

**TECHNICAL UNIVERSITY OF CRETE  
PRODUCTION ENGINEERING AND MANAGEMENT DEPARTMENT**



**Master's thesis:**

# **Simulation-based energy auditing**

**Parthena Exizidou**

**Supervisor:**

**Dr. Dimitrios Rovas**

Chania, 2012



## Acknowledgements

I gratefully acknowledge the valuable assistance of the supervisor of this thesis, Dr. Dimitrios Rovas. I would like to thank him for his guidance and for the chance he gave me to participate in his research team enriching my knowledge and experiences.

I am particularly thankful for the help and advice that Dr. Denia Kolokotsa offered me as a member of the research team and as a professor.

I could not miss referring to the contribution of my student colleagues and especially the contribution of Giorgos Giannakis to this effort.

Finally I wish to thank my parents, my brother, my sister and my closest friends for their love and support throughout all my academic years.

## Table of Contents

Executive Summary .....	1
1. Introduction.....	3
1.1 Harmonization of the EU regulations by the Greek legislation. ....	4
1.1.1 TEE-KENAK simulation software (Energy Performance Certificate) .....	5
1.2 Simulation based energy auditing-Benefits .....	6
2. Applying simulation-based energy auditing-A case study.....	6
2.1 Building’s description .....	7
2.1.1 General Description .....	9
2.1.2 Climate data.....	13
2.1.3 Geometric analysis and zoning .....	19
2.1.4 Wall definitions and Glazing .....	21
2.1.5 Shading .....	25
2.1.6 Ventilation and Infiltration .....	26
2.1.7 HVAC system .....	29
2.1.8 Internal Gains .....	34
2.2 Simulation results analysis .....	36
3. CFD external/internal airflow analysis in the TUC building.....	43
3.1 Introduction to CFD .....	43
3.2 Mathematical Model.....	46
3.2.1 CFD partial differential equations.....	46
3.2.2 Finite Volume Discretization Method .....	48
3.2.3 Relaxation methods .....	50
3.2.4 The SIMPLER Algorithm .....	51
3.2.5 CFD Boundary Conditions.....	53
3.3 Setting up a CFD analysis in DesignBuilder .....	54
3.3.1 External CFD analysis .....	54
3.3.2 Internal CFD analysis.....	57
3.3.3 Calculation options data .....	58
3.4 Applying external and internal CFD analysis in the TUC building .....	61
3.4.1 External CFD Analysis Results .....	61
3.4.2 Internal CFD analysis results .....	67
4. Energy auditing process-Further actions.....	75
4.1 Thermographic inspection .....	75
4.2 Building Energy Performance Rating.....	80

4.2.1 Calculation Parameters.....	80
4.2.2 Results .....	81
4.2.3 Modeling assumptions- Comparison with EnergyPlus .....	81
Conclusions .....	85
References.....	86
Appendix: Building’s envelope information and comfort results .....	88

## List of Figures

Figure 1.1: EU-27 total primary energy consumption by energy source in 2008 (1). .....	3
Figure 1.2: Greece's heating energy consumption exceeding Finland's ( $\text{kgoe}/\text{m}^2$ ) (1). .....	4
Figure 1.3: Energy Performance Certificate. ....	5
Figure 2.1: The building's site.....	7
Figure 2.2: The building's site.....	8
Figure 2.3: Depiction of the main entrance of the building. ....	8
Figure 2.4: Depiction of the south-west side. ....	9
Figure 2.5: Depiction of the south-east side. ....	9
Figure 2.6: Roof openings.....	9
Figure 2.7: The indoor stairs and circulation area.....	9
Figure 2.8: Geometry of the simulation model created in DesignBuilder.....	10
Figure 2.9: Building shading at 21/12 at 09:00. ....	10
Figure 2.10: Building shading at 21/12 at 12:00. ....	11
Figure 2.11: Building shading at 21/12 at 15:00. ....	11
Figure 2.12: Building shading at 21/06 at 09:00. ....	11
Figure 2.13: Building shading at 21/06 at 12:00. ....	12
Figure 2.14: Building shading at 21/06 at 15:00. ....	12
Figure 2.15: Monthly maximum and minimum dry bulb temperatures ( $^{\circ}\text{C}$ ). ....	14
Figure 2.16: Monthly mean maximum and minimum dew point temperatures ( $^{\circ}\text{C}$ ). ....	15
Figure 2.17: Monthly statistics of relative humidity (%). ....	15
Figure 2.18: Monthly mean relative humidity (data period: 1958-1997) (10).....	17
Figure 2.19: Mean monthly rainfall and rain days (data period: 1958-1997) (10).....	17
Figure 2.20: Wind speed values. ....	18
Figure 2.21: Slab-in-grade illustration (11).....	19
Figure 2.22: Ground floor plan view.....	20
Figure 2.23: First floor plan view. ....	21
Figure 2.24: Facade view (glass surface: $42.5\text{m}^2$ ).....	23
Figure 2.25: Plan view (glass surface: $18.3\text{m}^2$ ). ....	23
Figure 2.26: Left side view (glass surface: $17.8\text{m}^2$ ). ....	24
Figure 2.27: Right side view (glass surface: $30.63\text{m}^2$ ). ....	24
Figure 2.28: Shading devices. ....	25
Figure 2.29: Dimensions of windows with blinds (black color) and of windows without shading devices (red color)-façade view. ....	25
Figure 2.30: Dimensions of windows with blinds-left side view. ....	26
Figure 2.31: Dimensions of windows with blinds-right side view. ....	26
Figure 2.32: Modeling of Calculated Natural Ventilation flow and control in EnergyPlus. ....	28
Figure 2.33: The heating circulation system.....	30
Figure 2.34: Ground-floor plan of the heating circulation system. ....	31
Figure 2.35: First-floor plan of the heating circulation system. ....	32
Figure 2.36: Modeling split unit type air conditioners in EnergyPlus.....	33
Figure 2.37: The lighting system.....	35
Figure 2.38: Simulated energy consumption. ....	37
Figure 2.39: Comparison of simulated inside temperatures and measured inside temperatures for office 11 during December 2012. ....	38
Figure 2.40: Comparison of simulated inside temperatures and measured inside temperatures for office 10 during December 2012. ....	38
Figure 2.41: Monthly HVAC energy consumption. ....	40

Figure 2.42: Comparison of natural lighting level and lighting electric consumption in Office 1 during November.....	41
Figure 2.43: Time not comfortable based on ASHRAE 55-2004.....	42
Figure 3.1: Example of an internal CFD analysis.....	44
Figure 3.2: Example of an external CFD analysis.....	45
Figure 3.3: CFD workflow. ....	46
Figure 3.4: Building space divided into contiguous control volumes (Finite Volume Grid) .....	48
Figure 3.5: Depiction of Finite Volume Grid .....	49
Figure 3.6: The continuous nature of the dependent variable $\phi$ (19). ....	49
Figure 3.7: One dimension finite volume grid.....	49
Figure 3.8: SIMPLER Algorithm procedure (19; 21).....	53
Figure 3.9: Example of uniform and non-uniform grid spacing type. ....	54
Figure 3.10: Modifying the CFD grid using a “Uniform” spacing type. ....	55
Figure 3.11: “Increasing power law” spacing type.....	55
Figure 3.12: “Decreasing power law” spacing type.....	55
Figure 3.13: “Symmetric power law” option.....	56
Figure 3.14: 225° Wind direction .....	56
Figure 3.15: 90° Wind direction .....	56
Figure 3.16: Case of flow imbalance when importing boundary conditions from EnergyPlus simulation. ....	58
Figure 3.17: Calculation options data.....	59
Figure 3.18: Geometry of the simulation model created in DesignBuilder.....	61
Figure 3.19: Residuals and Cell Monitor. ....	63
Figure 3.20: 3D Velocity contours (m/s).....	64
Figure 3.21: Horizontal Velocity contour slice (m/s). ....	64
Figure 3.22: Vertical velocity slice (m/s).....	65
Figure 3.23: Generation of eddies at the back side of the building. ....	65
Figure 3.24: Filled velocity contour horizontal slice (m/s). ....	66
Figure 3.25: Pressure distribution (Pa). ....	66
Figure 3.26: Dependent value residuals reaching the desired termination residuals.....	67
Figure 3.27: 3D contours temperature results in office 11 (°C). ....	68
Figure 3.28: Filled temperature contours results in office 11 (°C) .....	69
Figure 3.29: Velocity vectors of air moving in and out through an open window. ....	69
Figure 3.30: Filled temperature contours results in office 10 (°C) .....	70
Figure 3.31: The operation of the cooling system in office 10. ....	71
Figure 3.32: Dependent value residuals reaching the desired termination residuals.....	72
Figure 3.33: Filled temperature contours results in office 1 (°C). ....	72
Figure 3.34: The atrium geometry isolated from the rest of the building .....	73
Figure 3.35: Air circulation in the atrium area. ....	73
Figure 3.36: Age of air in the atrium area-3D contours (sec). ....	74
Figure 4.1: Summer thermal image of the building façade.....	75
Figure 4.2: Winter thermal image of the façade of the building.....	76
Figure 4.3: Winter thermal image of the façade of the building.....	76
Figure 4.4: Depiction of the south-west side of the building (Summer thermal image). ....	76
Figure 4.5: Depiction of the south-west side of the building during summer.....	77
Figure 4.6: Depiction of the south-west side of the building during winter. ....	77
Figure 4.7: Thermal imaging of the glazing part of the façade during winter. ....	77
Figure 4.8: Internal thermal imaging of the building. ....	78
Figure 4.9: Internal thermal imaging of the building. ....	78
Figure 4.10: Internal thermal imaging of the building. ....	79
Figure 4.11: Greek climatic zones.....	82

## List of Tables

Table 1.1: Rating according to primary energy consumption in comparison with the reference building.....	5
Table 2.1: Hourly statistics for dry bulb temperatures (°C).....	15
Table 2.2: Hourly relative humidity.....	16
Table 2.3: Monthly wind direction (N=0° or 360°, E=90°, S=180°, W=270°).....	17
Table 2.4: Monthly statistics for solar radiation (Direct Normal, Diffuse, Global Horizontal) in Wh/m <sup>2</sup> .....	18
Table 2.5: Monthly ground temperatures calculated using the “slab” preprocessor.....	19
Table 2.6: Thermal properties of construction materials.....	22
Table 2.7: Description and layers U-values.....	22
Table 2.8: Glazing characteristics (12).....	23
Table 2.9: Airtightness data for a “medium” crack template (12).....	27
Table 2.10: Natural ventilation and infiltration values.....	29
Table 2.11: Technical characteristics of the radiators.....	31
Table 2.12: Technical characteristics of the cooling system of each zone.....	33
Table 2.13: Density of people in each zone of the building.....	34
Table 2.14: Holidays schedule.....	34
Table 2.15: Artificial lights in each zone.....	35
Table 2.16: Office equipment and internal gains.....	36
Table 2.17: Heating and cooling energy demands.....	39
Table 2.18: Annual energy consumption converted to primary energy.....	39
Table 2.19: Conversion factors of energy consumption to primary energy (15; 16).....	40
Table 2.20: Annual energy consumption in each zone.....	41
Table 3.1: Depiction of CFD boundaries.....	53
Table 3.2: Grid statistics.....	57
Table 3.3: Grid Statistics.....	62
Table 3.4: Dependent variable control settings.....	62
Table 4.1: Simulation results through TEE-KENAK simulation software (23).....	81

## Executive Summary

Currently, due to the global economic crisis it is of high importance the understanding of engineering leading role towards the economic development and innovation in order to deal with global issues such as sustainable development and climate change. This effort requires innovation strategies and awareness of the environmental and social impact that technology application has. Improving energy-efficiency by altering strategies and pursuing sustainability is a way of responding to the shortage of traditional energy sources.

The European Union in order to improve energy efficiency adopts several legislation and regulation following the Kyoto protocols' goals by setting minimum requirements for energy performance of the Community's buildings. European countries are therefore called to increase their national regulation for energy efficiency of buildings embodying regulation under the general scope of reducing energy consumption and pollution, decreasing the need of imported energy in parallel.

The harmonization of the EU regulation to the Greek legislation took a lot of time and effort. Greece adopted the first, under the EU directions for energy performance of buildings law in 2008 accompanied after two years by the national regulation "KENAK- Regulation on the Energy Assessment of Buildings". The first official national tool (simulation software) for measuring energy performance of Greek buildings is released during the same year (2010).

Towards this general effort of the European Community for decreasing energy consumption in the building sector, the current study is aiming to evaluate the significance of simulation-based energy audits and to accent the capabilities of simulation software and thus its usefulness.

The first chapter presents a retrospection of the EU and Greek efforts in setting future goals for energy consumption reduction ameliorating the performance of the Community's buildings by adopting several legislation and regulation introducing building's identity through the Energy Performance Certificate. A short description of the Greek simulation software tool –TEE-KENAK-for measuring energy performance accompanied by an analysis of its benefits and restrictions is presented.

In the second chapter a case study of applying simulation based energy auditing is presented. The under-inspection building is a public office building, the Technical Services building of Technical University of Crete. All the appropriate data for measuring and simulating its energy performance are presented in detail including climatic data for the site location, characterization of the building's envelope including construction materials and their properties, detailed information concerning the HVAC and lighting system and information about internal gains caused by office equipment, lights and the activity of the building users.

For the thermal modeling, the building simulation engine EnergyPlus is utilized. The goal is to obtain as accurate a description of the building and its systems as possible. For this reason, a very fine zoning is performed and detailed calculation of infiltration and other parameters takes place at each time step. To corroborate the simulation results a validation scenario is considered in which the temperatures for the building are compared against measured values taken over a period in which the building was closed.

In addition, part of this effort comprises the application of external and internal CFD airflow analysis (third chapter) in order to gain information upon air velocities, pressures and temperatures not only for the building as a whole but also for specific parts of the building, internal and external. The calculation of these parameters take into account specified boundary conditions such as surface temperatures, weather conditions, internal gains from human activity, equipment, lights and the HVAC system of the building. Additionally the application of a CFD analysis is used to evaluate the efficiency of the HVAC system both for cooling and for heating the building and therefore derive information upon thermal comfort of occupants.

Finally, additional audit actions are presented in the final chapter comprising the energy auditing of the building through a thermal imaging camera in order to review its present state of performance and the application of the Greek energy certification system in order to conclude to a brief comparison between EnergyPlus and TEE-KENAK simulation software.

## 1. Introduction

A first step towards the confrontation of global warming is an international agreement, the Kyoto Protocol, linked to the United Nations Framework Convention on Climate Change. Under the Kyoto Protocol, all countries that endorsed it are committed to reduce greenhouse gas emissions (GHG) by 5.2% from the 1990 level in a five-year period, from 2008 until 2012. In order to meet the objectives of the Kyoto Protocol, the implementation of measures and policies to each country is considered crucial.

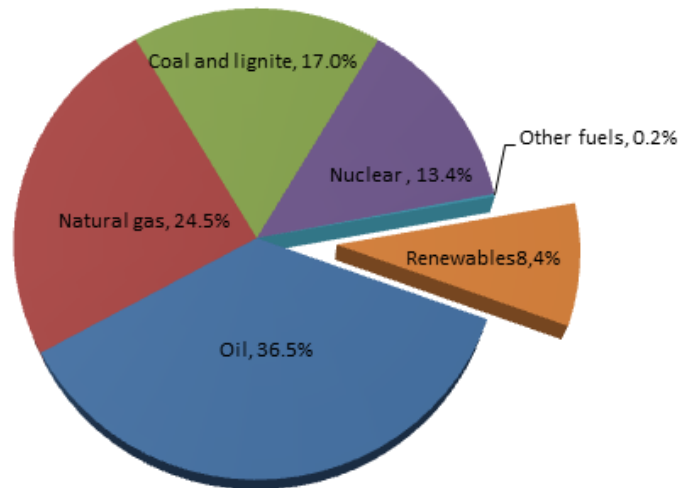


Figure 1.1: EU-27 total primary energy consumption by energy source in 2008 (1).

Complying with the Kyoto Protocol, Europe in order to meet its commitments adopts a package of policies and measures including the 2002/91/EC Directive of the European Parliament and of the Council of 16 December 2002 on the energy performance of buildings (EPBD). According to the Directive more than 40% of the energy consumption of the European Community is due to the buildings' sector (residential and tertiary). Hence it is aiming to the reduction of energy requirements, achieving security of energy supplies and meeting the Kyoto commitments. The requirements set by the Directive to the Member States are the adoption of a calculation methodology for the energy performance of buildings, the setting of minimum performance requirements for new and existing buildings, the energy performance certificate for constructed, sold and rented buildings and the regular inspection of the heating and cooling systems.

Furthermore, during March 2007, Europe, in order to strengthen its competitiveness and reduce its energy dependence combating climate change at the same time, adopted an energy policy known as the "20-20-20" targets. According to these energy targets Europe shall achieve by 2020 a 20% reduction of GHG comparing to the 1990s levels, to reach 20% energy consumption from renewable resources and 20% reduction of primary energy consumption.

The amending of the 2002/91/EC Directive, Directive 2010/31/EU of the European Parliament and of the Council of 19 May 2010 on the energy performance of buildings, is targeting to the reduce of the European Union's energy dependence and carbon dioxide emissions (2) under the general effort of achieving the 20% reduction of energy consumption of buildings by 2020. Towards this effort all the Member States of the Union are bounded to conform according to

the new Directive taking actions in order to reach cost-optimal levels of minimum energy performance requirements increasing, in parallel, the number of nearly zero-energy buildings.

### 1.1 Harmonization of the EU regulations by the Greek legislation.

During 1979 the first regulation in Greek history setting minimum requirements for thermal insulation on buildings envelope took place, meaning that buildings before 1979, representing the 75% of total building stock are uninsulated (3). Following this regulation, on May 2008 a first attempt of the mandatory harmonization of the EU regulation takes place with the national law N.3661/08 “Measures for the reduction of energy consumption in buildings and other provisions” enforced after one year by “KENAK-Regulation on the Energy Assessment of Buildings” (April 2010).

Taking into account that a 75% of the total amount of Greek buildings were built before 1980, the building stock in Greece is characterized by energy-intensive buildings due to their architecture, lack of insulation and material properties. Another parameter that accounts for the considerable increase in energy demands and therefore CO<sub>2</sub> emissions is the almost inexistent incentives and campaigns in order to amend end-users energy behavior and set a basis for the reinforcement of the environmental culture of Greek citizens.

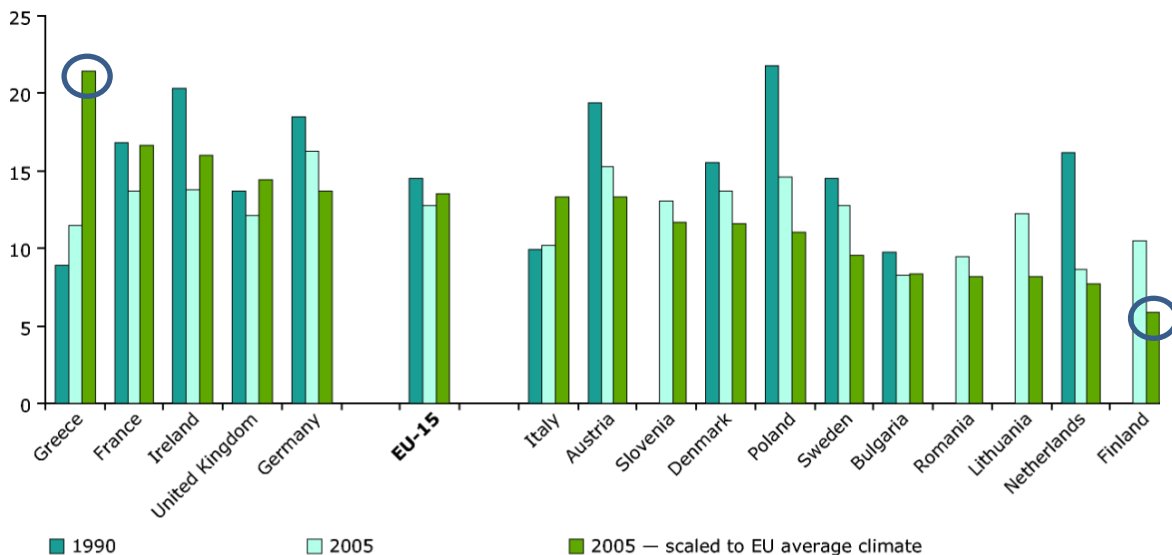


Figure 1.2: Greece's heating energy consumption exceeding Finland's (kgoe/m<sup>2</sup>) (1).

As part of the implementation of energy policies, KENAK through its provisions is targeting to the decrease of buildings' energy requirements for heating, cooling, lighting and hot water production through a better and more energy efficient design of the building cell and electromechanical equipment and through the use of renewable energy sources and CHP (Combined Heat and Power) systems. Within KENAK, the procedure and the contents of the calculation of energy performance of buildings are appointed and the form and content of the Energy Performance Certificate as well as the procedure of the buildings and HVAC energy inspection. KENAK and the four technical guidelines of the Technical Chamber of Greece (4; 5; 6; 7) are providing the methodology for calculating energy performance of buildings.

From January 2011 energy inspections are conducted by assessors and through simulation software a calculation of energy efficiency is performed. The official launch of the simulation software, called TEE-KENAK simulation software, took place during October 2010 and until today several editions containing improvements were released.

### 1.1.1 TEE-KENAK simulation software (Energy Performance Certificate)

TEE-KENAK software incorporates the Greek EPBD implementation. It is an energy-performance calculation software based on the IEE SAVE project EPA-NR. The calculation code adapted and upgraded through an agreement between the Technical Chamber of Greece (TEE) and the National Observatory of Athens (NOA). The official national software was developed according to the EN standards and national requirements in accordance to the Hellenic regulation (KENAK) and Technical Guidelines (4; 5; 6; 7).

The building rating procedure is based on the comparison of the under-study building with the characteristics of a reference building. The reference building is used as a benchmark for the construction procedure of new buildings and for the evaluation of energy performance of refurbished ones. The software specifies the characteristics of the reference building according to the characteristics and location of the under-study building. Thus, a reference building has the same geometry, orientation, use and climatic data as the under-study one. The reference building reflects the minimum requirements for the energy performance of the building according to the buildings envelope, HVAC system, use of renewable energy sources and library weather data.

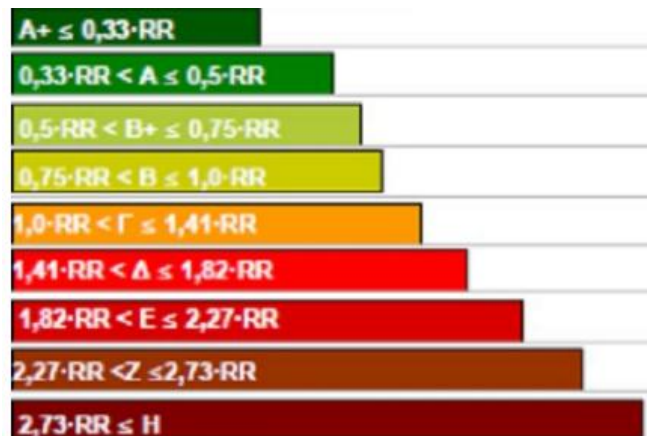


Figure 1.3: Energy Performance Certificate.

Rate	Boundaries
A+	$EP \leq 0.33R$
A	$0.33R < EP \leq 0.50R$
B	$0.50R < EP \leq 0.75R$
B+	$0.75R < EP \leq 1R$
Γ	$1R < EP \leq 1.41R$
Δ	$1.41R < EP \leq 1.82R$

Table 1.1: Rating according to primary energy consumption in comparison with the reference building.

The energy performance certificate is an asset rating of the building characterizing its energy efficiency. The most efficient building with almost zero energy consumption is rated with an A+

and the least efficient with an H. It is also used as an environment impact indicator calculating the carbon-dioxide emissions according to the primary energy consumption of the building.

## **1.2 Simulation based energy auditing-Benefits**

To account for further improvement of buildings energy performance, a detailed modeling and simulation is considered essential. Under this scope climatic and local conditions as well as the buildings geometry, heating and cooling installations, energy generation from renewable sources, lighting systems, natural lighting and ventilation and the use of the building are playing a significant role.

Reducing energy requirements whereas maintaining comfort conditions, entails realistic and accurate representation of the under-examination buildings through advanced simulation models (8). Thus, calculation models play a significant role in terms of evaluating different energy conservation alternatives, evaluate buildings' current state and facilitate assessors to undertake feasible and cost-effective measures.

Simulation-based energy auditing, unlike traditional energy audits, uses models which represent the actual building virtually including not only its geometry and construction materials but also its use and the operation of its HVAC and lighting system. The simulation models can be used not only for the calculation of the energy performance of a building but also for isolating specific parts of it identifying occurring problems and simulating the implementation of possible solutions evaluating their impact. Traditional energy audits lack in accuracy and can be more time consuming and expensive. Measures taken using a traditional audit are irreversible and therefore risky usually disregarding the effects of the application of more than one measure.

In order to apply a simulation-based energy auditing there are several types of simulation software tools available varying in terms of functions, complexity, accuracy and price.

In the following chapters an application of simulation-based energy auditing is discussed by a case study that comprise the energy audit and simulation of a public building using EnergyPlus simulation software tool along with a CFD internal and external airflow analysis using DesignBuilder. A review of the current performance of the building is achieved through thermal imaging inspection concluding with a brief comparison of the potential and results of the simulation process with the Greek energy performance rating software TEE-KENAK.

## **2. Applying simulation-based energy auditing-A case study**

In order to evaluate a simulation based energy auditing and explore the capabilities of such a procedure, a case study is used. For the thermal modeling, the building simulation engine EnergyPlus is utilized. The goal is to obtain as accurate a description of the building and it's systems as possible.

EnergyPlus is an energy simulation software performing dynamic sub-hourly thermal load calculations. As an energy analysis tool it is used to model and calculate the building's heating, cooling, lighting energy consumption and ventilation. Using EnergyPlus, a detailed design of HVAC systems and natural ventilation as well as infiltration can be achieved performing

comfort analysis at the same time using activity, humidity and dry bulb data. It can also calculate greenhouse gas emissions due to the amount of primary energy consumption. Moreover it contains a detailed weather database with hourly or sub-hourly climatic data.

Although EnergyPlus is a stand-alone simulation program without a “user-friendly” graphical interface there are plenty available such as DesignBuilder, Google SketchUp, CYPE-Building Services, EFEN, EPlusInterface and more. In the current case study DesignBuilder graphical user interface is used. DesignBuilder is developed around EnergyPlus containing a large variety of construction, glazing and blind materials providing visualization of site layouts and solar shading. DesignBuilder contains a CFD 3D simulation tool which is also used in the current study. Through DesignBuilder and EnergyPlus a very fine zoning is performed and detailed calculation of infiltration and other parameters takes place at each time step.

In the following paragraphs, information concerning the building and the area where it is situated as well as the production of a representative model using DesignBuilder and EnergyPlus are presented and discussed.

## 2.1 Building's description

The under-examination building used in this case study is located at the Technical University Campus situated at Kounoupidiana in the Akrotiri peninsula. The area is at the suburbs of Chania, thinly built-up, with an open view towards the north. The distance of the area from the sea is nearly 2.97 km from south and 2.02 km from north. The elevation of the area above the sea level is 156 m, the latitude is 35°31'36.58" and the longitude 24°04'13.01". *Figure 2.1* and *Figure 2.2* show a satellite picture of the area with the building marked.



*Figure 2.1: The building's site.*



*Figure 2.2: The building's site.*

The building comprises two stories with a basement with a total surface area of 426 m<sup>2</sup>. The overall construction is currently used for the University's technical services' offices. It has a North-North-West orientation with large openings and an atrium. Several views of the building can be seen from *Figure 2.3* to *Figure 2.7*.

The region is characterized by long-hot summers and cool/cold-humid winters and long periods of sunlight during the year, typical of a Mediterranean climate. The heating period starts in October and ends in April and cooling period starts in May and ends in September.



*Figure 2.3: Depiction of the main entrance of the building.*



*Figure 2.4: Depiction of the south-west side.*



*Figure 2.5: Depiction of the south-east side.*



*Figure 2.6: Roof openings.*

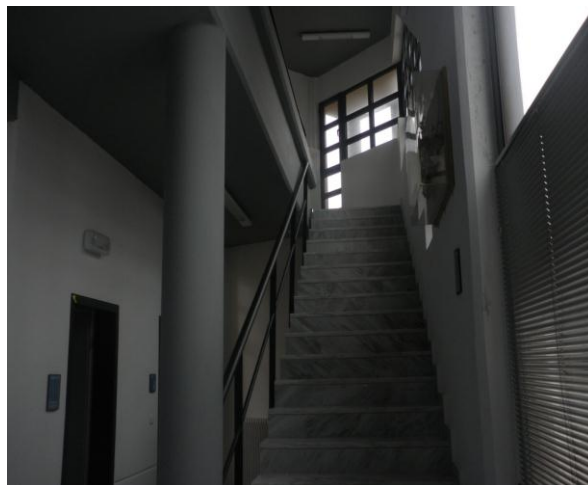


*Figure 2.7: The indoor stairs and circulation area.*

### **2.1.1 General Description**

A detailed representation of the building geometry, presented in *Figure 2.8*, was created according to the floor plans using the DesignBuilder drafting environment which allows for the automatic creation of the idf (EnergyPlus input) files. DesignBuilder is designed to act as a graphical interface to EnergyPlus.

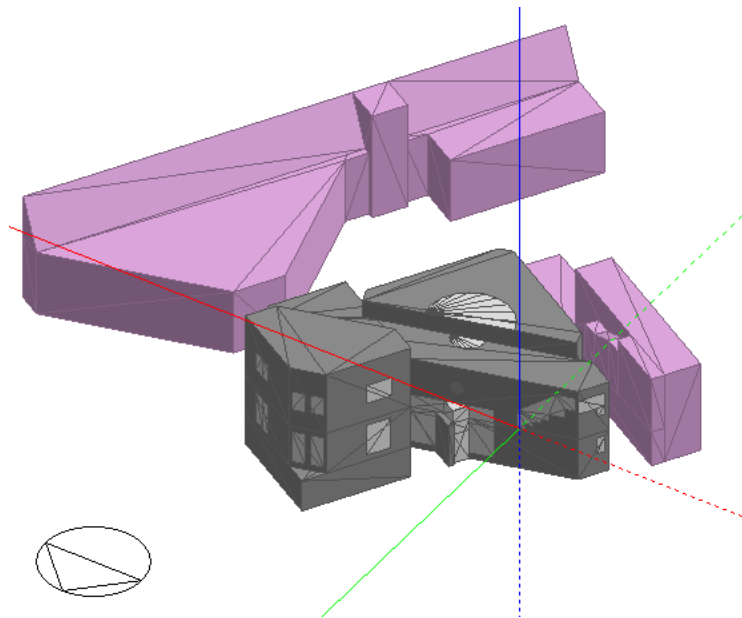


Figure 2.8: Geometry of the simulation model created in DesignBuilder.

To account for shading from nearby buildings, along with the building geometry, the shapes of nearby buildings were introduced. In the following Figures (Figure 2.9 to Figure 2.14) indicative examples of shading during different hours in the winter and summer solstice are presented.

The building, due to its construction, has three levels of height (see Figure 2.9) where the installation of photovoltaic panels is planned to be done in the near future. The shading of these three levels of roof will affect a great deal the efficiency of the panels. Observing Figure 2.9 to Figure 2.14 can be easily concluded that throughout the year the level of the building which is shaded is level 3 during winter solstice, mostly in morning hours (Figure 2.9). The shading of the rest of the levels are not affected by the nearby buildings nor by the building itself throughout the year.



Figure 2.9: Building shading at 21/12 at 09:00.



*Figure 2.10: Building shading at 21/12 at 12:00.*



*Figure 2.11: Building shading at 21/12 at 15:00.*



*Figure 2.12: Building shading at 21/06 at 09:00.*



*Figure 2.13: Building shading at 21/06 at 12:00.*



*Figure 2.14: Building shading at 21/06 at 15:00.*

To correctly account for internal gains due to occupant presence, activity data were collected for the building and imported. The types of data imported include occupant density (people/m<sup>2</sup>) on each zone, occupancy timetables (including holiday schedules), and metabolic rates for office activities. Moreover comfort temperatures (set points and setbacks) were imported as well as humidity set points, minimum fresh air levels (l/s-person) and desirable lighting levels according to the use of each zone. Finally, at this point computer and equipment gains were introduced for each zone of the building.

Furthermore, based on the building construction data, templates were created for each of the walls (internal partitions, external walls, roof etc.) detailing thermal characteristics. Appropriate templates were created for each of the construction elements so that they can be easily modified according to actual measurements.

With reference to the glazing data, apart from the glazing type and characteristics of internal and external windows, data of shading devices were introduced as well as an operation schedule which will allow their function. A percentage of the total window area that can open is introduced. An assumption of 20% of the total window area that opens was made according to the employees' habits. The air flow opening is assumed to be a gap in the side of the

window which takes on the full height of the window. Windows can only open if the operation schedule allows it and whenever the inside temperature is higher than the comfort one and higher than the outside temperature. The ventilation rate is calculated based on the pressure difference across the opening calculated from wind and stack pressure effects.

Moreover, lighting data were imported regarding the type of lights, energy requirement, visible and radiant fractions. To more realistically simulate lighting energy requirements (and consequent gains) lighting control was engaged to turn on the lights whenever the levels of natural light were below accepted comfort levels.

With reference to HVAC of the building, heating is achieved through a central system using an oil boiler and hot water radiators in each room. A packaged terminal heat pump is positioned in each office to cool the zone during summer but it is also used as a supplementary heating system whenever the central system does not cover the heating needs of each space during winter. Thus, whenever the capacity of the radiators is not enough (cannot reach the heating setpoint temperature) it is assumed that the employee is turning on the split unit so that the inside temperature reaches the desirable level.

To model the HVAC system in EnergyPlus, a dual setpoint thermostat was introduced for each of the 14 zones that are heated and/or cooled with separately heating and cooling setpoint temperatures. Data regarding the heating and cooling function of each type of split unit in each zone, were introduced such as availability schedule, air flow rates, EER, COP, capacity.

The central heating system was modeled with details referring to the boiler (fuel type, thermal efficiency, water temperature), to the radiators located in each zone (average water temperature, water mass flow rate, capacity, surfaces and fractions of radiant energy to surfaces) and to the connection of the boiler with the radiators in each zone (branches, splitter, mixer).

### **2.1.2 Climate data**

A weather station is installed at the terrace of the building in order to have local to the building information collected and available in real-time at a frequency of one per minute. However due to lack of annual weather data collected, the weather file that will be used in the current study is the Athens weather file of the EnergyPlus weather file library for annual simulations. Concerning the validation scenarios, data collected from the installed weather station will be used instead.

Once the weather data have been collected on an annual or any other basis, a semi-automatic procedure for the generation of the relevant weather files, (given as input to EnergyPlus) has been developed so that the data can be used by the simulation tools (9).

In any event, the data presented below give a reasonable estimate of weather characteristics in the building location on an annual basis.

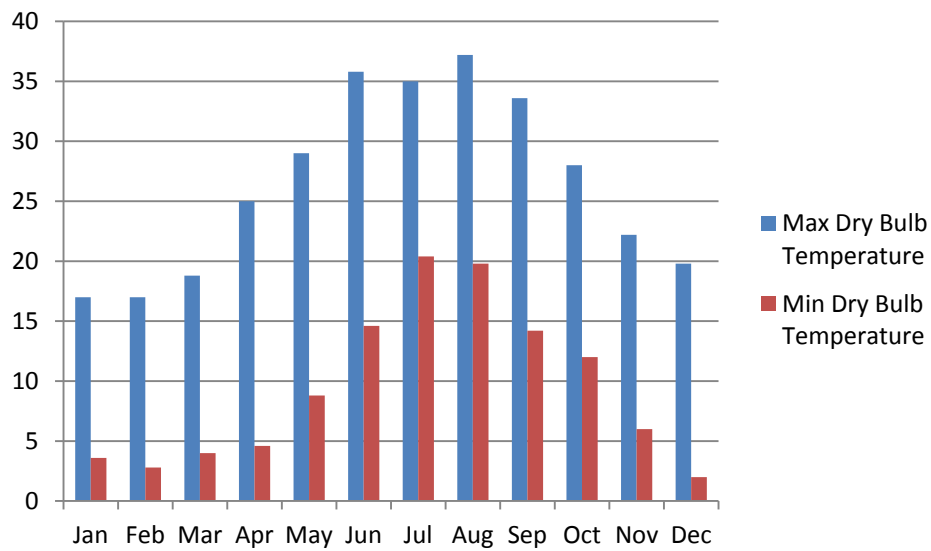


Figure 2.15: Monthly maximum and minimum dry bulb temperatures (°C).

The maximum-minimum mean dry bulb temperature can be seen in *Figure 2.15*. The maximum dry bulb temperature is 37.2°C on August 6 while the minimum dry bulb temperature is 2°C on December 26. The highest temperatures of the year are observed in months July and August whereas the minimum temperatures in months December, January and February. Average hourly statistics for dry bulb temperatures can be seen in *Table 2.1*.

	Jan	Feb	Mar	Apr	May	Jun	Jul	Aug	Sep	Oct	Nov	Dec
0:01- 1:00	9.4	8.1	9.6	12.7	17.5	21.8	25.3	24.9	21.8	17.1	12.9	9.6
1:01- 2:00	9.2	8.4	10.2	12.5	17.7	21.3	24.1	24.5	21.4	17.4	13.3	10.4
2:01- 3:00	9.1	7.9	9.4	12	16.8	21	24.5	24.3	21	16.6	12.3	9.3
3:01- 4:00	9.1	7.5	9.2	11.9	16.4	20.8	24.3	24.1	20.5	16.6	12.1	9.1
4:01- 5:00	9.1	8	9.7	11.7	16.5	20.5	23	24	20.1	16.9	12.8	9.8
5:01- 6:00	9.2	7.4	8.9	12.3	16.2	21.7	24.1	24.7	21	16.3	12.2	8.9
6:01- 7:00	9.2	7.5	9	13	17.3	22.9	24.8	25.5	21.9	16.1	12.3	9
7:01- 8:00	9.3	8.2	10.3	13.6	19.6	24.1	26.1	26.2	22.7	17.7	13.1	9.7
8:01- 9:00	10.2	8.3	10.7	14.9	19.7	25.1	27.4	27.5	23.9	19.6	14.4	9.4
9:01-10:00	11.1	9.3	11.5	16.1	20.5	26.1	28.5	28.9	25.1	20.7	15.7	10.6
10:01-11:00	12	11.4	13.5	17.3	22.1	27.2	29	30.2	26.3	21.8	16.7	12.9
11:01-12:00	12.4	11	12.8	17.7	21.4	27.5	29.5	30.8	26.7	22.4	17.2	12
12:01-13:00	12.9	11.5	13.4	18.2	22	27.9	30.1	31.4	27.1	22.6	17.4	12.4
13:01-14:00	13.4	13	14.6	18.7	23.2	28.3	30.4	32	27.6	22.9	17.8	14
14:01-15:00	13.1	12	13.7	18.5	22.5	27.9	30.7	31.5	27.2	22.4	17	12.7
15:01-16:00	12.8	11.9	13.6	18.2	22.6	27.7	30.9	31	26.9	21.9	16.3	12.7
16:01-17:00	12.5	12.2	14	18	22.7	27.8	30	30.5	26.6	21.3	16.2	12.8
17:01-18:00	11.8	10.8	12.6	17.1	21.5	26.8	29.8	29.5	25.7	19.7	14.8	11.3
18:01-19:00	11.1	10	12	16.2	20.5	25.9	29.1	28.5	24.7	19	14.5	11
19:01-20:00	10.5	10.1	12	15.3	20.1	25	27.5	27.5	23.8	19.2	14.8	11.5
20:01-21:00	10.2	9.2	10.8	14.7	18.8	24.3	27.5	26.9	23.4	18.4	13.8	10.5
21:01-22:00	10	8.8	10.6	14.1	18.5	23.6	27	26.3	23	17.9	13.6	10.2
22:01-23:00	9.7	9.1	11	13.5	18.6	22.9	25.7	25.7	22.6	18	13.8	10.9

23:01-24:00	9.5	8.5	10	13.2	17.8	22.4	25.8	25.3	22.2	17.1	13.1	9.9
-------------	-----	-----	----	------	------	------	------	------	------	------	------	-----

Table 2.1: Hourly statistics for dry bulb temperatures (°C).

In Figure 2.16 monthly maximum-minimum dew point temperatures can be seen.

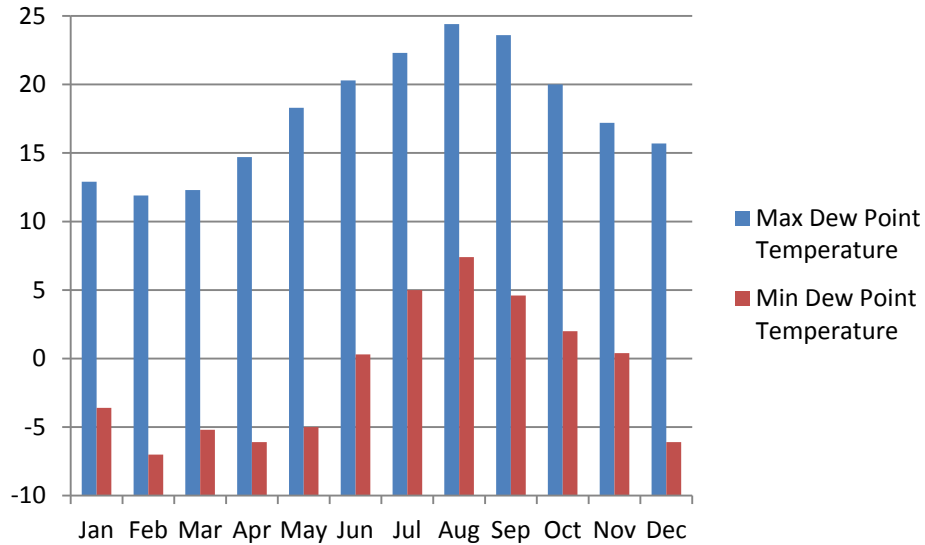


Figure 2.16: Monthly mean maximum and minimum dew point temperatures (°C).

The maximum dew point temperature is 24.4°C on 27<sup>th</sup> of August while the minimum dew point temperature is -7°C on 27<sup>th</sup> of February.

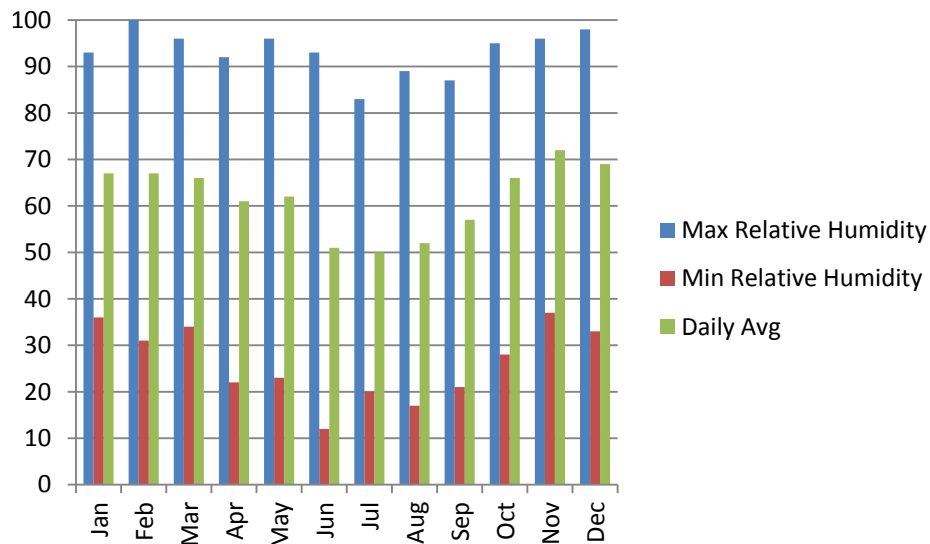


Figure 2.17: Monthly statistics of relative humidity (%).

The maximum and minimum values of mean monthly relative humidity can be seen in Figure 2.17 whereas the average hourly relative humidity (%) can be seen in Table 2.2. Chania is characterized by very humid winters compared to comfortable humidity conditions during summer months. Observing Table 2.2 June, July and August have the smallest average percentages in humidity while the maximum (more than 70%) occurs in November and December in the early morning hours.

Simulation-based energy auditing

	Jan	Feb	Mar	Apr	May	Jun	Jul	Aug	Sep	Oct	Nov	Dec
0:01-1:00	71	71	71	69	66	60	55	59	64	72	77	70
1:01-2:00	72	76	75	70	71	62	63	61	63	74	78	76
2:01-3:00	72	71	72	70	69	63	56	62	64	75	80	72
3:01-4:00	72	71	71	71	69	64	56	62	66	75	81	72
4:01-5:00	73	75	75	72	75	64	64	63	67	75	79	79
5:01-6:00	73	70	71	69	70	59	56	60	64	75	80	73
6:01-7:00	73	70	71	67	70	54	54	57	61	76	80	72
7:01-8:00	73	75	72	64	66	50	53	55	58	70	78	78
8:01-9:00	70	71	66	60	63	48	48	51	55	63	73	71
9:01-10:00	67	68	64	56	61	47	47	47	52	60	68	68
10:01-11:00	64	64	61	53	58	45	50	44	49	57	64	67
11:01-12:00	62	63	60	52	58	43	48	42	48	54	62	64
12:01-13:00	60	61	59	51	56	41	46	41	47	54	61	62
13:01-14:00	59	57	57	50	53	39	44	40	46	52	60	61
14:01-15:00	59	59	57	51	53	41	42	41	47	54	62	60
15:01-16:00	59	58	57	51	53	43	42	42	48	55	65	60
16:01-17:00	60	59	57	51	55	42	45	43	50	57	65	66
17:01-18:00	62	63	60	54	57	44	44	46	52	64	70	64
18:01-19:00	65	64	62	57	58	46	44	48	55	66	70	65
19:01-20:00	67	70	68	60	61	48	48	51	58	65	71	71
20:01-21:00	68	68	67	62	62	50	47	53	60	67	73	67
21:01-22:00	69	70	67	63	63	53	48	55	62	68	73	67
22:01-23:00	70	73	73	65	67	56	55	57	63	70	75	72
23:01-24:00	70	70	69	67	65	58	53	58	63	72	76	68

*Table 2.2: Hourly relative humidity.*

To further illustrate the local climate in Chania, data concerning the relative humidity and rainfall were obtained (10) for the period 1958-1997. In *Figure 2.18* the average humidity over each month (for that period) is given. As can be easily ascertained Chania have hot-dry summers followed by warm humid winters. Humid winters in Chania are accompanied with a respective number of rain days. According to *Figure 2.19* during January the maximum mean monthly rainfall of 122.9mm occurs with approximately 15 days of raining. Summers are very dry having almost no rainfall especially in July the lowest average rainfall of 0.5mm is observed. The mean values of data in *Figure 2.18* and *Figure 2.19* are referring to mean values of years 1958 to 1997.

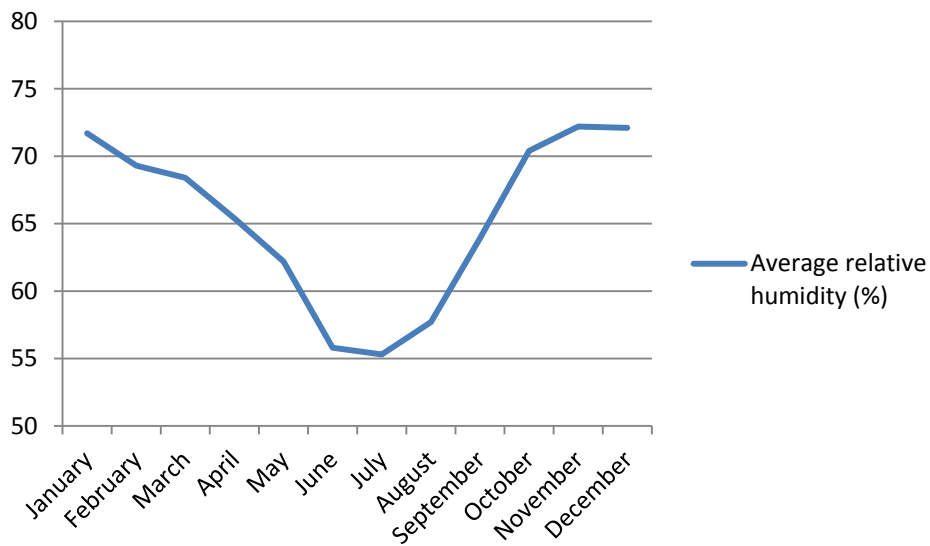


Figure 2.18: Monthly mean relative humidity (data period: 1958-1997) (10).

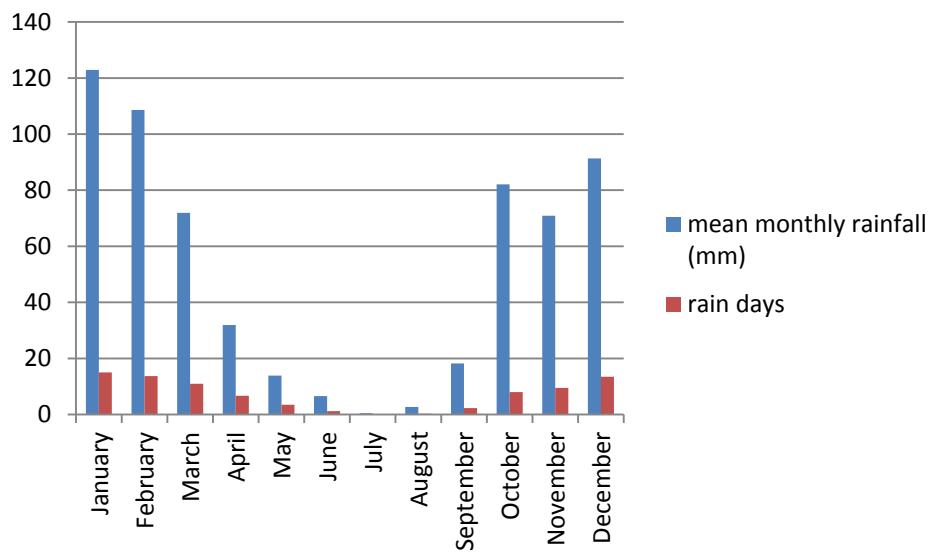


Figure 2.19: Mean monthly rainfall and rain days (data period: 1958-1997) (10).

	Jan (%)	Feb (%)	Mar (%)	Apr (%)	May (%)	Jun (%)	Jul (%)	Aug (%)	Sep (%)	Oct (%)	Nov (%)	Dec (%)
North	3	7	3	4	3	6	4	7	12	10	7	3
NorthEast	13	2	3	10	3	4	4	3	14	7	6	2
East	10	7	9	20	6	4	4	4	18	7	5	6
SouthEast	17	6	12	9	7	6	2	3	7	14	12	13
South	4	4	6	3	5	3	3	2	4	4	9	8
SouthWest	31	35	32	14	20	14	21	18	10	24	30	36
West	15	20	22	22	19	32	26	16	7	15	15	21
NorthWest	7	19	14	17	36	30	35	48	29	19	15	11

Table 2.3: Monthly wind direction (N=0° or 360°, E=90°, S=180°, W=270°).

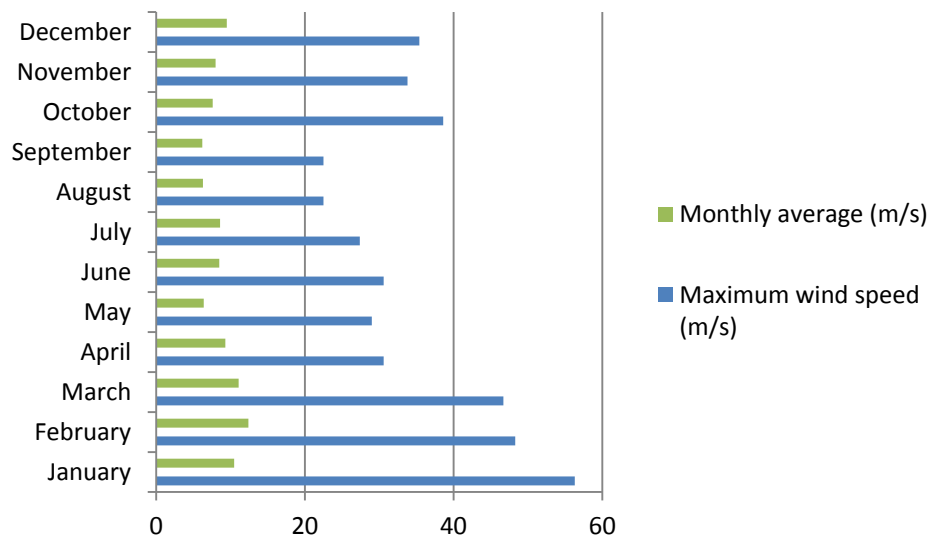


Figure 2.20: Wind speed values.

From Figure 2.20 the maximum wind speed of 56.3m/s occurs on January 22<sup>nd</sup> while the maximum direct normal solar radiation of 15968 Wh/m<sup>2</sup> occurs on June 15<sup>th</sup> according to Table 2.4.

	Jan	Feb	Mar	Apr	May	Jun	Jul	Aug	Sep	Oct	Nov	Dec
Direct	2421	320	5538	576	8601	1011	1055	8741	6568	5100	4596	287
Avg		6		6		7	2					7
Direct	7300	754	9103	883	1312	1596	1540	1593	1256	1150	1444	554
Max		8		2	1	8	4	9	5	6	0	1
Day	26	21	29	25	10	8	17	9	12	2	15	1
Diffuse	1030	130	1704	214	2300	2512	2471	2333	1967	1498	1174	100
Avg		7		9								5
Global	1995	281	4734	540	6957	7663	7599	6819	4825	3744	2995	216
Avg		4		5								3

Table 2.4: Monthly statistics for solar radiation (Direct Normal, Diffuse, Global Horizontal) in Wh/m<sup>2</sup>.

Apart from the environmental climate data that take part in the heat transfer calculations from the building to the environment and vice versa, the temperature of the ground is necessary for the calculation of heat transferred between zones and ground. To model ground thermal storage and calculate the temperatures applied to the underside of the ground floor surface, the external preprocessing “slab” tool of EnergyPlus was used. The input information needed to run the slab program was slab dimensions, slab thickness, mean monthly inside set point temperatures, ground temperatures and depth. In addition, soil and slab properties and boundary conditions were needed, such as thermal conductivity, density, specific heat, slab thickness. The slab configuration used in slab model is a ‘slab in grade’ model. It is assumed that the slab top surface to be in the same level as the outside earth surface (Figure 2.21). Typical values were used concerning material properties of the slab such as:

Slab material density=2300kg/m<sup>3</sup>

Soil density=1200kg/m<sup>3</sup>

Slab c<sub>p</sub>=650 J/kg K

Soil  $c_p=1200\text{J/kg K}$

Slab  $k=0.93\text{W/m K}$

Soil  $k=1\text{ W/m K}$

The actual building height was introduced to calculate the building shadowing on the ground as well as the indoor setpoint temperatures for each month of the year ( $22^\circ\text{C}$  for heating periods and  $26^\circ\text{C}$  for cooling periods).

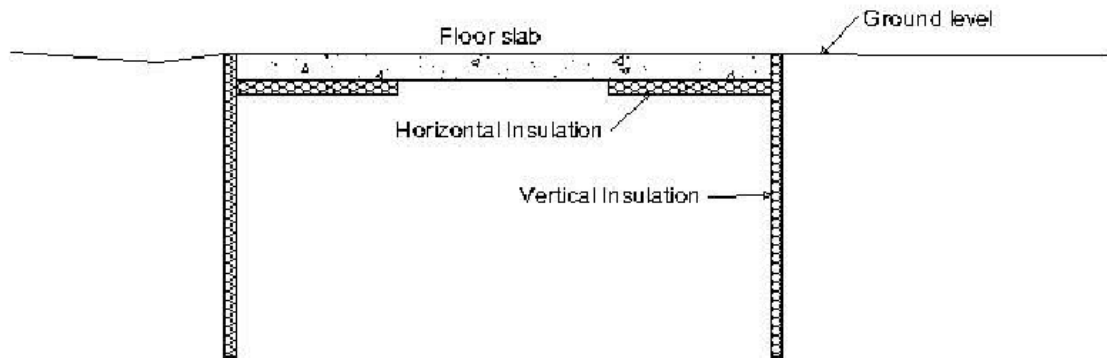


Figure 2.21: Slab-in-grade illustration (11).

The preprocessor obtained values are given in Table 2.5. These are direct inputs to simulation and provide information on mean monthly ground temperatures.

Month	Mean Ground Temperature ( $^\circ\text{C}$ )
January	20.36
February	20.32
March	20.35
April	20.40
May	20.45
June	23.38
July	23.73
August	23.81
September	23.92
October	21.02
November	20.59
December	20.45

Table 2.5: Monthly ground temperatures calculated using the “slab” preprocessor.

### 2.1.3 Geometric analysis and zoning

The shape of the building is triangular. The office building comprises 10 office rooms, an open meeting space, two corridors (one in each floor), the main entrance, an equipment room, a toilet and a basement that is used as a storage area. In both floors (ground floor and first floor) there is a central corridor along the length of the building with offices on either side. In the middle of the corridor there is an open meeting space in semicircle form. The plan of the second floor is similar with the first floor (Figure 2.22 and Figure 2.23). The only difference is

that in the middle of the second floor's corridor there is a semicircle space which connects the first floor meeting space with a 15.2m<sup>2</sup> roof glazing.

The 3D geometry modeling of the building in DesignBuilder graphical environment was based on existing 2D plans. The plans were designed in 1988 but the buildings construction started in 2006. There were several cases in which the plans did not agree with the actual construction, e.g. different window dimensions, zones were added later on, and more partitions were added. The lack of information from the 2D plans led to actual measurements of wall distances and window surfaces so as to have a more accurate geometry in the model. The connection between the two floors was succeeded by creating holes in the second floor of the model so as to merge zones in different blocks. Holes represent a constant flow path in the fabric. Since split type air conditioners are installed on each of the office rooms the temperature can be independently adjusted. For this reason each room of the building is defined as a separate thermal zone. Unconditioned zones include the main corridor and the basement.

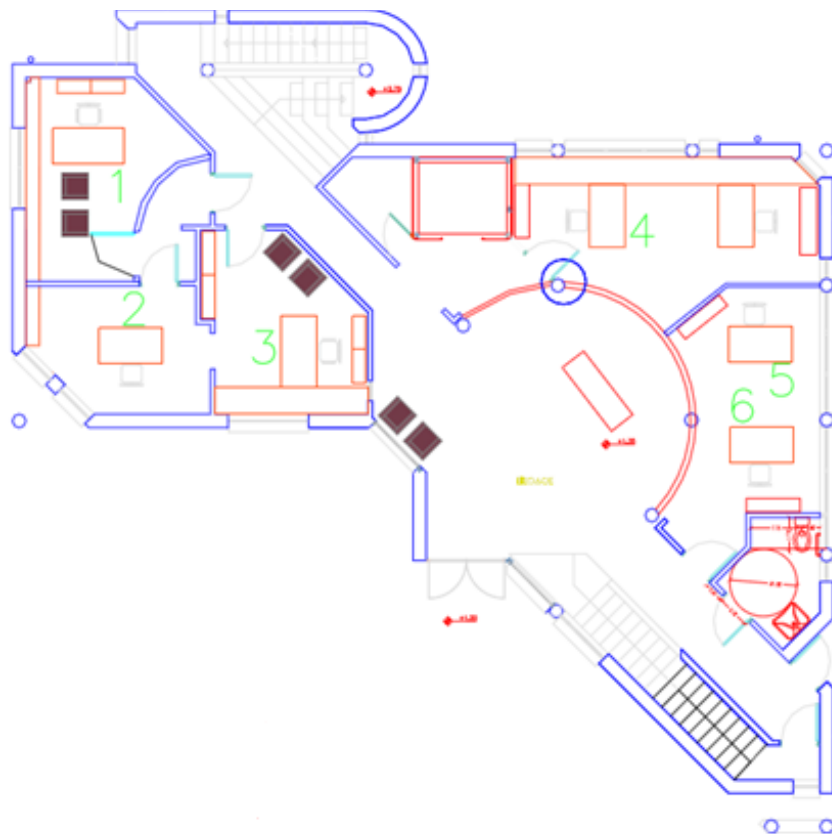


*Figure 2.22: Ground floor plan view.*

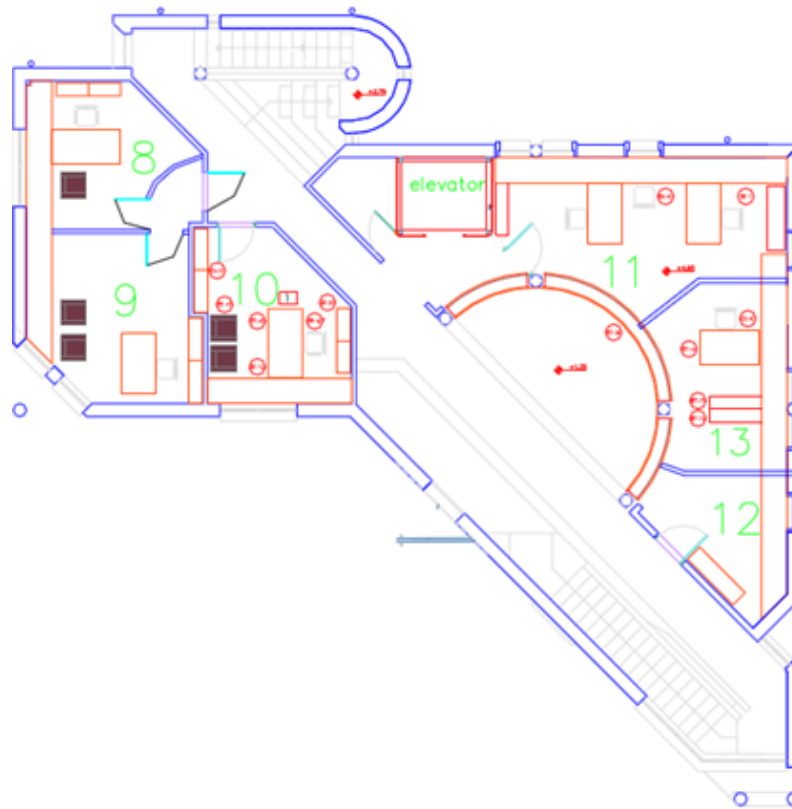


Figure 2.23: First floor plan view.

#### 2.1.4 Wall definitions and Glazing

The characteristics of the construction materials are described in detail by *Table 2.6* while each layers construction is described by

Layer	Layer bedding	U-value
External walls	0.02m coating, 0.19m concrete, 0.03m stone wool, 0.09m brick and 0.02m coating	1.026 W/m <sup>2</sup> K
External walls	0.02m coating, 0.31m concrete and 0.02m coating	4.3 W/m <sup>2</sup> K
Internal partitions	0.02m coating, 0.2m concrete, 0.02m coating	5.65 W/m <sup>2</sup> K
Internal walls-round partitions	0.05m gypsum plastering, 0.05m gypsum plastering	4 W/m <sup>2</sup> K
Roof	0.1m concrete, density 500kgr/m <sup>3</sup> , double asphaltpane 0.08m, extruded polysterine 0.04m, gravel 0.2m	0.41 W/m <sup>2</sup> K
Floor	white marble 0.03m and 0.3m concrete	4.44 W/m <sup>2</sup> K
External windows	double clear 3mm/6mm air (aluminum frames)	3.159 W/m <sup>2</sup> K
Internal windows	double clear 3mm/6mm air (aluminum frames)	3.159 W/m <sup>2</sup> K

*Table 2.7. Table 2.8* provides information on thermal, solar, visible and infra-red properties of the glazing of the building.

The external walls are constructed by concrete, brick and stone wool as insulation material with the exception of some specific parts in the front and back of the building that are constructed by concrete only. Some of the internal partitions are brick, some concrete and others added later on to separate the space are constructed by gypsum plastering. The U-values of the external, internal walls and windows are quite high which reveals the thermal attitude of the building. The building has a significant amount of thermal losses due to its construction materials and heat gains during summer due to the roof glazing. As part of the retrofitting efforts for the building the addition of external insulation is planned along with the installation of a shading device to protect from significant heat gains from the roof glazing. The thermal simulation model will be updated to reflect such changes when the retrofitting is completed.

Material	Thermal Bulk Properties			Surface Properties		
	Conductivity (W/mK)	Specific Heat (J/kg K)	Density (kg/m <sup>3</sup> )	Thermal Absorptance	Solar Absorptance	Visible Absorptance
Coating	0.85	1085	1900	0.9	0.7	0.7
Cast concrete (dense)	1.4	840	2100	0.9	0.6	0.6
MW Stone Wool	0.038	840	40	0.9	0.6	0.6
Brick	0.72	840	1920	0.9	0.6	0.6
Gypsum plastering	0.4	1000	1000	0.9	0.5	0.5
Aerated concrete slab	0.16	840	500	0.9	0.6	0.6
Expanded Polystyrene	0.035	1400	25	0.9	0.6	0.6
Asphalt	0.7	1000	2100	0.9	0.85	0.9
Gravel	0.36	840	1840	0.9	0.29	0.29
Marble (white)	2.77	802	2600	0.9	0.58	0.58

*Table 2.6: Thermal properties of construction materials.*

Layer	Layer bedding	U-value
External walls	0.02m coating, 0.19m concrete, 0.03m stone wool, 0.09m brick and 0.02m coating	1.026 W/m <sup>2</sup> K
External walls	0.02m coating, 0.31m concrete and 0.02m coating	4.3 W/m <sup>2</sup> K
Internal partitions	0.02m coating, 0.2m concrete, 0.02m coating	5.65 W/m <sup>2</sup> K
Internal walls-round partitions	0.05m gypsum plastering, 0.05m gypsum plastering	4 W/m <sup>2</sup> K
Roof	0.1m concrete, density 500kg/m <sup>3</sup> , double asphaltpane 0.08m, extruded polysterine 0.04m, gravel 0.2m	0.41 W/m <sup>2</sup> K
Floor	white marble 0.03m and 0.3m concrete	4.44

External windows	double clear 3mm/6mm air (aluminum frames)	W/m <sup>2</sup> K 3.159
Internal windows	double clear 3mm/6mm air (aluminum frames)	W/m <sup>2</sup> K 3.159

Table 2.7: Description and layers U-values.

Generic clear glass	
<b>Thermal Properties</b>	
Thickness (mm)	3
Conductivity (W/m K)	0.9
<b>Solar Properties</b>	
Solar transmittance	0.837
Outside solar reflectance	0.075
Inside solar reflectance	0.075
<b>Visible Properties</b>	
Visible transmittance	0.898
Outside visible reflectance	0.081
Inside visible reflectance	0.081
<b>Infra-red Properties</b>	
Infra-red transmittance	0
Outside emissivity	0.84
Inside emissivity	0.84

Table 2.8: Glazing characteristics (12).

The surface of each opening in each side of the building is depicted in the following figures.

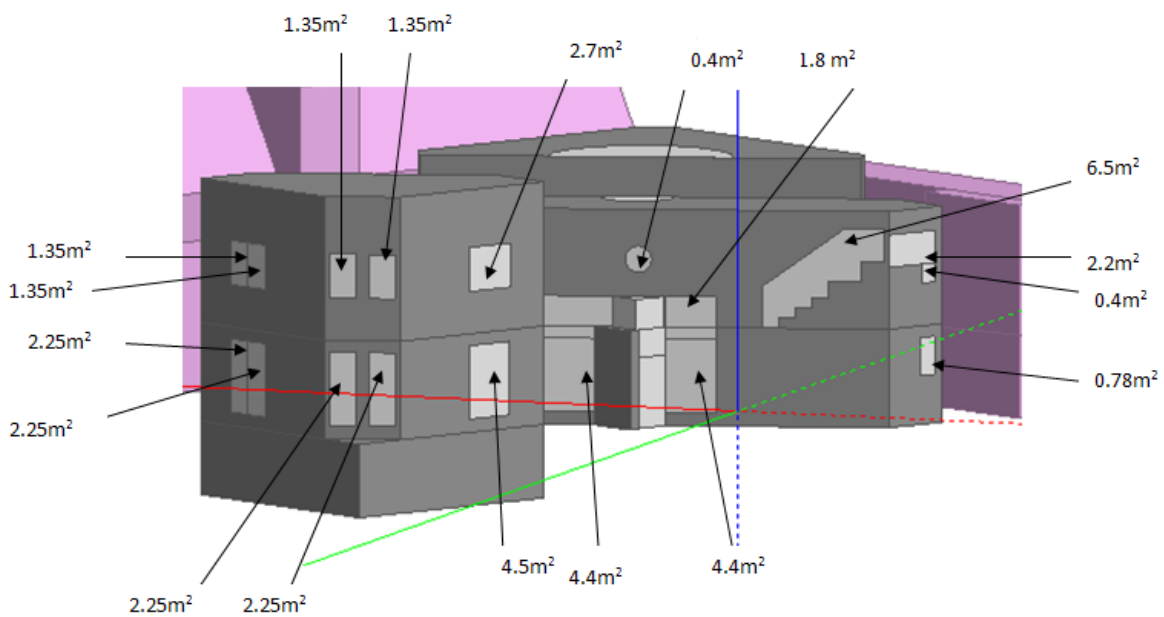


Figure 2.24: Facade view (glass surface: 42.5m<sup>2</sup>).

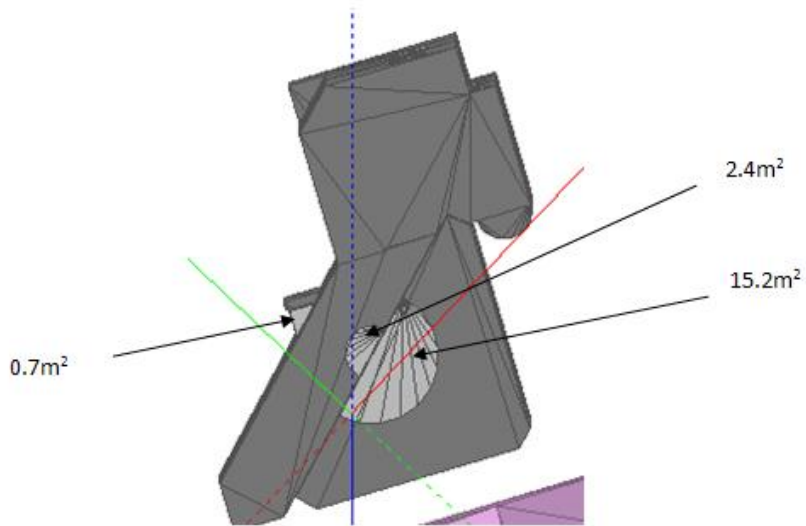


Figure 2.25: Plan view (glass surface: 18.3m<sup>2</sup>).

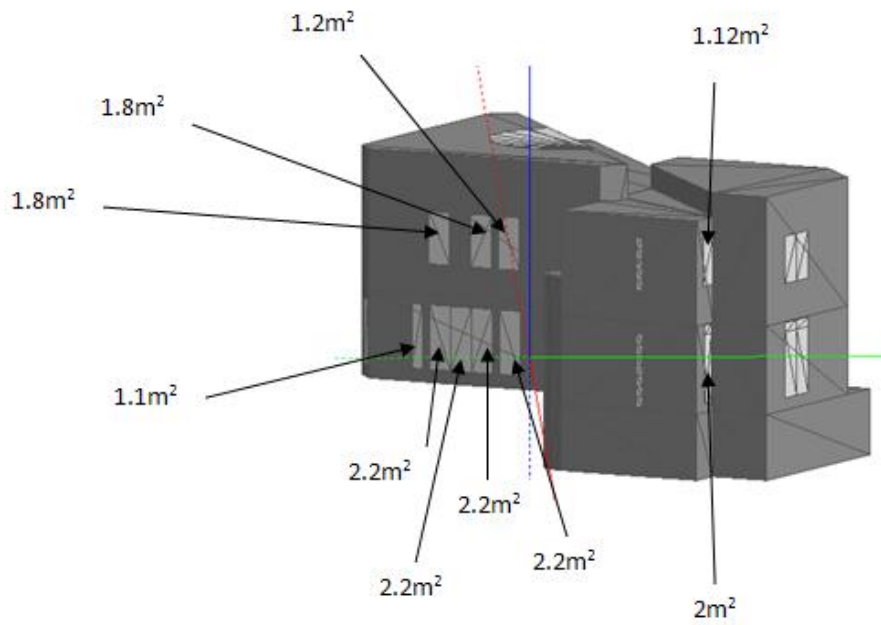
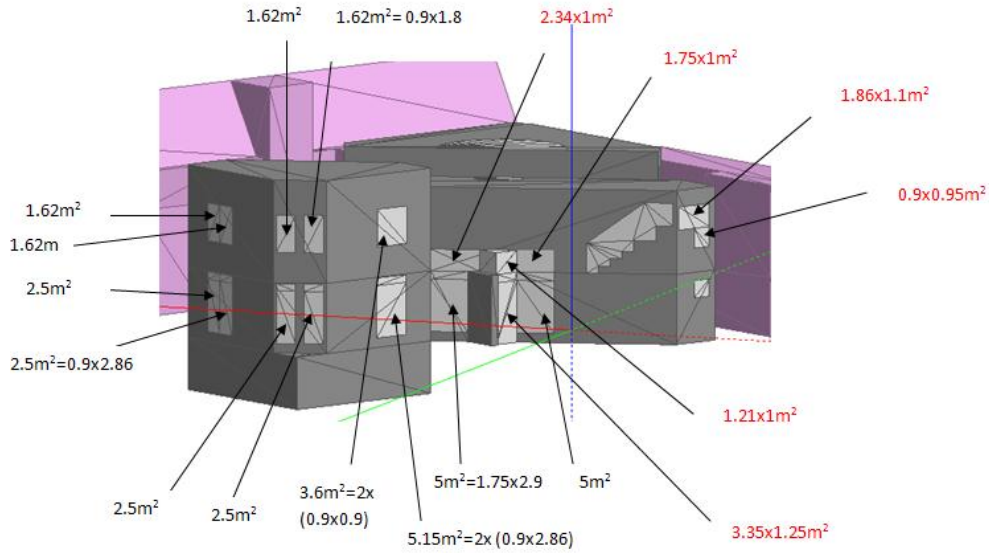


Figure 2.26: Left side view (glass surface: 17.8m<sup>2</sup>).



on other sides of the building contain shading devices and their dimensions can be seen in *Figure 2.30* and *Figure 2.31*.

An automatic system is planned to be used for the raising and lowering the blinds and also for changing the angle of the slats, as part of the renovation activities to be undertaken.



*Figure 2.29: Dimensions of windows with blinds (black color) and of windows without shading devices (red color)- façade view.*

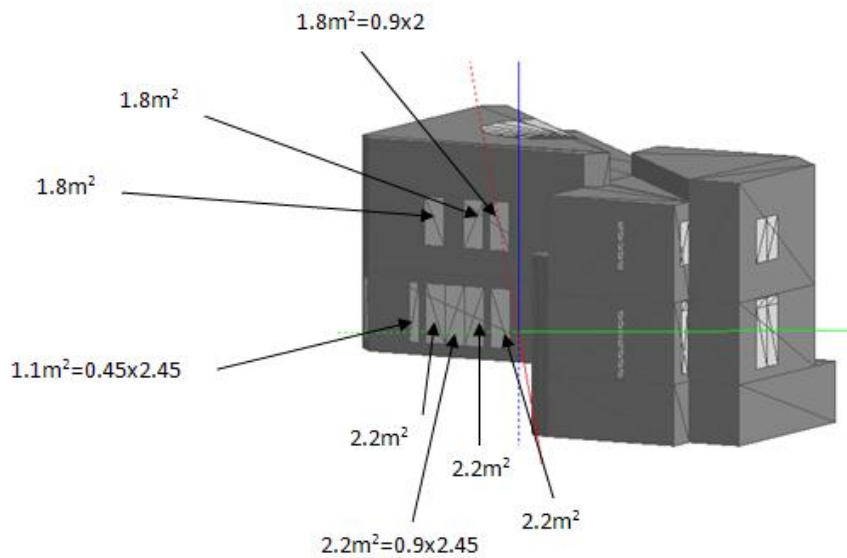


*Figure 2.30: Dimensions of windows with blinds-left side view.*

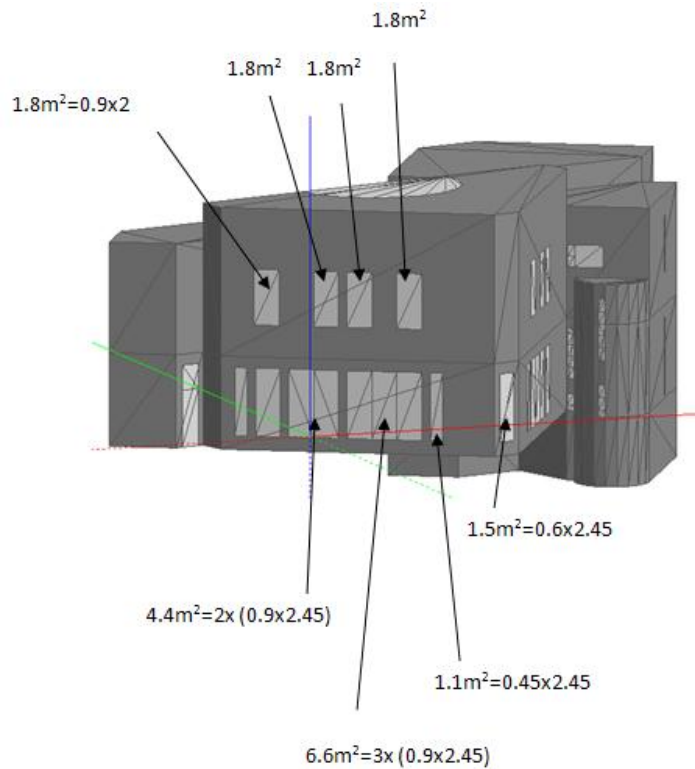
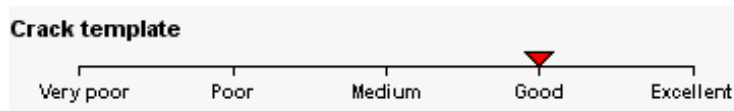


Figure 2.31: Dimensions of windows with blinds-right side view.

### 2.1.6 Ventilation and Infiltration

The natural ventilation and infiltration calculations are based on window openings, cracks, buoyancy, and wind driven pressure differences. Heat gains due to infiltration can be significant and for this reason a detailed modeling of the infiltration was performed using EnergyPlus. To calculate infiltration data concerning the airtightness of the building a crack template from Design Builder was used (that is created based on standards recommendations). In this case, airtightness is defined by a position on a five point scale:



The five settings correspond to the five crack templates. According to this type of modeling every surface in the model has a crack and its size (characterized by flow coefficient and exponent) is determined. The value of Airtightness is used as a key to look up corresponding crack sizes in the Cracks database. The cracks database has been set up empirically to give typical air change rates for each of the five Airtightness categories in a range of building types.

The ventilation rate ( $q$ ) through each opening and crack in the model is calculated based on the pressure difference using wind and stack pressure effects (12) according to the following formula:

$$q=C(\Delta P)^n$$

Where  $q$  is the volumetric flow through the opening,  $\Delta P$  is the pressure difference across the opening/crack,  $n$  is the flow exponent varying between 0.5 for fully turbulent flow and 1.0 for

fully laminar flow,  $C$  is the flow coefficient, characterizing the size of the opening/crack. The air mass flow coefficient specifies the properties of airflow through a crack and it is defined for a 1 Pa pressure difference across the crack. Reference conditions under which the air mass flow coefficient was determined were:

- Temperature: 20°C
- Barometric Pressure: 101320 Pa
- Humidity ratio: 0.005 kg/kg

An assumption of “medium” airtightness for TUC building was made based on its construction and its exposure to winds. The library of DesignBuilder provides information concerning the air mass flow coefficient and air mass flow exponent depending on the crack template. For a “medium” crack template the exported data can be seen in *Table 2.9*.

Air mass	windows		doors		walls		Floors		roof
	Ext.	Int.	Ext.	Int.	Ext.	Int.	Ext.	Int.	
Flow coefficient	0.0001	0.0001	0.0001	0.0	0.000	0.00	0.000	0.000	0.000
(kg/s)	4	4	4	2	1	3	7	9	1
Flow exponent	0.65	0.65	0.65	0.6	0.7	0.75	1	0.7	0.7

*Table 2.9: Airtightness data for a “medium” crack template (12).*

Concerning wind-driven ventilation, whenever wind impinges on the surface of a rectangular building, a positive pressure is induced on the upwind face. The flow separates at the corners resulting in negative pressure regions on the side of the building and a negative pressure distribution on the leeward facade. The pressure distribution on the roof varies according to pitch - the pressure on the upwind face being negative for roof pitches of 30° and positive for steeper pitches. The pressure on any point on the surface of a building facade can be comprehensibly estimated using (12)

$$P_w = 0.5 C_p \rho u_z^2$$

Where  $P_w$  is the surface pressure due to wind,  $\rho$  is the density of air,  $C_p$  is the wind pressure coefficient at a given position on the surface, and  $u_z$  is the mean wind velocity at height  $z$ .

The wind pressure coefficient,  $C_p$ , is a function of wind direction, position on the building surface and side exposure. Some typical approximate values for buildings subjected to varying degrees of shelter and wind directions is given in an AIVC publication A guide to energy-efficient ventilation. This data is also quoted in the CIBSE A Guide. DesignBuilder uses this data to populate the pressure coefficients templates and provide default pressure coefficients suitable for use in basic design calculations for buildings having no more than three stories. The  $C_p$  data are applicable for buildings of 3 stories or less, with square surfaces and for 3 levels of site exposure (the data is given in 45° increments).

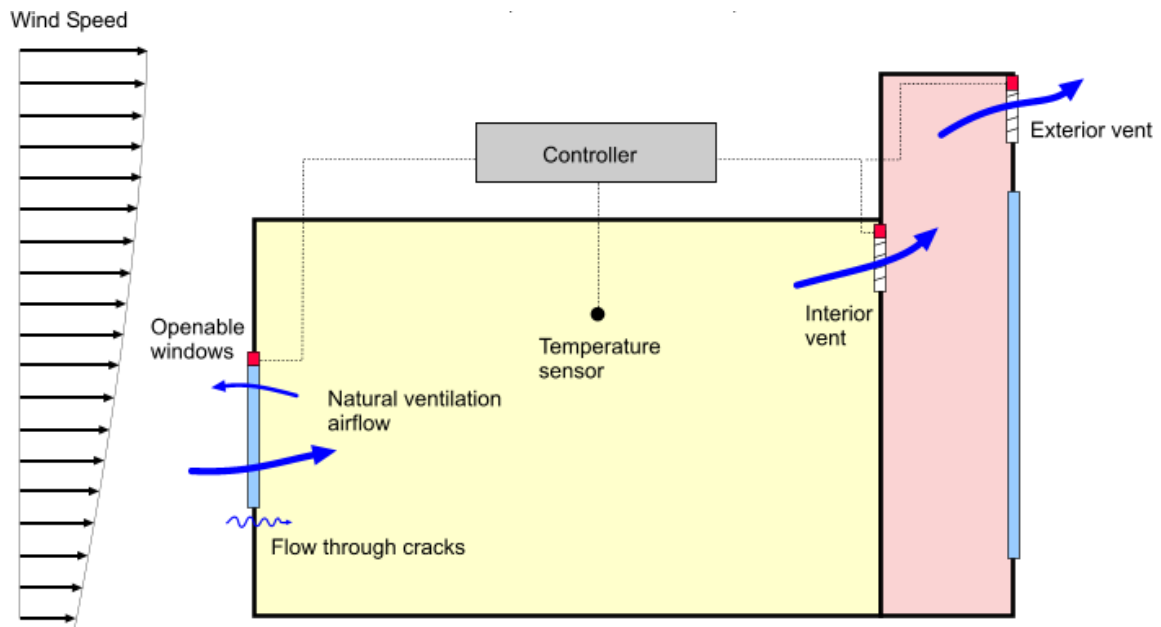


Figure 2.32: Modeling of Calculated Natural Ventilation flow and control in EnergyPlus.

EnergyPlus AirflowNetwork model provides the ability to simulate the performance of an air distribution system, including supply and return leaks, and calculate multizone airflows driven by outdoor wind and forced air during HVAC system operation. The model is used to simulate thermal conduction and air leakage losses. Pressure at each node and airflow through each linkage (given wind pressures and forced airflows) are determined through pressure and airflow calculations. Given zone air temperatures and zone humidity ratios, the model then calculates node temperatures and humidity ratios. Using these node temperatures and humidity ratios, the sensible and latent loads from duct system conduction and leakage are summed for each zone. These sensible and latent loads are then used in the zone energy balance equations to predict HVAC system loads and to calculate the final zone air temperatures, humidity ratios and pressures.

Table 2.10 depicts the calculated values of (air changes per hour) ACH as a sum of infiltration and natural ventilation of each zone for the specific building.

Zone	Surface (m <sup>2</sup> )	ACH
Office 1	21.89	0.34
Office 2	10.5	0.81
Office 3	13.58	0.76
Office 4	23.26	0.89
Office 5,6	17.8	1.05
Office 8	16.9	0.21
Office 9	15.19	0.28
Office 10	13.58	0.39
Office 11	23.8	0.43
Office 12 (equipment room)	7.9	0.48

Office 13	14.9	0.59
WC	5.079	1.05

*Table 2.10: Natural ventilation and infiltration values.*

These data are average values obtained for an annual simulation period. Detailed infiltration data are calculated at each time step of the simulation. As can be seen there are rather sizable infiltration, and the building geometry enters indirectly through the values of the pressure coefficients. External CFD calculations can be used to more carefully ascertain the infiltration gains and particularize the pressure coefficients to the building.

### 2.1.7 HVAC system

The heating system of the building is a central system with an oil boiler and hot water radiators in each zone. The efficiency of the boiler is estimated at 0.8. The thermal bodies are depicted in *Figure 2.33*. The technical characteristics of the radiators such as dimensions, capacity can be seen in *Table 2.11*.

During winter the heating system is available according to the work time schedule. The thermal heat pump is activated only when the capacity of the radiators is not sufficient to reach the desired (set) temperature level within a zone. That means that whenever the employees do not feel comfortable, they are turning on the split-type unit even if the radiators are heating the zone.

The cooling of the zone is again available according to the work time schedule during the summer period. This is an ideal usage pattern in which the building occupants turn on the A/C units when they are in the building and switch them on when they leave from their offices. Obviously deviations exist from this “ideal” use case that is very hard to *a priori* ascertain.

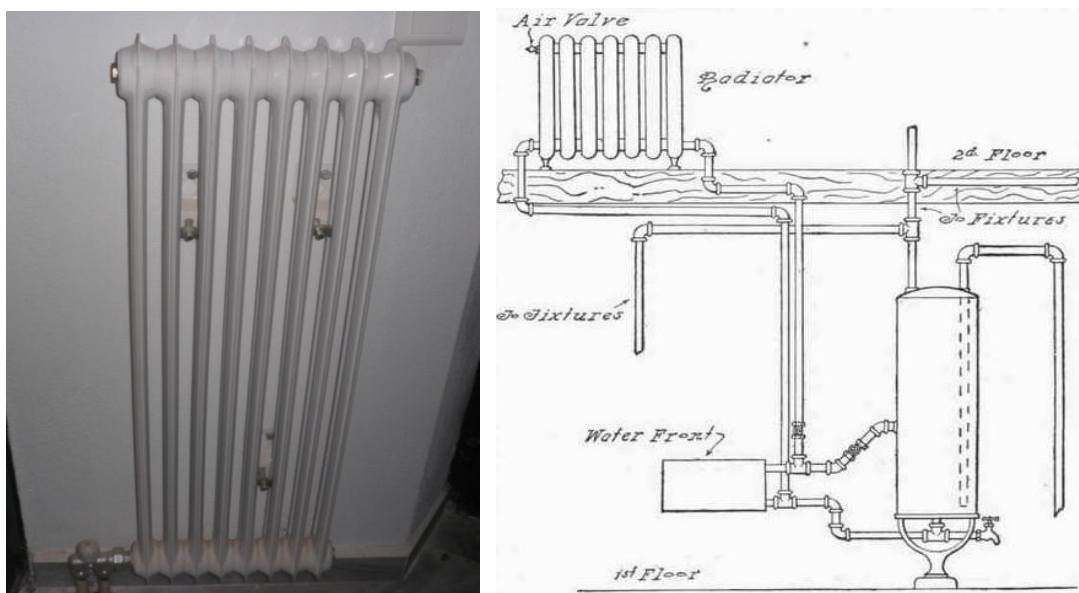
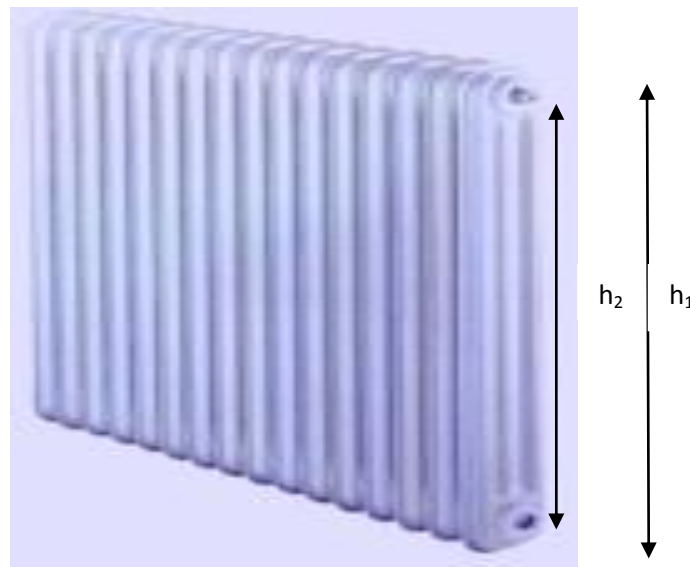


*Figure 2.33: The heating circulation system.*



Zone	Slices	Columns	Length (mm)	$h_2$ (mm)	$h_1$ (mm)	Capacity (kW)
Office 1	10	3	380	905	995	1.51
Office 2	10	3	380	905	995	1.51
Office 3	10	3	380	905	995	1.51
Office 4	10	3	380	905	995	1.51
Office 5-6	18	3	684	905	995	2.72
Office 8	10	3	380	905	995	1.51
Office 9	10	3	380	905	995	1.51
Office 10	10	3	380	905	995	1.51
Office 11	10	3	380	505	595	0.93
Office 11	10	3	380	905	995	1.51
Office 13	12	4	456	905	995	2.37
WC	10	2	380	905	995	1.04
Corridor 1a	10	3	380	905	995	1.51
Corridor 1a	22	2	836	905	995	2.3
Corridor 2a	10	3	380	905	995	1.51
Corridor 2a	24	2	912	905	995	2.51
Corridor 2b	14	2	532	355	445	0.89
Corridor 1b	8	3	304	905	995	1.2

*Table 2.11: Technical characteristics of the radiators.*

The oil boiler serves three buildings. The connection between the central boiler and the building is achieved through underground pipes in two central points (see *Figure 2.34*, red arrows) and then from these points hot water is distributed from the pipes to the radiators of each zone. Due to the fact that the building does not own the boiler, no thermostat can act on its operation which means that the availability schedule of the boiler is controlled by one person in charge who decides whether the heating should be on and for how long. For the moment, an availability schedule of the HVAC system was inserted to the model according to the working time schedule of the occupants which more or less gives us a good estimation on



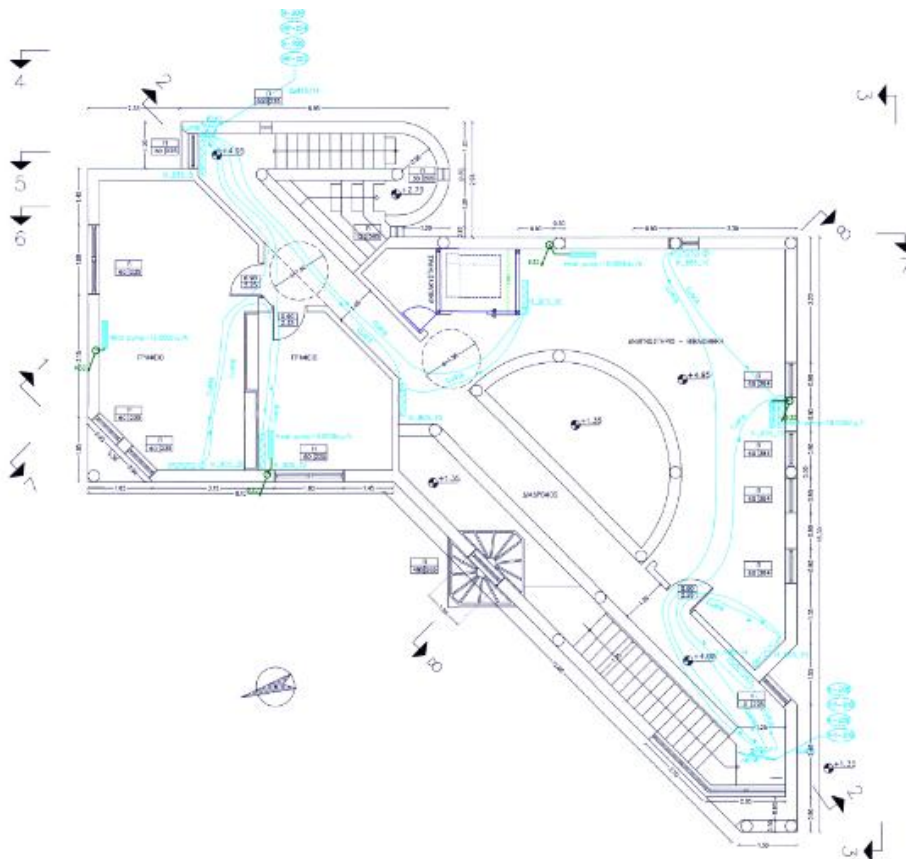


Figure 2.35: First-floor plan of the heating circulation system.

The cooling of the building is achieved by split units. The EER, COP and the capacity of the system vary depending of the model of the split unit. The type and characteristics of each split unit are shown in *Table 2.12*.

Zone	Split unit type	Cooling characteristics			Heating characteristics		
		EER	Cooling capacity (kW)	Rated air flow rate (m <sup>3</sup> /s)	COP	Heating capacity (kW)	Rated air flow rate (m <sup>3</sup> /s)
Office 1	Haier HSU-09 HC03/R2	3.82	2.6	0.153	3.66	3.45	0.153
Office 2	MITSUBISHI MSH-AXV12WV	2.41	3.5	0.131	3.03	4	0.141
Office 3	MITSUBISHI MSH-AXV12WV	2.41	3.5	0.131	3.03	4	0.141
Office 4	MITSUBISHI GA50VB	2.81	5	0.178	3.23	5.3	0.178
Office 5-6	MITSUBISHI MCFH-A24WV	2.45	6	0.206	2.5	6.8	0.206
Office 8	Haier HSU-09 HC03/R2	3.82	2.6	0.153	3.66	3.45	0.153
Office 9	MITSUBISHI MSH-	2.41	3.5	0.131	3.03	4	0.141

	AXV12WV						
Office 10	MITSUBISHI	2.41	3.5	0.131	3.03	4	0.141
	MSH-AXV12WV						
Office 11	MITSUBISHI	2.81	5	0.178	3.23	5.3	0.178
	GA50VB						
Office 13	MITSUBISHI	2.81	5	0.178	3.23	5.3	0.178
	GA50VB						

Table 2.12: Technical characteristics of the cooling system of each zone.

The modeling of the split type units in EnergyPlus was achieved by modeling a Packaged Terminal Heat Pump (PTHP) taking into account some assumptions such as:

- 1) The air that is drawn into the split unit is drawn through a node that belongs to the inside of the zone. No outside air is introduced to the unit.
- 2) The supplemental heating coil was modeled using an availability schedule that doesn't permit its function. In reality such a coil doesn't exist but it is necessary to be modeled using the PTHP in EnergyPlus.
- 3) Both heating and cooling coils were modeled as single speed direct expansion coils with all the characteristics that appear in Table 2.12.
- 4) The fan that was modeled is an "On-Off Fan".

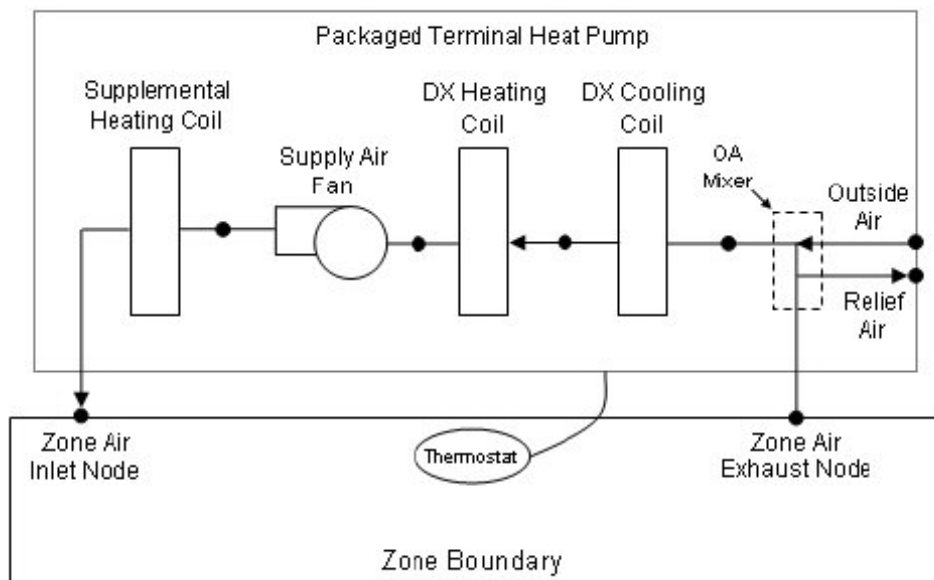


Figure 2.36: Modeling split unit type air conditioners in EnergyPlus.

Apart from the split units of each office, there is another air conditioning system (FYROGENIS) situated near the entrance that is only used in extreme weather conditions with heating capacity 15.95kW and cooling capacity 15.7kW.

### 2.1.8 Internal Gains

The working days are Monday till Friday except from Christmas break, Easter break summer break and some local holidays. The building is occupied, during working days, from 08:00 to 15:00.

Zone	Surface (m <sup>2</sup> )	Employees	Density (people/m <sup>2</sup> )
Office 1	21.89	1	0.04
Office 2	10.5	1	0.09
Office 3	13.58	1	0.07
Office 4	23.26	1	0.04
Office 5,6	17.8	2	0.11
Office 8	16.9	1	0.06
Office 9	15.19	1	0.06
Office 10	13.58	1	0.07
Office 11	23.8	1	0.04
Office 12 (equipment room)	7.9	-	0.01
Office 13	14.9	1	0.07
WC	5.079	-	0.01

Table 2.13: Density of people in each zone of the building.

Holidays	2009	2010	2011	2012
Christmas	23/12-6/1	23/12-6/1	23/12-6/1	23/12-6/1
Easter	16/4-22/4	1/4-7/4	21/4-27/4	12/4-18/4
National holiday	28/10	28/10	28/10	28/10
National holiday	25/3	25/3	25/3	25/3
National holiday	17/11	17/11	17/11	17/11
Labor day	1/5	1/5	1/5	1/5
Local holiday	21/11	21/11	21/11	21/11
Lent Monday	2/3	15/2	7/3	27/2
Holy spirit Monday	8/6	24/5	13/6	4/6
Summer holidays	9/8-15/8	9/8-15/8	9/8-15/8	9/8-15/8

Table 2.14: Holidays schedule.

Artificial lights are located in each office providing sufficient lighting when natural cannot reach the desirable lux levels (500lux for offices). The type of lighting tubes is TL-D 36 fluorescent of 25mm diameter and 1.5m length. The power per tube is 36 Watt and the voltage 230V. There is also a smaller type of lighting tubes TL-D 18 placed in the corridor of the ground and first floor, 4 tubes in each zone. The luminaire type is surface mount with radiant fraction of 0.72 and visible fraction 0.18 (13). The number of lighting tubes and their efficiency can be seen in Table 2.15. The lighting system is controlled according to the day lighting luminance on the working plane and according to the working time schedule.

Zone	Surface (m <sup>2</sup> )	Lighting tubes	Total power demand (W)	W/m <sup>2</sup>
------	---------------------------	----------------	------------------------	------------------

Zone	Surface (m <sup>2</sup> )	Number of Lights	Power (W)	Power Density (W/m <sup>2</sup> )
Ground floor-corridor	91.85	6+4	288	3.13
1 <sup>st</sup> floor-corridor	49	6+4	288	5.87
WC	5.079	1	36	7.08
Office 1	21.89	4	144	6.57
Office 2	10.5	4	144	13.7
Office 3	13.58	8	288	21.2
Office 4	23.26	8	288	12.38
Office 5,6	17.8	10	360	20.2
Office 8	16.9	4	144	8.52
Office 9	15.19	4	144	9.48
Office 10	13.58	8	288	21.2
Office 11	23.8	14	504	21.17
Office 12 (equipment room)	7.9	2	72	9.11
Office 13	14.9	6	216	14.5

Table 2.15: Artificial lights in each zone.



Figure 2.37: The lighting system.

The internal gains due to the operation of office equipment and computers can be seen in the following table. It is assumed that computers are operating during the work-time schedule except the one positioned in office 11 that is always on according to information provided by the user, the rest are off when the building is closed. Concerning office equipment such as printers, it is assumed that they are always in sleep mode because of the small frequency of operation.

Zone	Surface (m <sup>2</sup> )	Office Equipment	Computer Gains (W/m <sup>2</sup> )	Equipment Gains (W/m <sup>2</sup> )
Office 1	21.89	1 PC (100 Watt)	4.57	-
Office 2	10.5	1 PC (100 Watt), 1 printer (15 Watt, sleep mode)	9.52	1.42
Office 3	13.58	1 PC (100 Watt), 1 printer (15 Watt, sleep mode)	7.36	1.1
Office 4	23.26	1 PC (100 Watt), 1 printer (15 Watt, sleep mode)	4.3	0.64

		printer (15 Watt, sleep mode)		
Office 5,6	17.8	2 PC (200 Watt)	11.23	-
Office 8	16.9	1 PC (100 Watt), 1 printer (15 Watt, sleep mode)	5.9	0.88
Office 9	15.19	1 PC (100 Watt), 1 printer (15 Watt, sleep mode)	6.58	0.94
Office 10	13.58	1 PC (100 Watt)	7.36	-
Office 11	23.8	1 PC (100 Watt)	4.2	-
Office 12 (equipment room)	7.9	1 plotter (HP designjet 800ps- 15 Watt sleeping mode, 150 Watt max), OKI C7300 (45 Watt sleep mode), Samsung SF-560 R (12 Watt, sleep mode), refrigerator Goldstar GR-1410 GS (30 Watt)	-	22.4
Office 13	14.9	1 PC (100 Watt)	6.7	-

*Table 2.16: Office equipment and internal gains.*

In addition, human activity in the building (light office work) gives a metabolic rate of 65W/m<sup>2</sup> (14).

## 2.2 Simulation results analysis

All the above information was integrated to generate the thermal model for the building. According to EnergyPlus simulation results the building's total annual energy consumption in primary energy per conditioned area is approximately 126kWh/m<sup>2</sup>/yr. The electric consumption of the cooling system is nearly 27% while the energy consumption for heating is around 22% (baseboard+ DX heating). During summer months the temperature is quite high and differs a lot from the comfort one. Concerning the construction of the building and the presence of the atrium, big amounts of heat are stored inside which causes the rising of the inside temperature. The amount of energy consumption is typical for buildings in Greece as the heating needs in Crete are generally less than the ones in northern Greece or northern Europe. Moreover the building is operating 6-7 hours per day, five days per week. Concerning the lighting energy consumption, EnergyPlus through "Daylight control" allows the operation of the lighting system whenever the natural light does not reach the comfort one which is 500lux for office buildings. In reality the consumption is much less due to the users' habits.

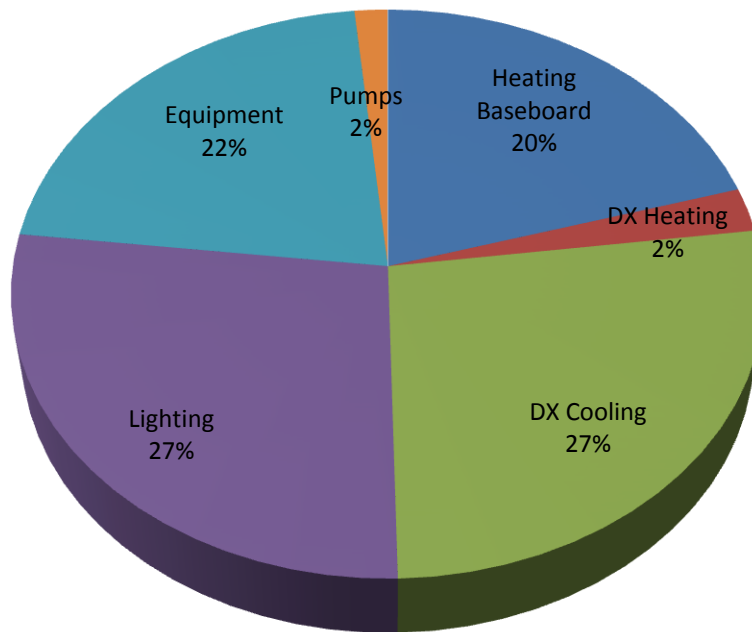


*Figure 2.38: Simulated energy consumption.*

The first step to validate the model is to compare the simulated inside temperatures with actual measurements that took place in the building during a heating period from 10<sup>th</sup> of December until 30<sup>th</sup>. The building from 23<sup>rd</sup> until 27<sup>th</sup> was not operating due to Christmas holidays. The measured data were exported from two temperature sensors installed in the south side of the building (office 11) and in the north side (office 10). The following two figures depict the simulation results vs. the measured values in the offices during December including Christmas holidays when the building was not operating. The weather file that was used in EnergyPlus contained actual data of the period taken from the weather station installed at the terrace of the building.

In *Figure 2.39* for office 11 the maximum temperature difference when the building is closed (23/12 until 27/12) is 1.16°C, the minimum 0.16°C and the average 0.6°C which reveals a quite good accordance of the two curves. Observing the curve with the simulated values it appears that the inside temperature of the office whenever it is occupied is 22°C which is set as the comfort level while measured values reveal that the temperature could be under 20°C and the user is not turning on the split type unit for heating. In office 10 (*Figure 2.40*), the maximum difference between the measured and the simulated values is 0.96°C while the minimum is 0.005°C and the average 0.5°C. As it occurs in office 11, during holiday period the two curves in office 10 seem to agree enough as their average difference is acceptable. For the rest of the period it is quite difficult to predict the user's behavior as this might vary concerning the comfort conditions, the working hours and the absence of information concerning the operation of the central heating system. Further simulation scenarios concerning the validation of the model are planned in the near future.

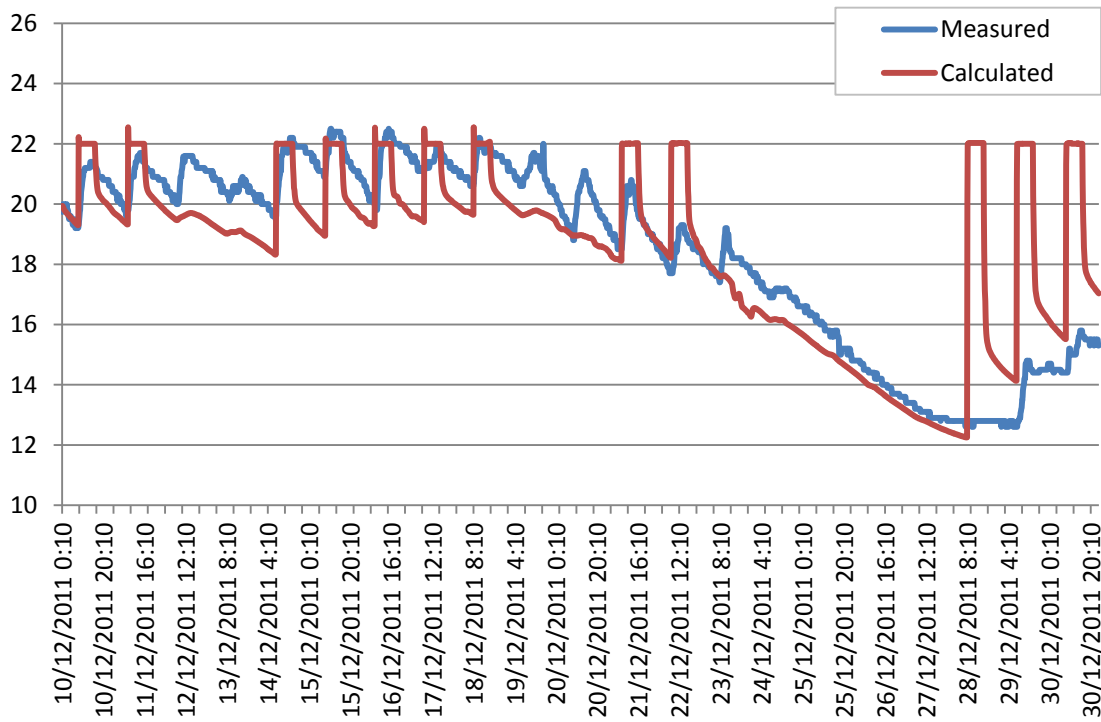


Figure 2.39: Comparison of simulated inside temperatures and measured inside temperatures for office 11 during December 2012.

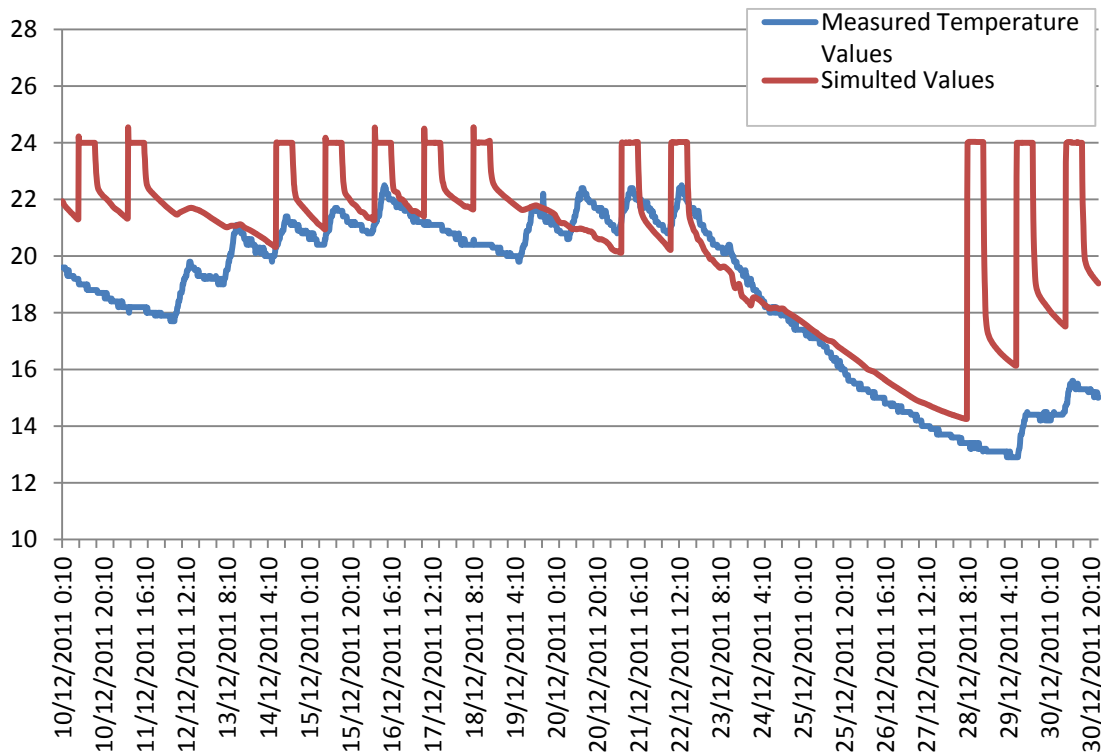


Figure 2.40: Comparison of simulated inside temperatures and measured inside temperatures for office 10 during December 2012.

The results in the following tables and figures are annual results from the simulation in EnergyPlus. The aim of the simulation was to compute annual consumption values for the

building and to estimate energy performance. According to the weather file used for the annual simulation, the buildings' heating and cooling energy demands are calculated based on weather conditions of the 26<sup>th</sup> of December and 6<sup>th</sup> of August where the peak values of temperature occurred. On 27<sup>th</sup> of December the minimum dry-bulb temperature was 2°C while on 5<sup>th</sup> of August the maximum dry-bulb temperature was 37.2°C. The system sizing calculation was based on the heating and cooling setpoint temperatures set. In order to meet comfort conditions the heating setpoint temperature was set to 22°C and the cooling setpoint temperature to 26°C. Thus, the ideal heating system is designed to cover around 20°C which is the temperature difference between the heating setpoint temperature and the outside dry-bulb temperature while the ideal cooling system is designed to cover a temperature difference of 11°C. The heating and cooling energy demands can be seen in *Table 2.17*.

	Energy Demands (Watt)	Energy Demands/Conditioned Floor Area (W/m <sup>2</sup> )
Heating	15686	63.7
Cooling	6737	40.5

*Table 2.17: Heating and cooling energy demands.*

The total energy consumption presented in *Table 2.18* is calculated based on the heating, cooling and lighting characteristics of the actual HVAC and lighting system of the building and the total power of the offices equipment that was set for the calculations. The primary energy consumption result is the annual energy consumption multiplied with the conversion factors of *Table 2.19*.

	Annual Consumption (kWh/yr)	Primary energy consumption (kWh/yr)	Primary Energy Consumption/Conditioned Floor Area kWh/m <sup>2</sup> /yr
Heating Baseboard	5784.1	6362.5	25.85
DX Heating Coil	265	768.5	3.12
DX Cooling Coil	1931.2	5600.5	33.66
Lighting	2915.1	8453.8	34.33
Equipment	2313.5	6709.15	27.25
Pumps	167.6	486.04	1.97
Total	13376.55	28380.5	126.18
Total in kWh/m <sup>2</sup> /yr	31.37	66.55	126.18

*Table 2.18: Annual energy consumption converted to primary energy.*

Fossil fuel	Conversion factor for primary energy	CO <sub>2</sub> emissions (kgCO <sub>2</sub> /kWh)
Natural Gas	1.05	0.196
Oil	1.1	0.264
Electric	2.9	0.989

Energy	
Biomass	1

Table 2.19: Conversion factors of energy consumption to primary energy (15; 16).

Figure 2.41 depicts the monthly HVAC energy consumption. The heating of the building is achieved primarily by the radiators and secondly by the heat pump. During April and May the building has no heating needs and the central heating system is not operating while for the rest of the winter months the heating pump supplements the central heating system. The warmest months in Chania are July and August comparing to June and September. The annual electricity consumption of the cooling system is less from the one of the heating system. This is due to the fact that the heated area of the building contains the central corridors of the building while the cooling area comprises only the offices.

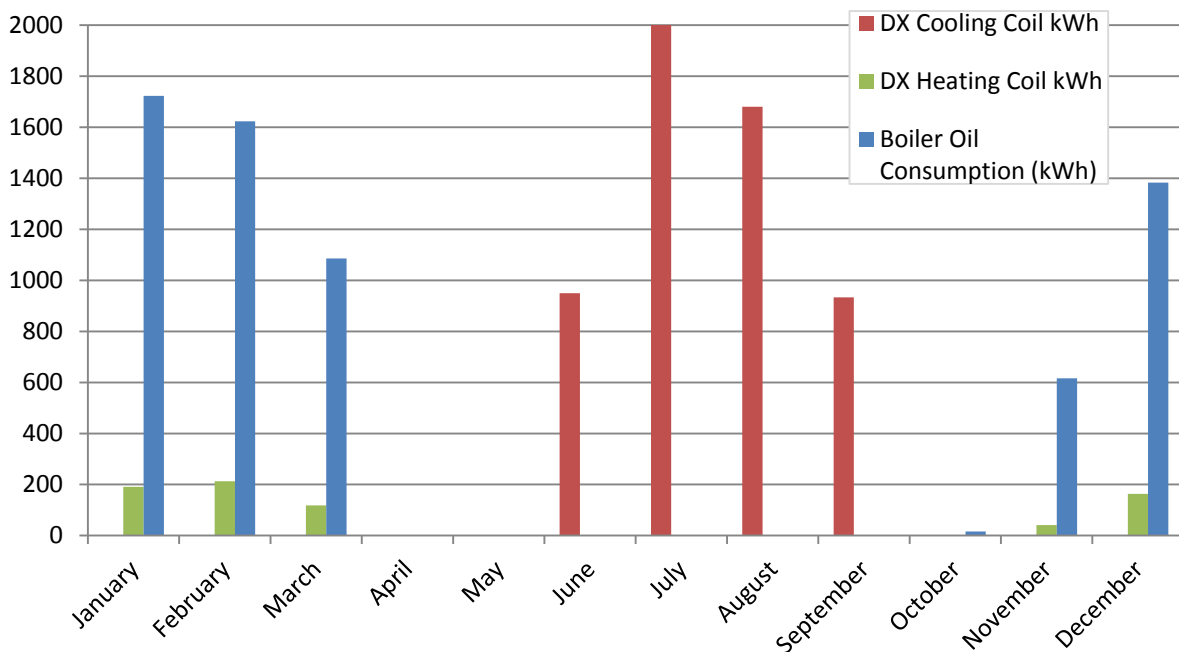


Figure 2.41: Monthly HVAC primary energy consumption.

	Lighting consumption (kWh/yr)	Computers and office equipment consumption (kWh/yr)	DX Heating consumption (kWh/yr)	DX Cooling consumption (kWh/yr)
Office 1	310,3	559,7	46,4	220,4
Office 2	368,3	643,8	14,5	292,9
Office 3	783	643,8	60,9	371,2
Office 4	493	643,8	60,9	858,4
Office 5-6	849,7	559,7	20,3	542,3
Office 8	374,1	643,8	98,6	319
Office 9	522	643,8	78,3	449,5
Office 10	1397,8	559,7	249,4	597,4
Office 11	1160	559,7	87	1305
Office 13	609	559,7	8,7	635,1
Equipmen	368,3	672,8	0.00	0.00

t room				
WC	200,1	0.00	0.00	0.00
First floor-corridor	484,3	0.00	0.00	0.00
Ground floor-corridor	513,3	0.00	0.00	0.00
Stairs	0.00	0.00	0.00	0.00

Table 2.20: Annual primary energy consumption in each zone.

Figure 2.42 depicts the function of lighting control modeled in EnergyPlus. Whenever the natural lighting level does not reach the desirable levels, artificial lights are (4) on. The desirable lighting level for office buildings is set to 500 lux (14).

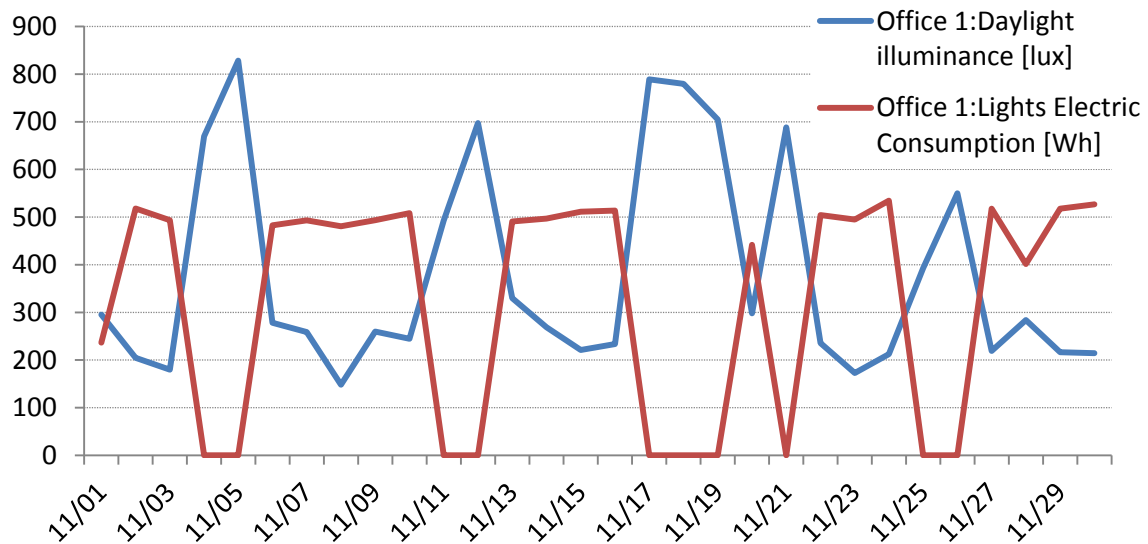
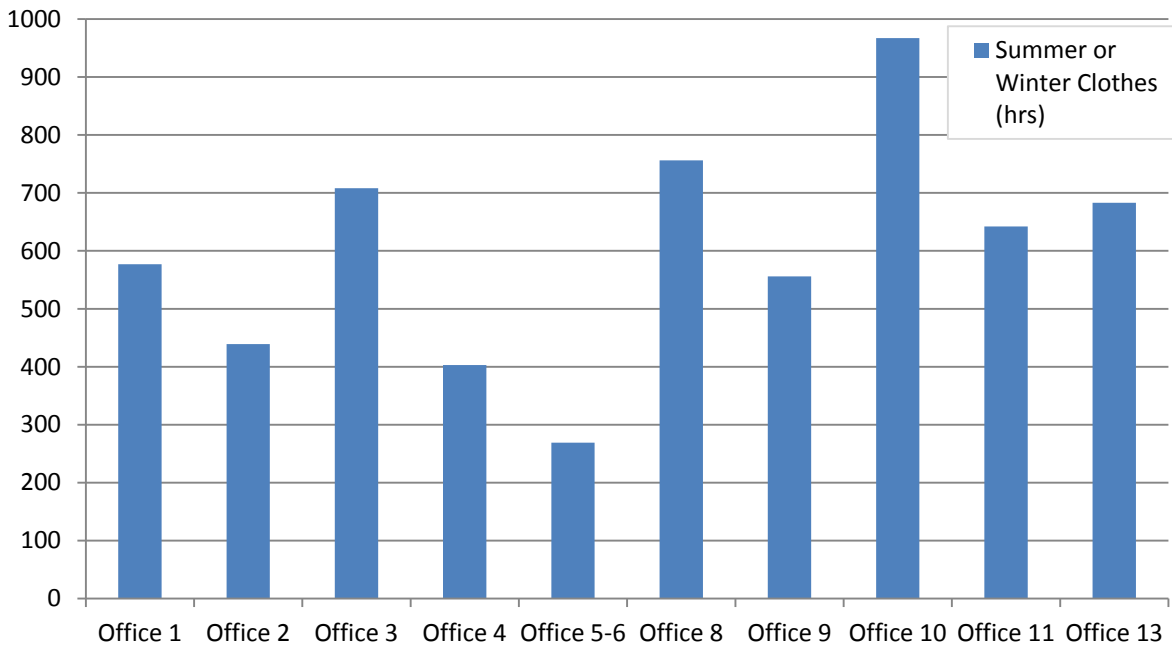


Figure 2.42: Comparison of natural lighting level and lighting electric consumption in Office 1 during November

Figure 2.43 presents the total discomfort hours based on ASHRAE 55-2004 for each of the conditioned zone of the building. The calculation of discomfort hours was based upon the weighted average:

$$\frac{\sum \text{floor area} * \text{discomfort hrs}}{\sum \text{floor area}}$$



*Figure 2.43: Time not comfortable based on ASHRAE 55-2004.*

The presence of the skylight affects a great deal the comfort conditions of the offices around it, especially during summer. The internal partitions of these offices are made by gypsum plasterboard and thus the thermal gains due to solar radiation are causing an augmented temperature rise.

In the next paragraph, CFD calculations will further illustrate and evaluate the efficiency of the heating and cooling system and derive conclusions upon thermal comfort of building occupants. The EnergyPlus simulation results concerning the surface temperatures of each thermal zone will be used in the next section as boundary conditions in order to conduct internal CFD airflow analysis.

### **3. CFD external/internal airflow analysis in the TUC building**

The scope of the application of a DesignBuilder CFD external and internal airflow analysis in the Technical Services building is to gain information upon air velocities, pressures and temperatures not only for the building as a whole but also for specific parts of the building, internal and external. The calculation of these parameters take into account specified boundary conditions such as surface temperatures, weather conditions from the imported to the program weather file, internal gains from human activity, equipment, lights and the HVAC system of the building.

In order to calculate the dependent variables (temperature, velocity, pressure etc.) in the partial differential equations, a Finite Volume grid was used together with the k-e turbulence model. The chosen relaxation method uses false time steps to replace time steps in transient terms of the equations. In regard to the boundary conditions, an EnergyPlus simulation run was used to import boundary surface temperatures into the CFD model.

Apart from the external CFD analysis, various internal analysis are conducted for summer and winter weather conditions in order to evaluate the efficiency of the HVAC system both for cooling and for heating the building and therefore derive information upon thermal comfort of occupants.

#### **3.1 Introduction to CFD**

CFD-Computational Fluid Dynamics is a method of predicting the movement of the air and its characteristics such as velocity, temperature, pressure, age of air, both in the inside environment of a building (internal CFD analysis) and in the outdoor (external CFD analysis) (17; 18).

Through an internal CFD analysis, information on thermal comfort of occupants and on the distribution of air velocity, pressure and temperature can be gained, within any predefined volume of the building. In addition it provides information on the age of the internal air. The results of an internal CFD analysis are actually not only a prediction of the field of the airflow but also of the heat transfer, consequently the use of CFD is considered quite a useful study for the appropriate design of any HVAC system determining the outdoor air intakes and exhausts. Being able to use an accurate weather file, one can study the introduction of outside air to the inside of the building through the position and the size of the openings and take advantage of the benefits of natural ventilation, cross ventilation and their effects to the energy consumption and thermal comfort of occupants. Concerning the thermal comfort of occupants, DesignBuilder CFD uses the Predicted Mean Vote (PMV) of the Fanger Comfort Model.

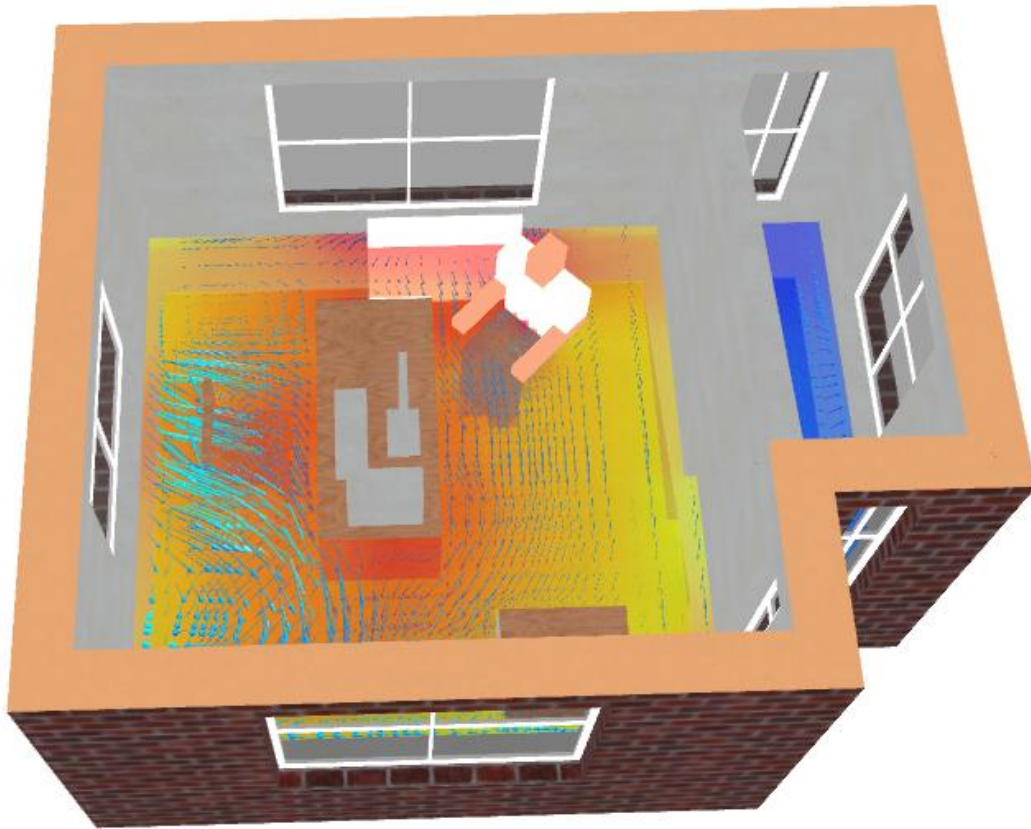


*Figure 3.1: Example of an internal CFD analysis*

Conducting an external CFD analysis, information concerning the distribution of air velocities and pressures caused by the effect of wind around the building envelope can be provided. This information can be used so as to obtain more accurate values about pressure coefficients for the calculation of natural ventilation conducted by EnergyPlus. Moreover, the significant effect of neighbor buildings that act as obstacles to the wind, designating its strength and direction, can be studied in order to understand better the microclimate around the building envelope.

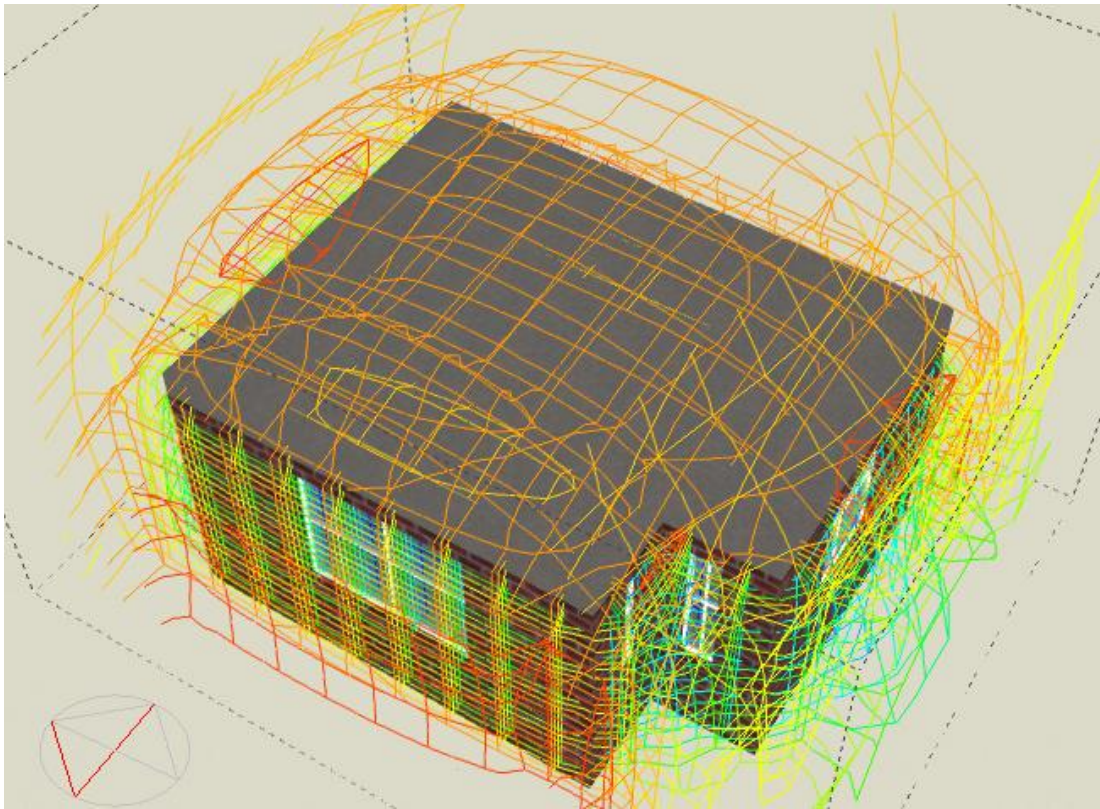


*Figure 3.2: Example of an external CFD analysis*

In the current study an internal/external CFD analysis will be conducted using DesignBuilder CFD tool. The general DesignBuilder CFD workflow is described by a flow chart depicted in *Figure 3.3*. In the following paragraphs the mathematical model that the chosen CFD tool is using will be promptly analyzed.

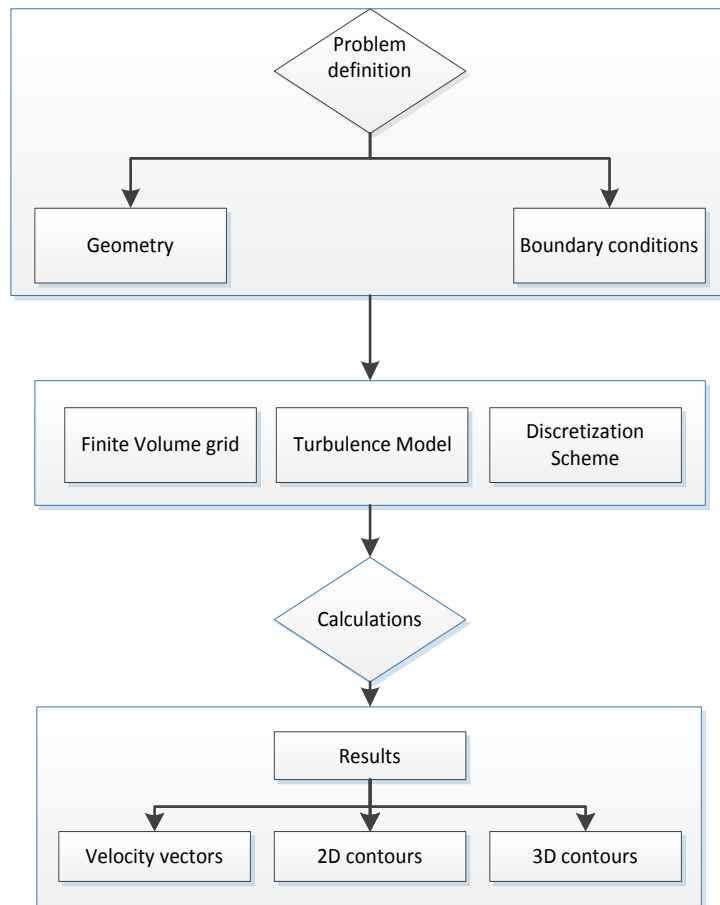


Figure 3.3: CFD workflow.

## 3.2 Mathematical Model

DesignBuilder CFD uses a finite volume method so as to solve a set of partial differential equations that represent the conservation of mass, the conservation of energy and the second law of Newton (momentum equation). The equation set comprises the three velocity component momentum equations, called Navier-Stokes equations, the energy equation using the k- $\epsilon$  turbulence model and equations for turbulence kinetic energy and the dissipation rate of turbulence kinetic energy (12).

### 3.2.1 CFD partial differential equations

Partial differential equations describe the variation of a dependent variable, such as temperature or velocity, with a number of independent variables, such as time and distance. The general vector-form of the non-linear, second order partial differential equation is:

$$\frac{\partial}{\partial t}(\rho\phi) + \text{div}(\rho u\phi) = \text{div}(\Gamma \text{grad}\phi) + S \quad (3.1)$$

Where  $\phi$  represents any dependent variable such as temperature, velocity, mass, turbulence kinetic energy,  $\Gamma$  is a diffusion coefficient and  $S$  is a source term.

The term  $\frac{\partial}{\partial t}(\rho\phi)$  represents the unsteady term of the rate of change of any dependent variable in the equation. The term  $\text{div}(\rho u\phi)$  represents convection. The term  $\text{div}(\Gamma \text{grad}\phi)$

represents diffusion and the S is a source term. Depending on which quantity  $\phi$  represents, the diffusion coefficient  $\Gamma$  and the source term S will have an appropriate meaning.

The flow field should also satisfy the continuity equation (mass conservation) which is (19):

$$\frac{\partial \rho}{\partial t} + \text{div}(\rho u) = 0 \quad (3.2)$$

The Cartesian-tensor form of equations (3.1) and (3.2) is:

$$\frac{\partial}{\partial t}(\rho \phi) + \frac{\partial}{\partial x_j}(\rho u_j \phi) = \frac{\partial}{\partial x_j}(\Gamma \frac{\partial \phi}{\partial x_j}) + S \quad (3.3)$$

$$\frac{\partial \rho}{\partial t} + \frac{\partial}{\partial x_j}(\rho u_j) = 0 \quad (3.4)$$

Where the index j takes values 1, 2, 3 of the three space coordinates.

By using the general form of the differential equation, it is intended to conform the unsteady term, the convection and the diffusion term to the standard form for any chosen dependent variable. Then the coefficient in the diffusion term of  $\text{grad}\phi$  takes the expression of  $\Gamma$  and the source term S comprises the remaining terms on the right-hand side of the equation.

The general form of the equation derived from the energy equation, the momentum equation and the turbulence-kinetic-energy equation.

### 3.2.1.1 Energy Equation

Taking into account acknowledgements such as a steady low velocity flow, negligible viscous dissipation and a constant pressure coefficient, the energy equation can be written as (19):

$$\text{div}(\rho u T) = \text{div}\left(\frac{k}{c} \text{grad}T\right) + \frac{S_h}{c} \quad (3.5)$$

Where h is the specific enthalpy ( $h=cT$ ), k is the thermal conductivity, T is the temperature,  $S_h$  is the volumetric heat generation rate, c is the constant-pressure specific heat and  $\text{div}(k \text{ grad}T)$  describes the heat transfer due to conduction within the fluid (Fourier law of conduction).

### 3.2.1.2 Momentum Equation

As for the momentum equation, its derivation was based in the Stokes theory that the relation between shear, normal stresses and deformations in an isotropic elastic solid body is identical with the relation between stresses and deformation rate of a moving fluid element. Thus the shear modulus can be replaced by the dynamic viscosity. According to Newtons' law for the viscosity, there is a connection between the shear stresses and deformations and by replacing the normal and shear stresses in the equations of fluid motion, the Navier Stokes equations derive (19):

$$\frac{\partial}{\partial t}(\rho u) + \text{div}(\rho v u) = \text{div}(\mu \text{grad}u) - \frac{\partial p}{\partial x} + B_x + V_x \quad (3.6)$$

Where  $u$  is the x-direction velocity,  $\mu$  is the dynamic viscosity,  $p$  is the pressure,  $B_x(=\rho g_x)$  is the body force per unit volume in the x-direction and  $V_x=\mu\Delta u$  and  $\text{div}(\mu\text{grad}u)$  represent the viscous terms.

### 3.2.1.3 The turbulence-kinetic-energy equation

In cases where the velocity of the fluid is small, hence the inertia forces are smaller than the viscosity forces, any perturbation that can appear in the fluid flow is dumped quite quickly due to the viscosity forces that act as fluid stabilizers. When the velocity values rises the viscosity forces are not able to control the perturbations thus the flow is considered transient with random perturbations which tend to augment as the velocity values augment too and reach a specific point where the flow is characterized as turbulent. In order to describe this behavior of the flow, the Turbulence-Kinetic-Energy equation is introduced (19):

$$\frac{\partial}{\partial t}(\rho k) + \text{div}(\rho uk) = \text{div}(\Gamma_k \text{grad}k) + G - \rho\varepsilon \quad (3.7)$$

Where  $k$  denotes the kinetic energy,  $\Gamma_k$  the diffusion coefficient for  $k$ ,  $G$  the rate of generation of turbulence energy,  $\varepsilon$  the kinematic rate of dissipation and  $G-\rho\varepsilon$  describes the net source term of the equation.

### 3.2.2 Finite Volume Discretization Method

Due to the fact that partial differential equations cannot be solved numerically because coefficients themselves can contain the same dependent variables that they are associated with, it is intended to obtain an approximate solution numerically using a *discretization method*. Discretization methods involve the approximation of the partial differential equations by a set of algebraic equations for the variables at some set of discrete locations in time and space. The most widely used methods are the Finite Volume method (FV), the Finite Difference method (FD) and the Finite Element method (FE) (19; 20).

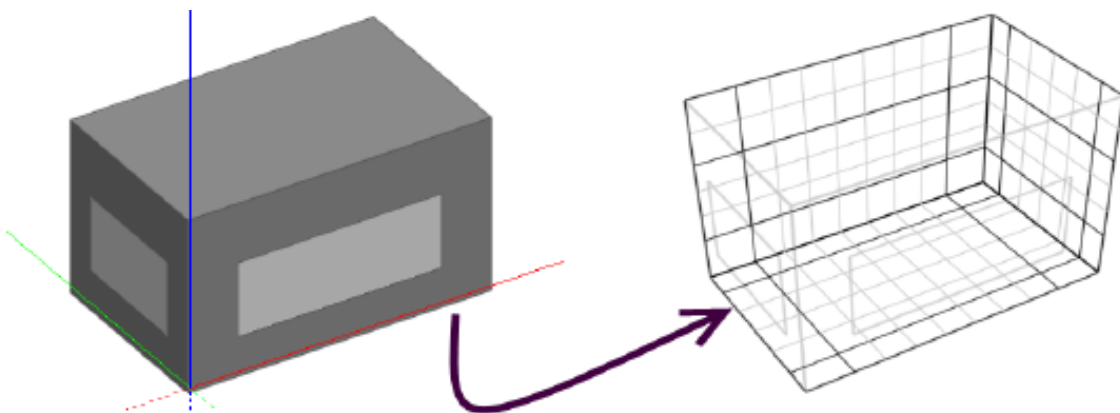
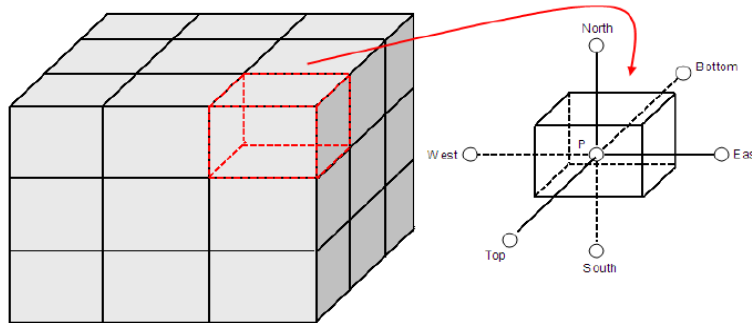


Figure 3.4: Building space divided into contiguous control volumes (Finite Volume Grid)

DesignBuilder CFD uses the Finite Volume Method (12), appropriate for any geometry including complex ones. Through the Finite Volume Method that DesignBuilder adopts, a finite volume grid is created that surrounds the building space or any domain that is analyzed. The domain is divided into a finite number of contiguous control volumes, cells. For each grid cell, the set of algebraic equations is solved by numerical methods. The center of each control

volume represents a computational node where the variables are calculated. *Figure 3.5* depicts the central node of a control volume and its neighbor points related to it.



*Figure 3.5: Depiction of Finite Volume Grid*

The continuous nature of the dependent variable  $\phi$ , represented by a curve in *Figure 3.6* is approximated by straight lines, linear relationships so that the equations will be solved easily. The variation of the dependent variable from the grid points and the neighbor ones is expressed by linear profiles.



*Figure 3.6: The continuous nature of the dependent variable  $\phi$  (19).*

As an example, the steady one dimensional heat conduction is considered, described by the equation (19):

$$\frac{d}{dx} \left( k \frac{dT}{dx} \right) + S = 0 \tag{3.8}$$

Where  $k$  is the thermal conductivity,  $T$  is the temperature and  $S$  is the rate of heat generation per unit volume.

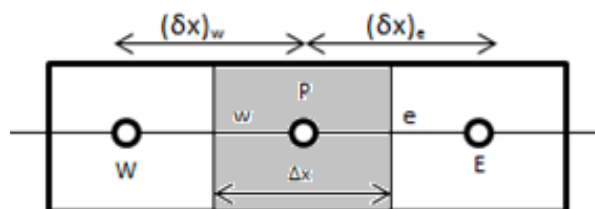


*Figure 3.7: One dimension finite volume grid.*

To apply discretization method, in order to calculate the dependent variable in  $P$  point of the grid, a control volume (in grey) is considered with dimensions  $\Delta x * 1 * 1$  (assuming a unit thickness for  $y$  and  $z$  directions, for a one dimensional problem). Points  $E$  and  $W$  are the neighbor points for  $P$  with  $E$  (east point) denoting the positive direction of  $x$  and  $W$  (west point)

denoting the negative direction of  $x$ . The discretization equation that derives by the integration of equation (3.8) over the control volume is (19):

$$\left(k \frac{dT}{dx}\right)_e - \left(k \frac{dT}{dx}\right)_w + \int_w^e S dx = 0 \quad (3.9)$$

Applying linear interpolation between the grid points (see *Figure 3.7* where  $\phi$  is the dependent variable  $T$ ), the discretization equation will take the form:

$$\frac{k_e(T_E - T_P)}{(\delta x)_e} - \frac{k_w(T_P - T_W)}{(\delta x)_w} + \bar{S} \Delta x = 0 \quad (3.10)$$

Where  $\bar{S}$  is the average value of  $S$  over the control volume. The standard form of the discretization equation is:

$$a_P T_P = a_E T_E + a_W T_W + b \quad (3.11)$$

Where  $a_E = \frac{k_e}{(\delta x)_e}$ ,  $a_W = \frac{k_w}{(\delta x)_w}$ ,  $a_P = a_E + a_W$ ,  $b = \bar{S} \Delta x$ .

The general form of the equation (3.11) is:

$$a_P T_P = \sum a_{nb} T_{nb} + b \quad (3.12)$$

Where  $nb$  is the neighbor grid point. For two and three-dimensional problems, the number of neighbor grid-point temperatures increases.

Now the form of the equation is simple algebraic and can be solved with basic numerical methods. The linear systems that arise by discretization process will be solved by iterative techniques which mean that the equations are reconstructed repeatedly until the dependent variables do not change. The iterative procedure comprises an inner iterative one so as for the dependent variable equations to be solved and an outer one, which contains the inner one, so as to update the coefficients of the dependent variables. Every time an outer iteration takes place, only the uncertain (tentative) values of the dependent variables are calculated so the number of the inner iterations that is required to take place is less.

The calculation loop for the outer iterations will continue to take place until the values of all the dependent variables satisfy the finite difference equation. The termination of this procedure is called convergence of the solution. Convergence is achieved when the residuals of each dependent variable in the forthcoming iteration descends to the termination residual that the user appoints, taking into account that this is an acceptable value for the dependent variable and so the simulation ends (12).

### 3.2.3 Relaxation methods

In order to avoid divergence in the iterative solution, especially if the equations are strongly non-linear, it is recommended to slow down the changes in the dependent variables that take place in each iteration. The method is called *underrelaxation*. The general form of the discretization equation can be written as:

$$T_P = \frac{\sum a_{nb} T_{nb} + b}{a_P} = T_P^* + \left( \frac{\sum a_{nb} T_{nb} + b}{a_P} - T_P^* \right) \quad (3.13)$$

Where  $T_p^*$  is the value of  $T_p$  from the previous iteration and the parenthesis denotes the change of the dependent variable T in the current iteration. If a relaxation factor  $\alpha$  is added to the equation it will take the form below:

$$T_p = T_p^* + \alpha \left( \frac{\sum a_{nb} T_{nb} + b}{a_p} - T_p^* \right) \quad (3.14)$$

Or

$$\frac{a_p}{\alpha} T_p = \sum a_{nb} T_{nb} + b + (1 - \alpha) \frac{a_p}{\alpha} T_p^* \quad (3.15)$$

The relaxation factor in the underrelaxation method takes the values from 0 to 1 so that the values of  $T_p$  remain close to the values from the previous iteration,  $T_p^*$ . The smaller the values of  $\alpha$ , the slower the changes in  $T_p$ . Convergence will be achieved when the value of  $T_p^*$  becomes equal to the value of  $T_p$  satisfying equation (3.15).

Furthermore, concerning the issue of convergence, another parameter that contributes to this achievement is a kind of relaxation method which uses false time steps in the transient term of the dependent variable of the differential equation. The calculations that DesignBuilder CFD tool conducts is a “snap-shot” in time (steady state), so the false time steps are replacing the time steps used in the equation. It is a way of slowing down the changes in the dependent variable to accomplish a more stable solution. Especially for the velocity components, reducing the value of the false time steps can lead to stability in the solution increasing at the same time the simulation run period. Comparing the relaxation factor and the false time steps as two methods of achieving relaxation, the false time step is preferred due to the fact that applying a relaxation factor in each iteration allows only part of the calculated dependent variable value to be assigned to the variable (19).

### 3.2.4 The SIMPLER Algorithm

A problem which arises in the approach of the overall solution is the calculation of the pressure field. In compressible flows, pressure can be obtained from the density and temperature using the equation of state  $p = p(\rho, T)$  due to the fact that the energy equation is a transport equation for temperature and the continuity equation can be used as a transport equation for density. However, in this case the flow is considered incompressible, thus the density has a unique constant value and cannot be linked to the pressure. This situation reflects the problem of correlation of pressure and velocity in the general approach of the flow field because the pressure field which is applied to the momentum equation should satisfy the continuity equation as well. In a two dimensional laminar steady flow problem the x-momentum equation would be (3.16), the y-momentum equation would be (3.17), and the continuity equation would be (3.18), (21).

$$\frac{\partial(\rho uu)}{\partial x} + \frac{\partial(\rho vu)}{\partial y} = \frac{\partial}{\partial x} \left( \mu \frac{\partial u}{\partial x} \right) + \frac{\partial}{\partial y} \left( \mu \frac{\partial u}{\partial y} \right) - \frac{\partial p}{\partial x} + S_u \quad (3.16)$$

$$\frac{\partial(\rho uv)}{\partial x} + \frac{\partial(\rho vv)}{\partial y} = \frac{\partial}{\partial x} \left( \mu \frac{\partial v}{\partial x} \right) + \frac{\partial}{\partial y} \left( \mu \frac{\partial v}{\partial y} \right) - \frac{\partial p}{\partial y} + S_v \quad (3.17)$$

$$\frac{\partial(\rho u)}{\partial x} + \frac{\partial(\rho v)}{\partial y} = 0 \quad (3.18)$$

Concertedly the problems that arise from the set of the equations are the nonlinear quantities contained in the convective terms of the momentum equation (3.16) ( $\rho uu$ ), the correlation of the three equations containing velocity components and the lack of a pressure equation. The lack of a pressure equation leads to the necessity of linking pressure and velocity. In order to achieve this and calculate the flow field, an iterative algorithm will be used which is called SIMPLER (Semi-Implicit Method for Pressure linked Equations Revised). SIMPLER algorithm is a revised algorithm developed by Patankar (1980). The step procedure of the algorithm is presented by the diagram depicted in *Figure 3.8*.

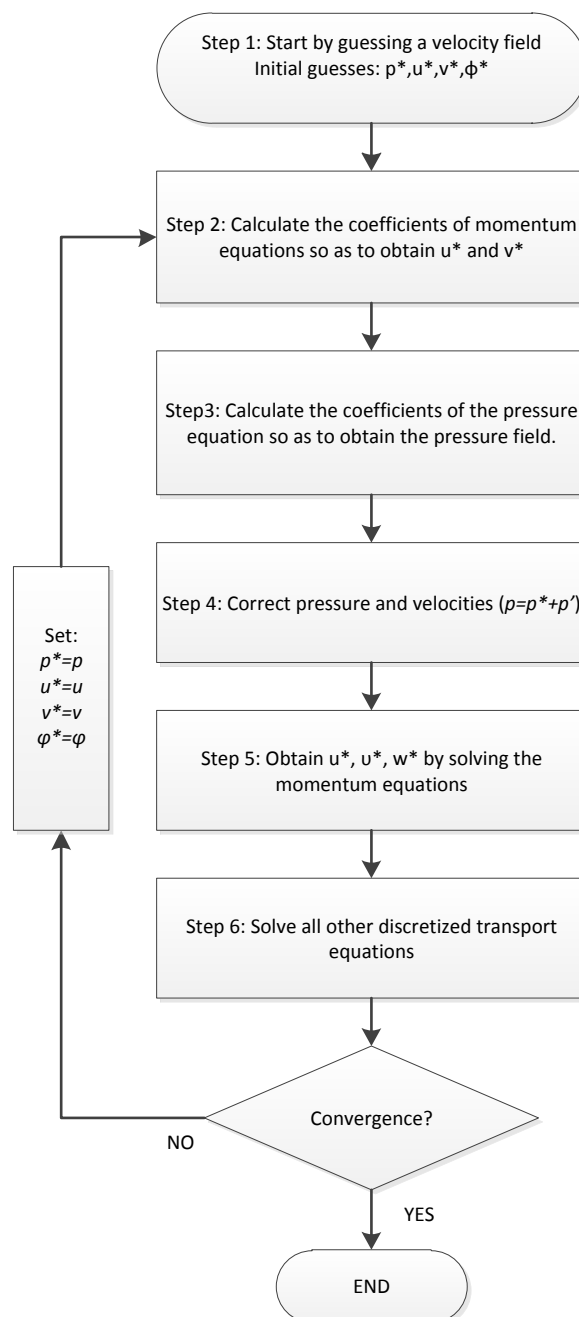


Figure 3.8: SIMPLER Algorithm procedure (19; 21).

### 3.2.5 CFD Boundary Conditions

To apply a CFD analysis, boundary conditions should be determined. Boundary conditions are initial values in the analysis domain that the user specifies at solution points. These values are going to be used in the dependent variable equations.

Conducting an external DesignBuilder CFD analysis, the necessary boundary conditions are the building wind exposure (open country, urban, suburban), the wind velocity and direction. The calculations in an external CFD analysis are isothermal (temperature remains constant  $\Delta T=0$ ) and only velocity and pressure are taken into consideration.

On the other hand, internal analysis require several boundaries such us surface temperatures for walls and windows, supply diffusers and extract grilles, heat fluxes patches and the position of assemblies in the analysis domain. Component blocks and component assemblies can represent any furniture, equipment, occupants, radiators, fan coil units that belong to the space and act either as obstacles or/and as temperature or heat flux boundaries.

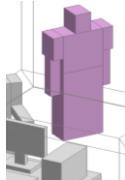
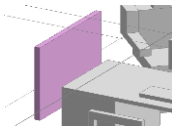
CFD Boundaries	Assemblies	Thermal Boundary Type
Furniture		None
Occupants		Heat Flux 45Watt
Radiators		Temperature 75°C-constant temperature surfaces
Computers-Equipment		Heat Flux 119Watt

Table 3.1: Depiction of CFD boundaries

In general, all of the momentum equation boundary conditions are specified through velocity components (Dirichlet boundary conditions) by combining specified flow rates with opening aperture areas. Energy equation boundary conditions may be defined using surface temperature or flux. Concerning wall and window boundary temperatures, they can be generated automatically after an EnergyPlus simulation. Pressure boundaries are not required due to the fact that the pressure equation boundary conditions are provided in terms of normal velocities. Relative pressure is calculated above and below the prevailing atmospheric pressure.

### 3.3 Setting up a CFD analysis in DesignBuilder

#### 3.3.1 External CFD analysis

After the creation of the building model in DesignBuilder graphical user interface, the modeling of an external CFD analysis requires the definition of special parameters concerning the grid, the wind and some site factors.

DesignBuilder generates automatically the CFD grid in the analysis domain. The grid spacing type can be uniform or non-uniform. A uniform grid is actually a simple grid that comprises identical cubic cells. The size of each cell is the default grid spacing. Concerning the non-uniform grid type spacing is an “almost” uniform grid, created by DesignBuilder, with the exception that the corners are located in the crossing lines of the grid. For this reason the “Grid line merge tolerance” parameter should be used so as for the variations in the grid to take place. The value of “Grid line merge tolerance” indicates the maximum dimension for allowing or not the grid lines to merge. By using “Grid line merge tolerance” instability in the equation solver is avoided that can happen due to the creations of cells with high aspect ratio. Additionally for the grid domain to be created, the user sets the site factors which are values that multiply the dimensions of the building (length, width, height) to shape the boundaries of the analysis domain.

By default DesignBuilder creates a Cartesian grid which is non-uniform. The lines are parallel with the major axis but because it is a non-uniform grid it can be edited changing the space between the lines.

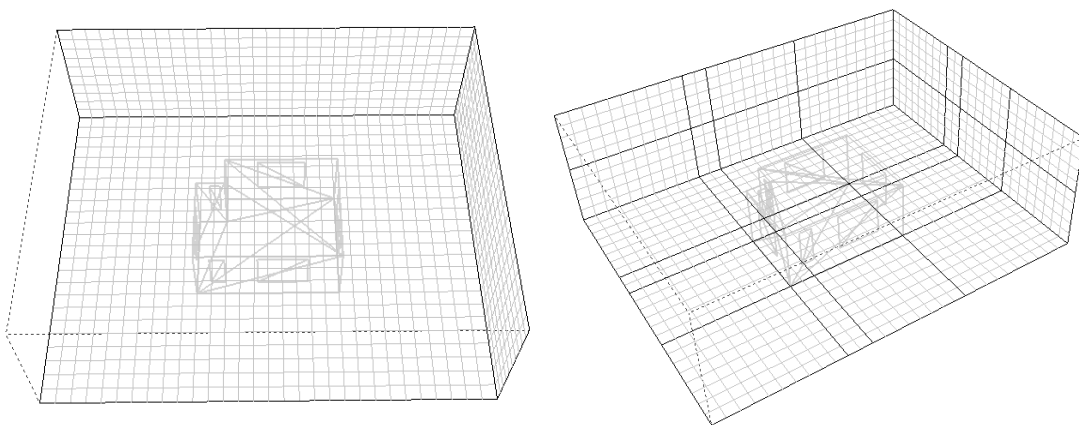


*Figure 3.9: Example of uniform and non-uniform grid spacing type.*

Although the grid is automatically created the user can edit it and transform it, according to the needs of each CFD problem, by inserting or removing regions and changing the spacing parameter.

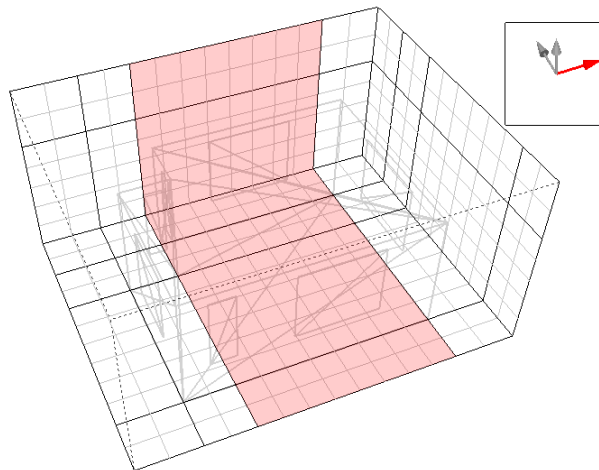


Figure 3.10: Modifying the CFD grid using a “Uniform” spacing type.

For the grid region (pink color) selected to be modified, there are several options concerning the spacing type. A “Uniform” spacing option is dividing the region into same geometry divisions with a spacing dimension that the user defines.

For “Increasing power law” option, according to the space power that the user sets, the location of each geometry divisions within the region increases starting from the beginning of the region.

$$x_i = (\text{region dimension}) \left( \frac{i}{n} \right)^{\text{spacingpower}} + x_s$$

Where  $i$  denote the index number of the grid line counted from the start of the region (12).

On the other hand by using “Decreasing power-law” option the opposite occurs, with the relationship that describes it to be the following (12):

$$x_i = (\text{region dimension}) \left[ 1 - \left( \frac{i}{n} \right)^{\text{spacingpower}} \right] + x_s$$

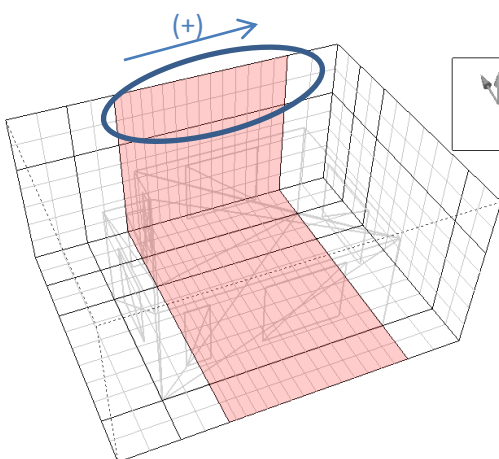


Figure 3.11: “Increasing power law” spacing type

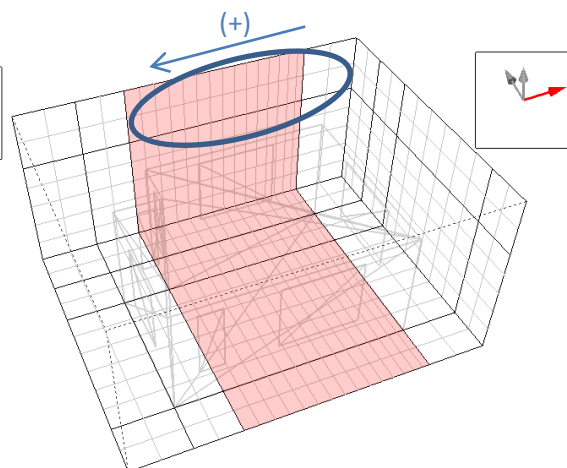


Figure 3.12: “Decreasing power law” spacing type

The “Symmetric power-law” option uses both Increasing and Decreasing power law relationships according to the following conditions (12):

$$\text{For } i \leq \frac{n}{2}: x_i = \frac{\text{region dimension}}{2} \left(\frac{2i}{n}\right)^{\text{power}} + x_s$$

$$\text{For } i \geq \frac{n}{2}: x_i = \frac{\text{region dimension}}{2} \left[2 - \left(\frac{2i}{n}\right)^{\text{power}}\right] + x_s$$

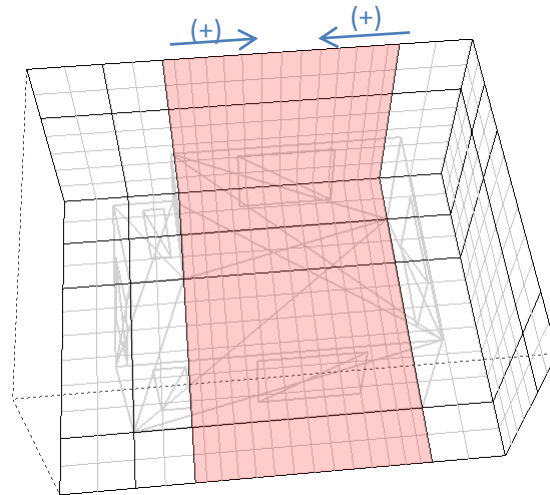


Figure 3.13: “Symmetric power law” option

All Figures depict the grid region, in pink color, which is created using 1.2 for spacing power and 15 subdivisions.

Apart from the grid parameters, information concerning the wind is considered essential. The user should define its direction and velocity (at 10m above ground) and the type of exposure of the building to the wind, i.e. urban, suburban and open country exposure. An empirical relationship is used to correct the free stream wind velocity for heights above ground and the area that surrounds the building. The correlation between the orientation of the analysis domain and the orientation of the wind is depicted in *Figure 3.14* and *Figure 3.15*.

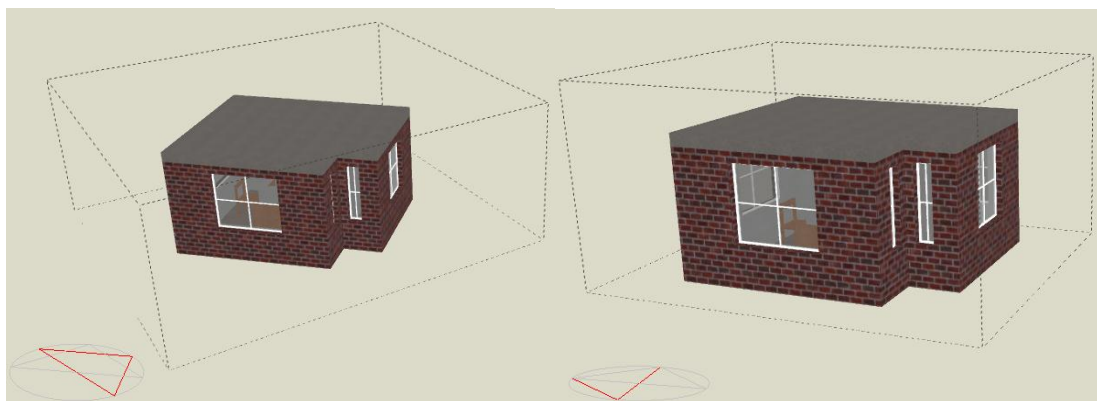


Figure 3.14: 225° Wind direction

Figure 3.15: 90° Wind direction

Before proceeding to the simulation, an automatic check is being conducted by DesignBuilder concerning the grid statistics. For any type of grid created, the “Show CFD grid statistics tool” displays *Table 3.2*.

Description	Data
Number X Cells	20
Number Y Cells	12
Number Z Cells	7
Max aspect ratio	3.228
Required Memory (MB)	0.2
Available Memory (MB)	1723.3
Check	OK

*Table 3.2: Grid statistics*

The limit of the maximum aspect ratio value is 50 which mean that if this limit is exceeded or if the required memory is above the available one then a failure in the check will be indicated in order for the user to apply changes and check again.

After confirming that the check is *OK*, the next step is to set the calculation options through an edit screen.

### 3.3.2 Internal CFD analysis

The first step for modeling an internal CFD analysis is to define the “Default grid spacing” and the “Grid line merge tolerance”. The procedure continues with the setting of boundary conditions. There are two ways of accessing these data. The first one is from the “CFD Boundary” where one can set default values from building level to block and surface level. These values are inside surface temperatures for internal and external surfaces, inside surface window temperature, incoming air temperature, aperture position (top, right, left, and bottom) and size of opening area which is the percentage of the total of opening area. The second way of accessing the boundary data is through the “CFD Boundary Conditions Editor”. The Editor is providing to the user information concerning the flow balance and window and wall temperatures. These data can be imported manually or they can be imported directly after an EnergyPlus simulation for a specific day and time (the CFD calculations are a snapshot in time). In particular the values that are imported are surface inside temperatures of walls, floors, roofs, partitions, ceilings, windows, doors and sub-surfaces and flow in and flow out of windows, vents, doors and holes.

In cases of flow imbalance, the CFD Boundary Conditions Editor is warning the user so as to manually correct the value of “Flow in” or “Flow Out” as seen in *Figure 3.16*.

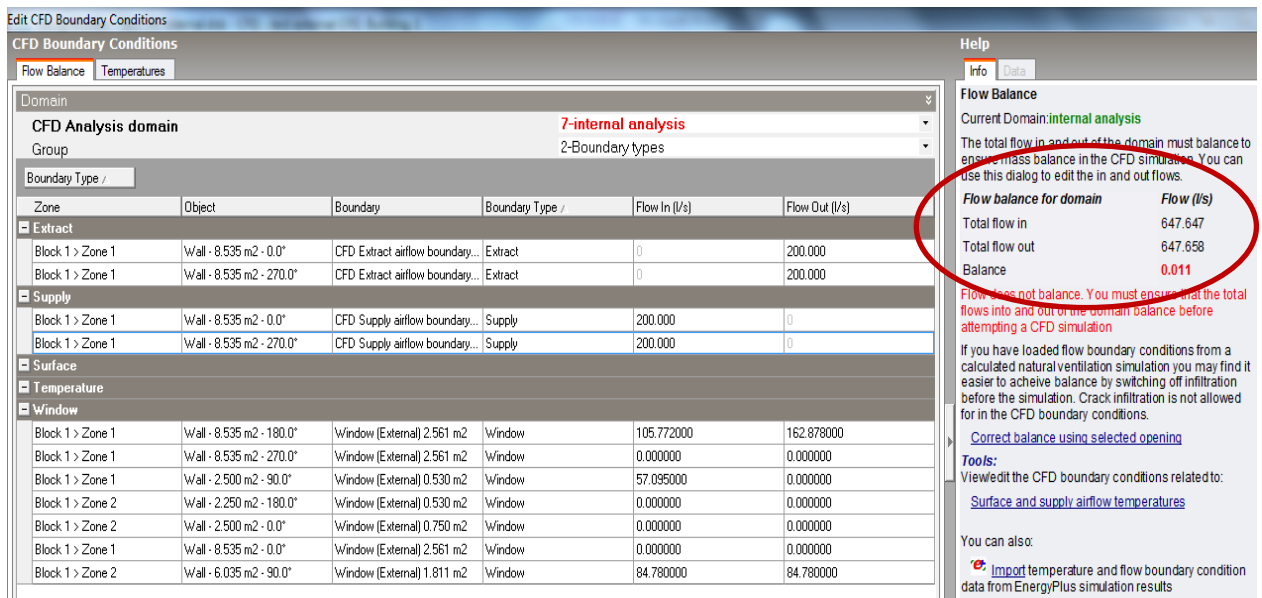


Figure 3.16: Case of flow imbalance when importing boundary conditions from EnergyPlus simulation.

All the boundary condition values can be edited manually either they are set by default or they are imported from an EnergyPlus simulation.

Boundary condition values concerning velocity for openings are very difficult to automatically derive. This is a problem of location and geometry of the windows taking into account that the velocity vectors for a casement and sash windows are different. The best case for accurate values would be the imported mass flows calculated by EnergyPlus and the specification of aperture position and size. The next step is setting the calculation options, a procedure that will be described in the following section.

### 3.3.3 Calculation options data

As long as the grid is generated correctly and all the boundary conditions are imported, the following step is setting the calculation options data. For both an external and internal analysis one can edit calculation options in the dialog depicted in Figure 3.17.

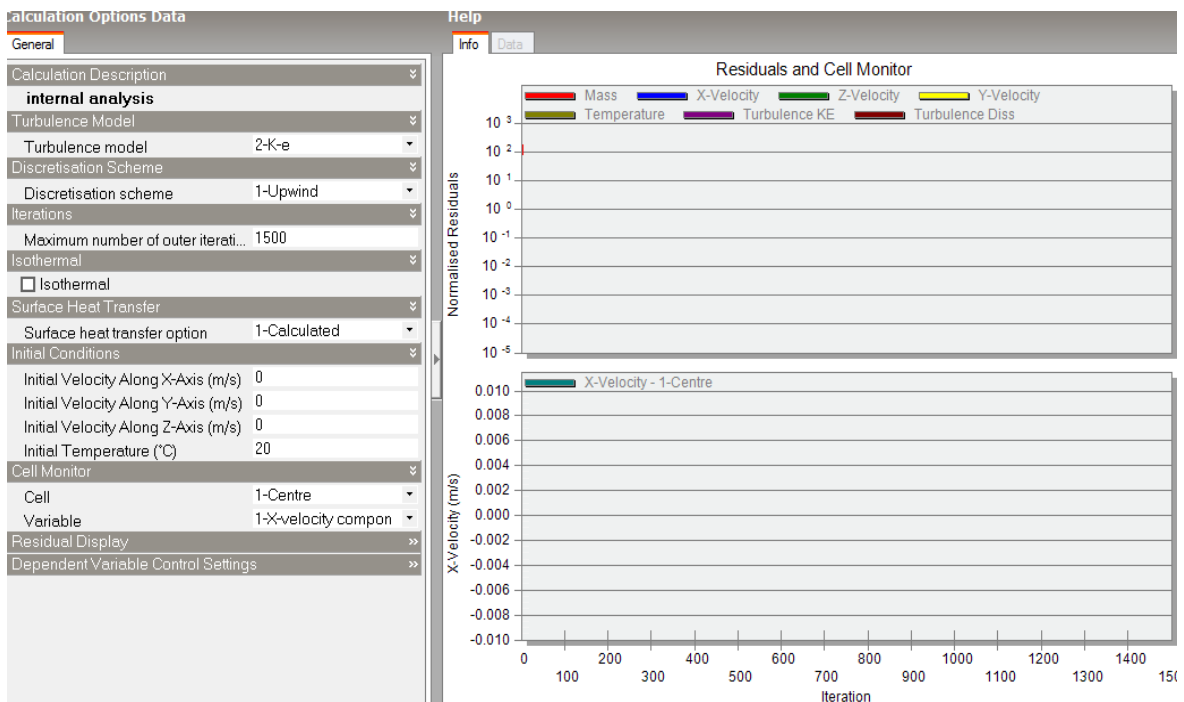
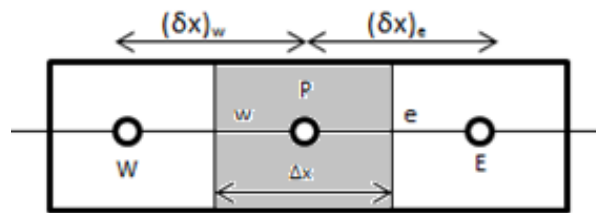


Figure 3.17: Calculation options data

With reference to the turbulence model there are two options, the “k-e” turbulence model and the “Constant effective viscosity” model. Turbulence models were developed in order to simulate the effects of turbulence since DNS (Direct Numerical Simulation) of turbulent flows is extremely expensive in terms of memory and computation. One of the most commonly used turbulence model is the k-e model which belong to the RANS (Reynolds Averaged Navier-Stokes) family. Using the k-e turbulence model transport equations are solved for the turbulent kinetic energy (k), and the rate of dissipation of the turbulent kinetic energy (e) representing the dependent variables (22). The instant velocity which is contained in the Navier Stokes and energy equations is replaced by a mean and oscillating component.

The second option regarding the turbulence model is the “Constant effective viscosity”. According to this model a constant effective viscosity is replacing a molecular viscosity in the Navier stokes equations. The disadvantage of the model lies in the ineffectiveness of modeling the transport of turbulence though is less expensive in terms of computation than the k-e model.

The next step is setting the discretization schemes. The available choices are the Upwind, the Hybrid and the Power-Law discretization scheme. The upwind scheme is based in the assumption that the dependent variable  $\phi$  at an interface is equal to the  $\phi$  value of the upwind side for the calculation of the convection term. Nevertheless diffusion is still calculated as the average of  $\phi_E$  and  $\phi_P$ .



The hybrid scheme is a combination of central difference and upwind schemes. It is more expensive than the upwind in terms of computation but at high values of  $P_e$  (Peclet) number it reduces numerical diffusion.

The final option is the power-law scheme which is more complicated and expensive to compute than the hybrid scheme yet providing a better representation of exponential behavior which makes it more accurate.

Proceeding, in the field “iterations” the user is called to set the maximum number of outer loop iterations. When the iterations reach this number then the calculations will stop either the solution is converged or not.

Concerning the heat transfer, the user decides whether the temperature will be assumed constant and consequently the energy equation will not take part into the calculations (Isothermal) or surface heat transfer coefficients should be set. In case of the k- $\epsilon$  turbulence model choice the surface heat transfer coefficients are calculated through the CFD scheme or the user can define them for surfaces such as ceilings, walls and floors.

Initial conditions referring to velocity and temperature values can be set for a less time consuming simulation.

The cell monitor point allows the user to set a point inside the calculation domain and observe the progress in the calculation of a dependent variable.

Moreover, the user defines the residuals that will be displayed in the result graphs. The residuals can be mass, x-velocity, y-velocity, z-velocity, temperature, turbulence KE and turbulence dissipation rate. A reliable indicator of convergence is the mass residual which is extracted from the continuity equation.

Finally in order to calculate the dependent variables some settings concerning the iterative procedure used in the calculations should take place. The user should define the number of the inner iterations conducted in the overall outer iterative loop, as discussed in previous chapter. In addition the false time step which is used in order to slow down the change in dependent variables should be defined. Alternatively a value for the relaxation factor can be set as a relaxation method. The last setting that should be done with reference to every dependent variable concerns the termination residuals. The termination residuals are the points in which the CFD calculation scheme is considered to have converged. For each dependent variable the solution is converged when the residual is less than the termination residual. The closer the value is to 0 the better the solution.

The only difference between an external and internal analysis relative to the calculation options data is that in an external analysis isothermal calculations take place so there is no option of setting surface heat transfer coefficients.

### 3.4 Applying external and internal CFD analysis in the TUC building

A detailed representation of the building geometry, presented in *Figure 3.18*, was created according to the floor plans using the DesignBuilder drafting environment, as discussed in Chapter 2. Nearby buildings were modeled as well to account for shading and due to their participation as wind obstacles to the surrounding environment.

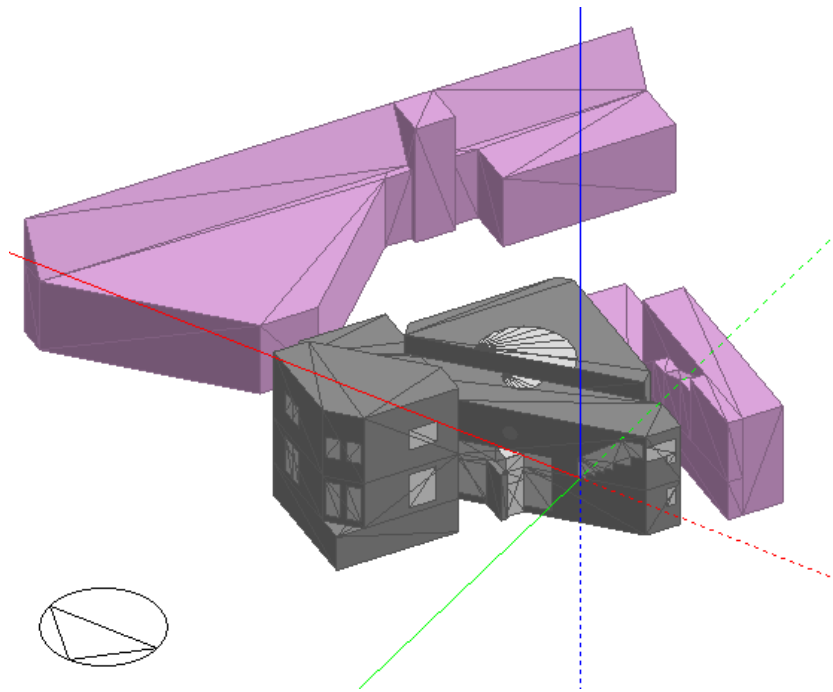


*Figure 3.18: Geometry of the simulation model created in DesignBuilder.*

All the imported data to the simulation model presented in the previous chapter will be also used in the CFD analysis such as activity data, comfort temperatures, lighting data, equipment gains, HVAC data in order to calculate boundary conditions.

#### 3.4.1 External CFD Analysis Results

Setting up the external analysis a non-uniform grid was selected with a default grid spacing of 0.5m and a grid line merge tolerance value of 0.1m. The wind velocity was set to 15m/s with 90° direction and suburban exposure. The grid statistics can be seen in *Table 3.3*.

Description	Data
Number X Cells	282
Number Y Cells	254
Number Z Cells	49
Max aspect ratio	9.666
Required Memory (MB)	452.4
Available Memory (MB)	2026.7
Check	OK

*Table 3.3: Grid Statistics.*

The selected turbulence model is the k-e and a choice of upwind discretization scheme was made. The maximum number of iterations was set to 4000. With reference to the dependent variable control settings Table comprise all the choices that were made for the calculations.

Dependent Variable	Inner iterations	False time step	Relaxation factor	Termination residual
x-axis velocity	3	0.0444	1	$10^{-5}$
y-axis velocity	3	0.0444	1	$10^{-5}$
z-axis velocity	3	0.0444	1	$10^{-5}$
Pressure	9	-	-	-
Mass	-	-	-	$10^{-5}$
Turbulence KE	6	0.0222	1	$10^{-5}$
Dissipation rate of turbulence KE	6	0.0222	1	$10^{-5}$
Viscosity	-	-	1	-

*Table 3.4: Dependent variable control settings.*

After 4000 iterations the solution is not converged but the residuals for almost all the dependent variables except mass reach  $10^{-4}$  which is considered to produce quite accurate results.

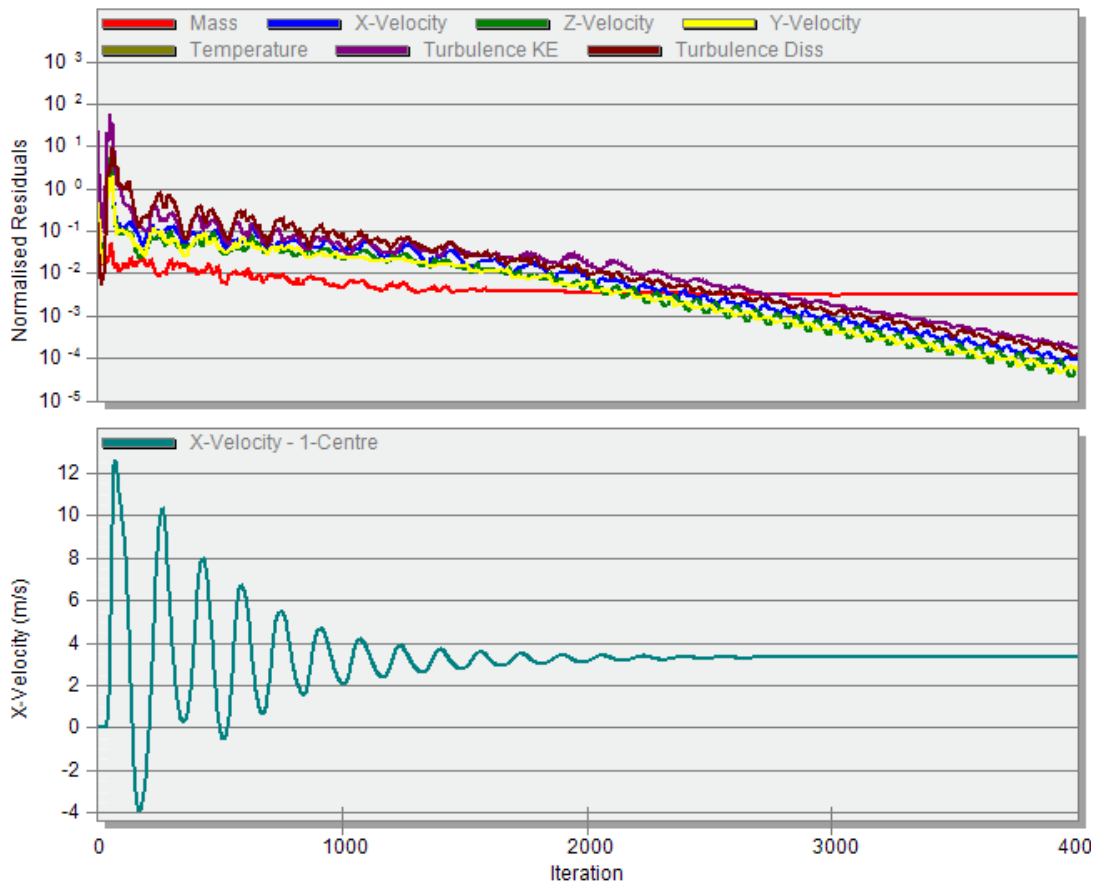


Figure 3.19: Residuals and Cell Monitor.

From *Figure 3.20* until *Figure 3.24* the distribution of air around the building structures is depicted. A color palette is used to depict the fluctuation of velocity. The velocity falls into smaller values as the air is moving towards the building. This phenomenon is depicted in blue color for a velocity of 0m/s. The velocity values rise as the distance from the building becomes bigger with the maximum velocity to reach the value of 16.3 m/s. Observing *Figure 3.20* one can easily notice that neighbor buildings act as obstacles in the wind movement. The red arrow depicted in the figures implies the wind direction.

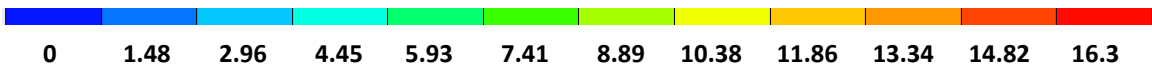
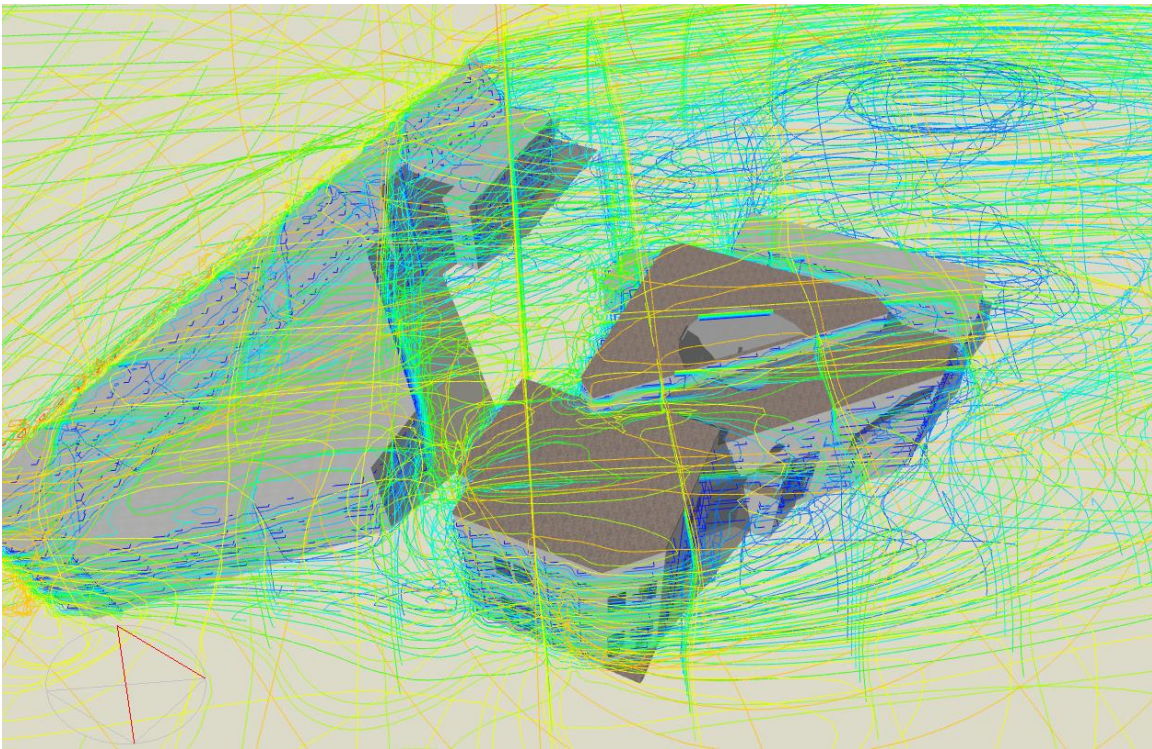


Figure 3.20: 3D Velocity contours (m/s).

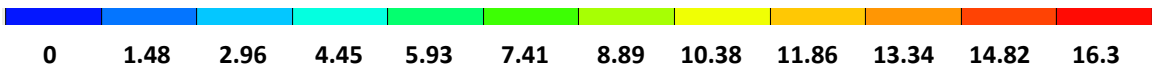
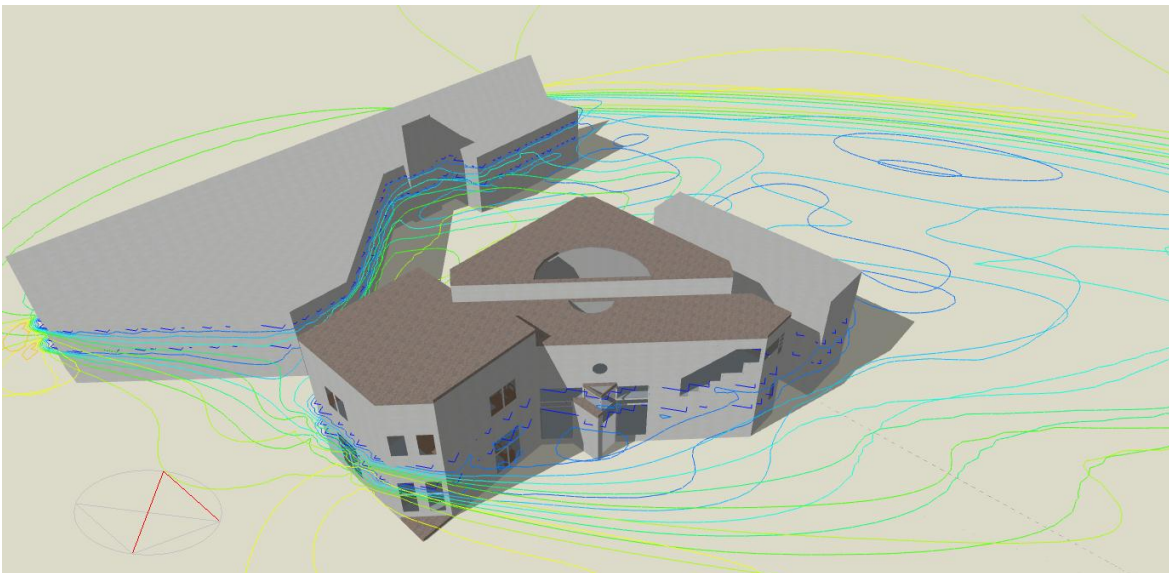


Figure 3.21: Horizontal Velocity contour slice (m/s).

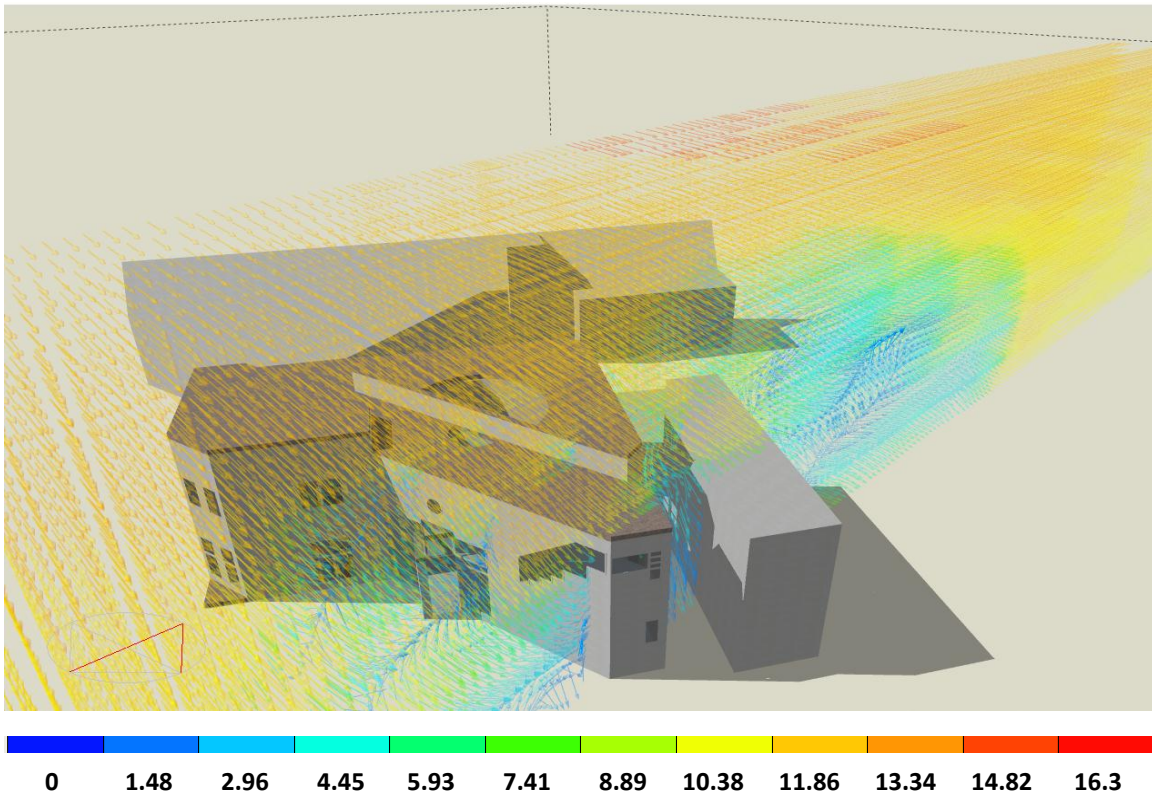


Figure 3.22: Vertical velocity slice (m/s).

Vertical velocity slices are depicting the generation of eddies colored in blue due to the wind direction and its effect on building structure.

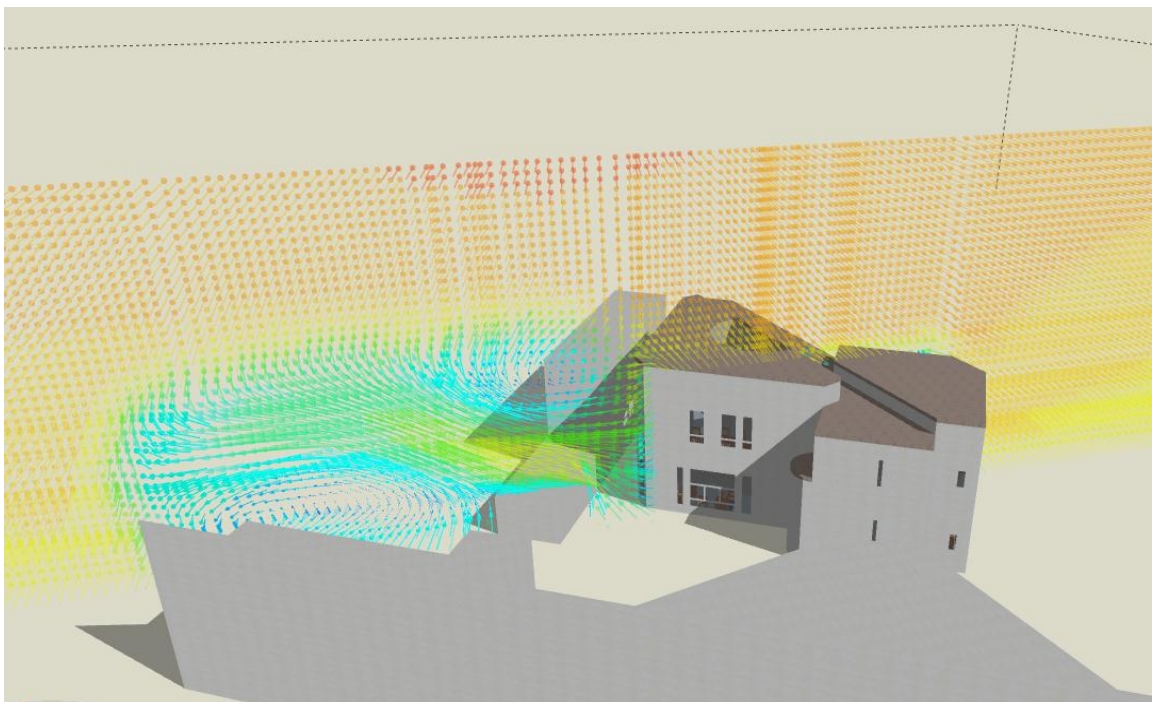


Figure 3.23: Generation of eddies at the back side of the building.

The maximum wind speed is detected around the buildings volume where the geometry has no longer an effect.

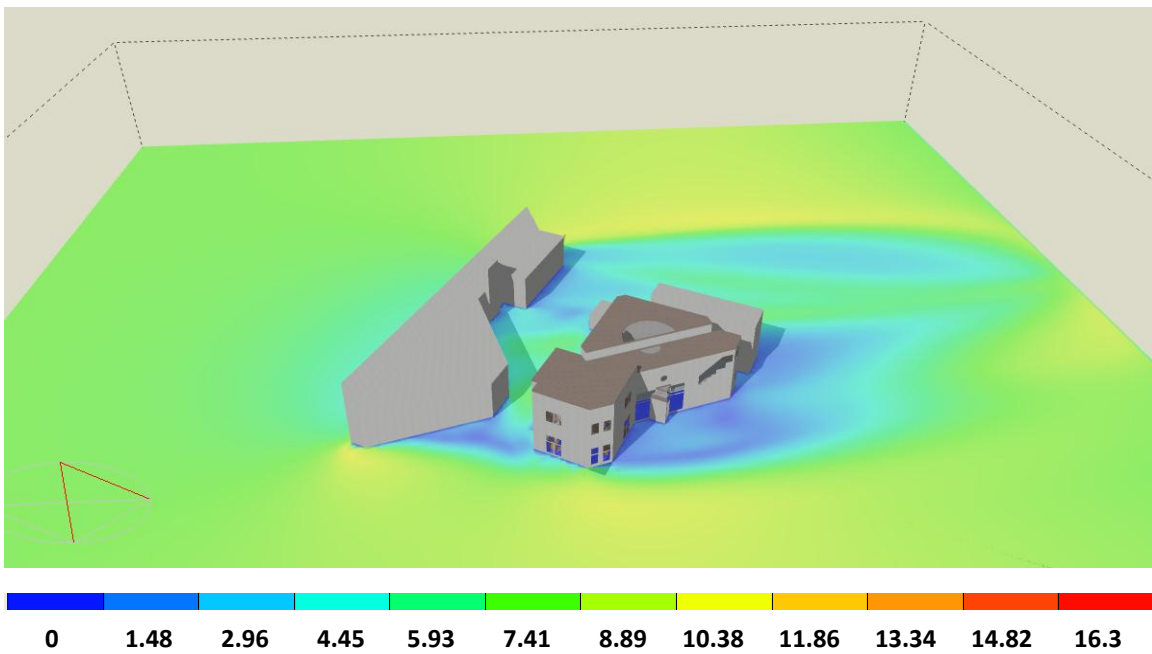


Figure 3.24: Filled velocity contour horizontal slice (m/s).

The maximum pressure deployed is around 35Pa depicted in *Figure 3.25*. The developed pressure depends also on the complexity of the geometry of the building. According to the direction of the wind, as the air flow impinges on the building surface, positive pressure depicted in dark orange and red color is induced on the upwind face of the building. As the flow separates around and above the building negative pressure depicted in yellow, green and blue is induced on the leeward façade. The pressure values also depend on the different heights of the building.

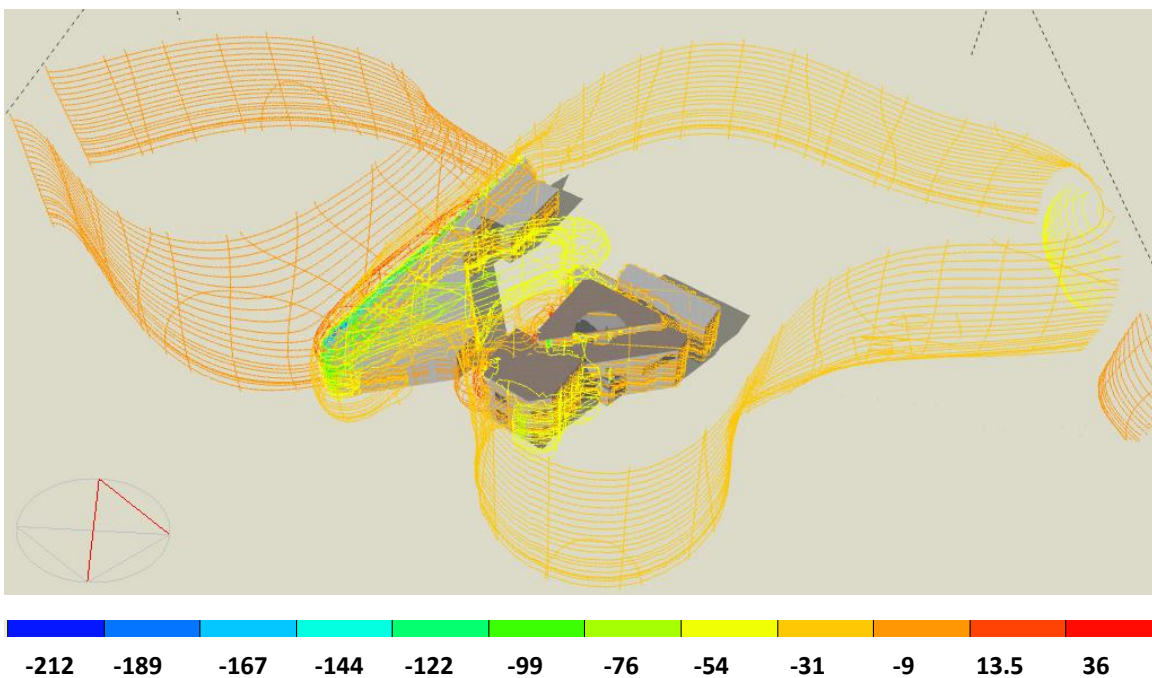


Figure 3.25: Pressure distribution (Pa).

Positive and negative pressure values represent the above and below calculated values from the prevailing atmospheric pressure.

### 3.4.2 Internal CFD analysis results

As far as the application of an internal CFD analysis is concerned, EnergyPlus simulation results were used as boundary conditions for the CFD calculations.

Since split type air conditioners are installed on each of the office rooms the temperature can be independently adjusted. For this reason each room of the building is defined as a separate thermal zone and thus as a separate control volume in which an internal CFD analysis of the airflow took place.

Apart from the assemblies' introduction as boundary conditions (people, furniture, equipment), radiators are modeled for winter CFD calculations and split type units for cooling each space are modeled for summer calculations. In order to model the cooling system in a CFD calculation domain as CFD boundary the parameters that should be set are the boundary type (Supply or Extract grille), the boundary temperature for the supply grille, the flow rate in l/s, the x and y discharge angle and the minimum discharge velocity. The radiators are modeled as volumes (component blocks) inside the space with their real dimensions and act both as obstacles and as constant temperature (75°C) objects. They can also be modeled with a Flux boundary type where the user should set the heat flux considering that only convection takes place.

#### 3.4.2.1 Internal CFD analysis of office 11

The first step of setting the boundary condition is to run an EnergyPlus simulation so as to generate results that will then be used as boundary conditions in the internal CFD analysis as discussed before. The simulation runs for a typical winter period during December. The CFD analysis took place for 10 of December at 13:00pm. The external mean air temperature at 13:00pm was 13.8°C and the average zone air temperature 16°C without the HVAC operation. The wall surface temperature was around 17°C. What distinct this office from the rest of the building is that the user of the office leaves a specific window always open so the flow balance imported from EnergyPlus was 54.192l/s.

The k-e turbulence model and the upwind discretization scheme were selected for the simulation. The residuals of the dependent variables reached the termination residual value of  $10^{-5}$  and the solution converged after 4000 iterations.



Figure 3.26: Dependent value residuals reaching the desired termination residuals

Observing the 3-D contour temperature results in *Figure 3.27*, it is clearly noticed the effect of radiators and open window in the room temperature. The user in this particular office leaves one window open throughout the day. Radiators can be distinguished by the red color and the air inserting the office by the blue color. The air around the radiators and in the upper space has a temperature of 20°C while the air temperature near the open window around 15°C. Computers, equipment and human activity and presence also contribute to the temperature augmentation of the inside air.

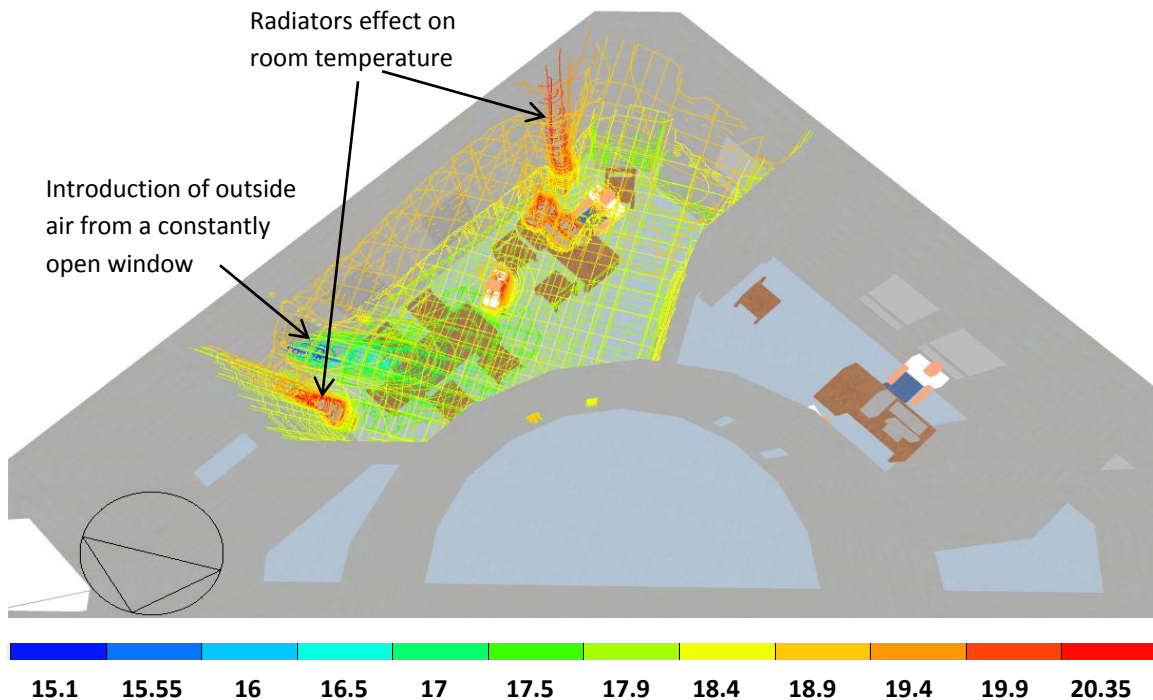


*Figure 3.27: 3D contours temperature results in office 11 (°C).*

The temperature slices in different heights inside office 11 depict the temperature bedding with the values to rise moving from the lowest to the highest levels having a temperature difference of around 2°C (see *Figure 3.28*) due to the stack effect. Higher air temperature values in red color are developed around the radiators. The general winter comfort temperature for Chania is between 20-22°C. The average temperature inside the office is around 19°C due to the open window. It seems that the capacity of the radiators is the appropriate one in order to achieve the desirable temperature according to the user behavior and preference.

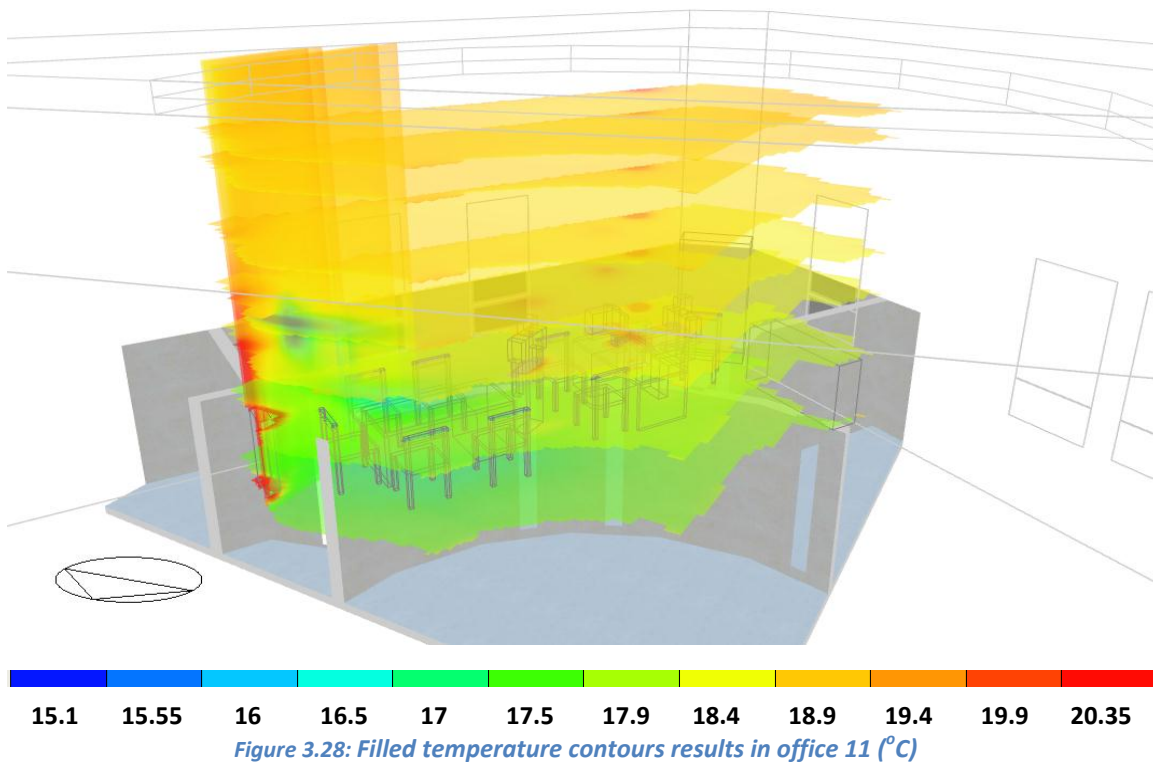
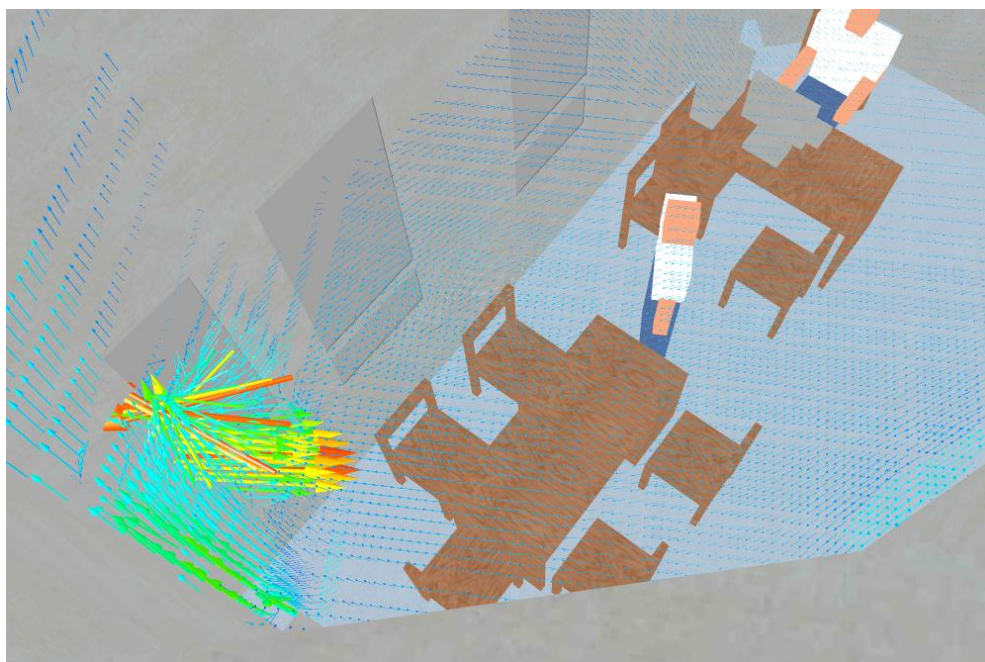


Figure 3.29 depicts the air movement in and out of the space through the open window. The warmer the colors the higher the velocity value is. Red arrows depict the maximum velocity while the rest of the space is covered by blue arrows which mean almost 0m/s wind velocity.



*Figure 3.29: Velocity vectors of air moving in and out through an open window.*

#### **3.4.2.2 Internal CFD analysis results of office 10**

In office 10 EnergyPlus simulation runs for the warmest period the summer which is the end of July. Simulation results, used as CFD Boundaries, were imported for the 31<sup>st</sup> of July at 15:00pm. The average zone air temperature is at 30.5°C while the external air temperature is 29°C.

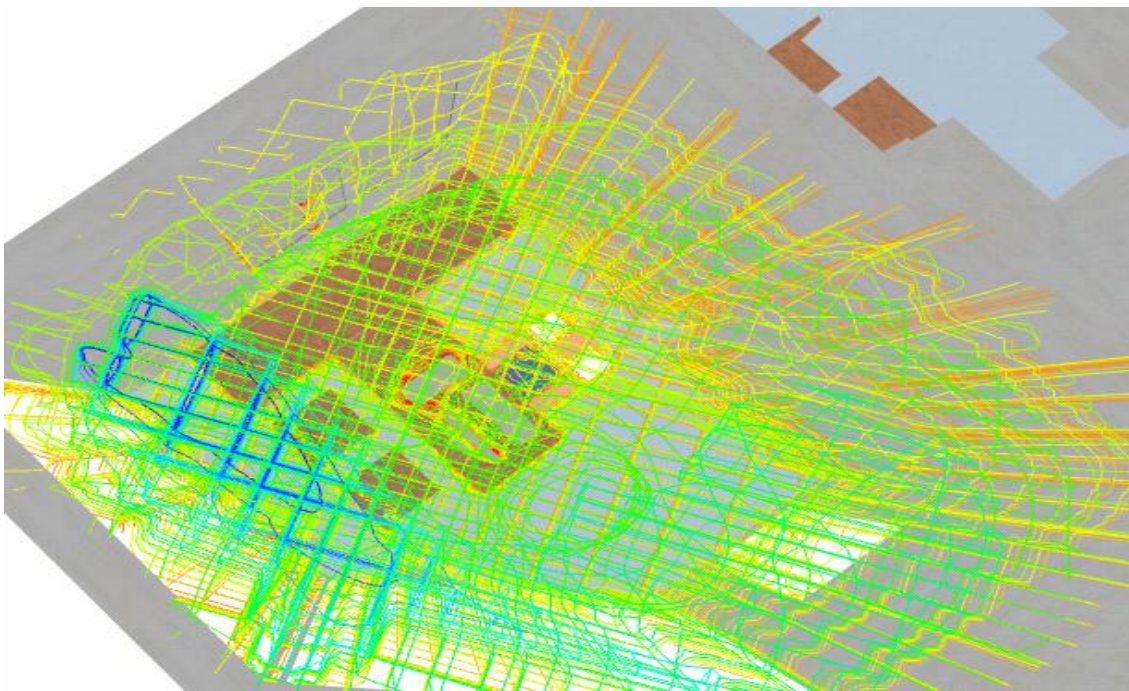


*Figure 3.30: Filled temperature contours results in office 10 (°C)*

The lowest temperature values appear due to the operation of the cooling system (*Figure 3.31*). The surface temperature for walls connecting the offices seem to be higher than the room air temperature and this is due to the fact that in the semi-detached offices the average air temperature is much higher because of the non-operation of the cooling system. These surface temperatures are the boundary conditions imported from the EnergyPlus simulation. *Figure 3.31* depicts the movement of the air in velocity vectors from the extract and the supply node of the cooling system. The extract node can be seen from the upper vectors while the supply nodes from the lower vectors.

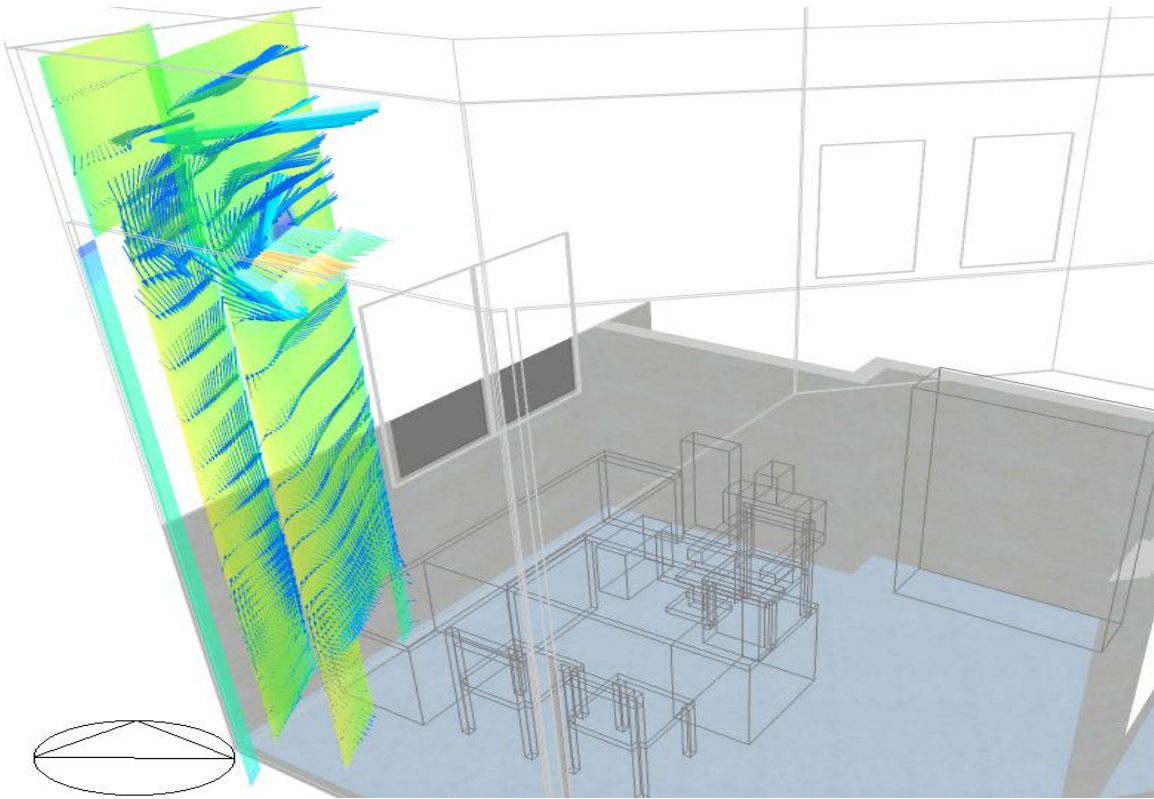
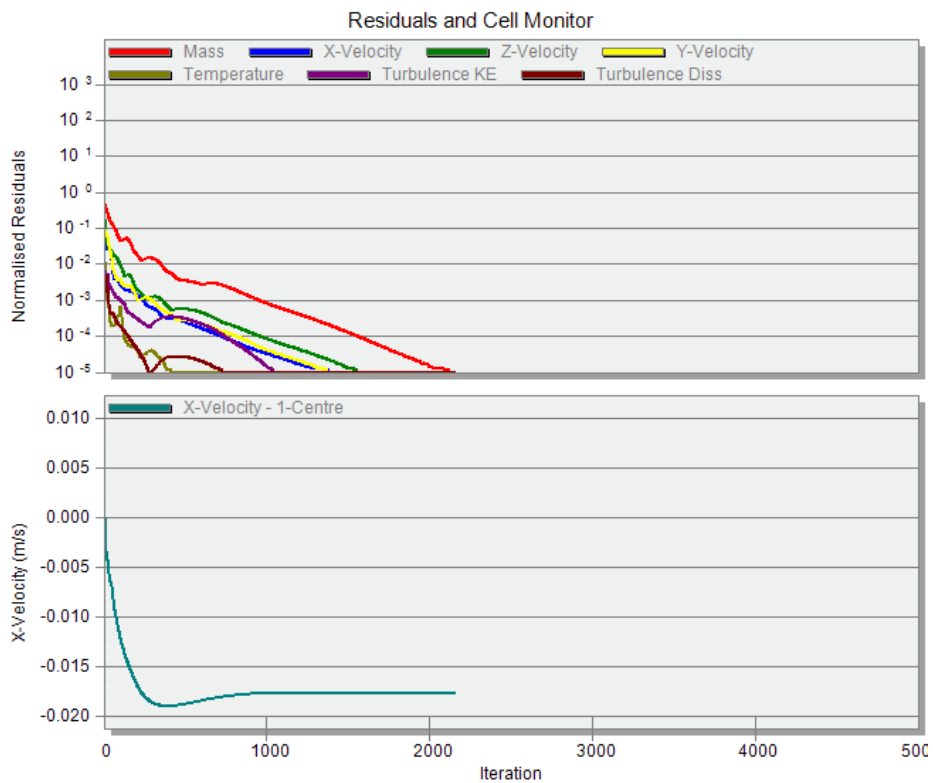


Figure 3.31: The operation of the cooling system in office 10.

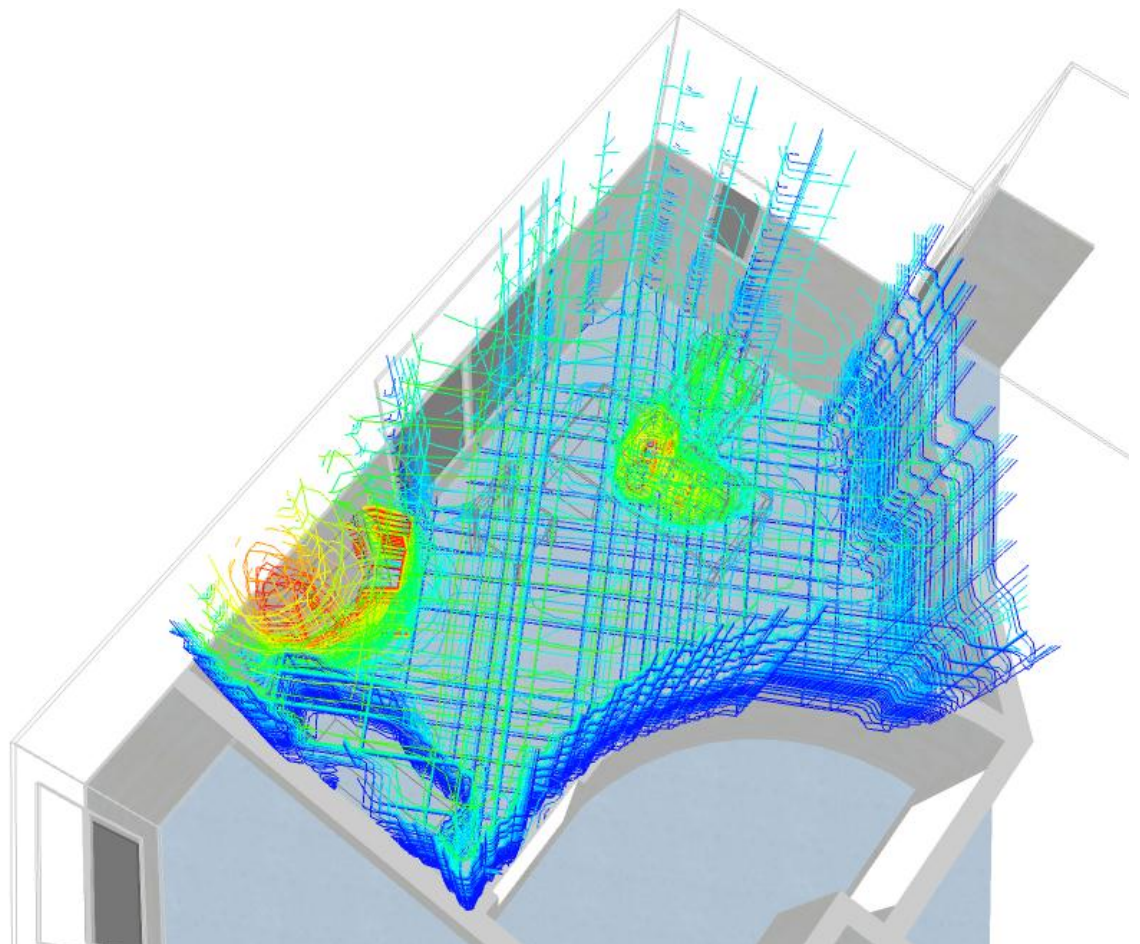
### 3.4.2.3 Internal CFD analysis results of office 1

Office 1 is located in the ground floor of the building. The CFD simulation runs on the 31<sup>st</sup> of January. The simulation converged after 2000 iterations.



*Figure 3.32: Dependent value residuals reaching the desired termination residuals.*

Figure 3.33 depicts the effect of the operation of the radiator in the room air temperature. The neighbor offices are not heated and thus the internal wall surface temperature is less than the average room air temperature. Temperature values rise around the radiator, around office equipment (computers) and around the user. The operation of the radiator due to its capacity seems to heat the space to the desirable comfort temperature.



21.14 21.61 22.08 22.5 23 23.5 23.9 24.4 24.9 25.3 25.8 26.3

*Figure 3.33: Filled temperature contours results in office 1 (°C).*

#### **3.4.2.4 Atrium CFD internal analysis**

Due to high temperature development during summer period in the atrium space it was considered purposive to isolate it from the rest of the building and contact an internal CFD analysis with a calculation domain extending from the ground floor corridor till the first floor. The two floors are not separated in the atrium area. The spaces under the skylight are corridors and a central meeting space. Even though they are spaces not used frequently, the absence of a cooling system provokes high temperature development due to the skylight which affects the neighbor offices through heat transfer.

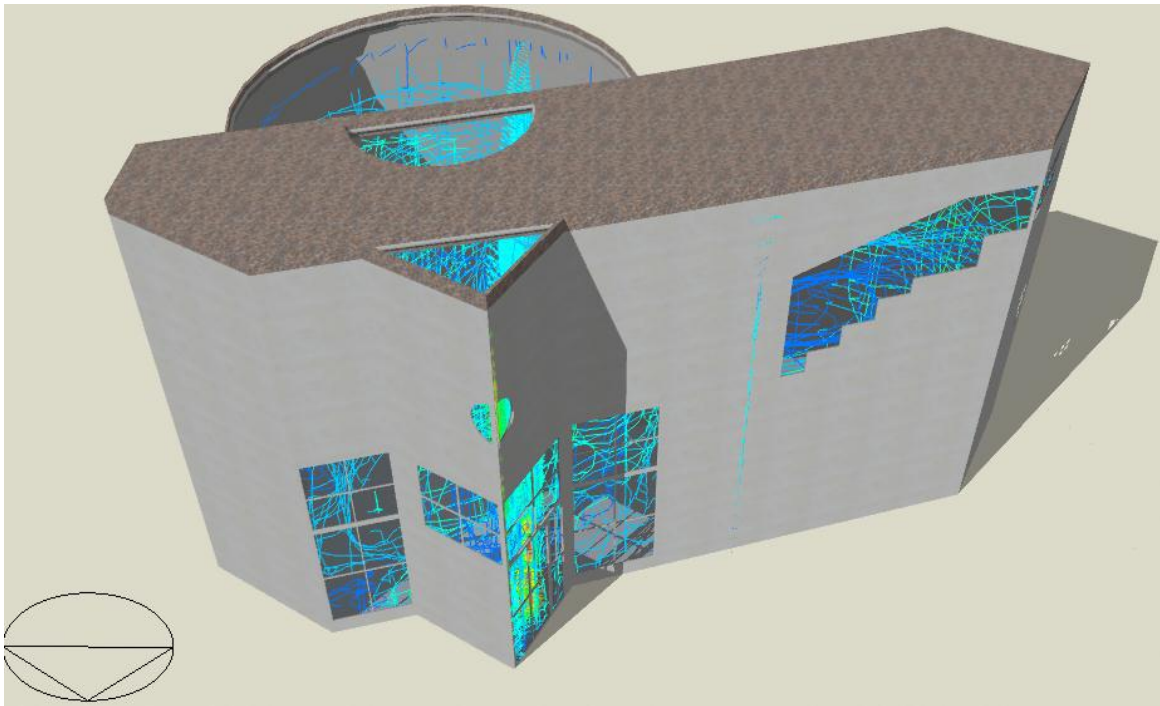


*Figure 3.34: The atrium geometry isolated from the rest of the building*

The CFD internal analysis was conducted in July 31<sup>st</sup> during midday. The central door of the building was left open as it usually occurs when the building is operating. *Figure 3.35* depicts the air circulation (velocity vectors) caused by the open central door.

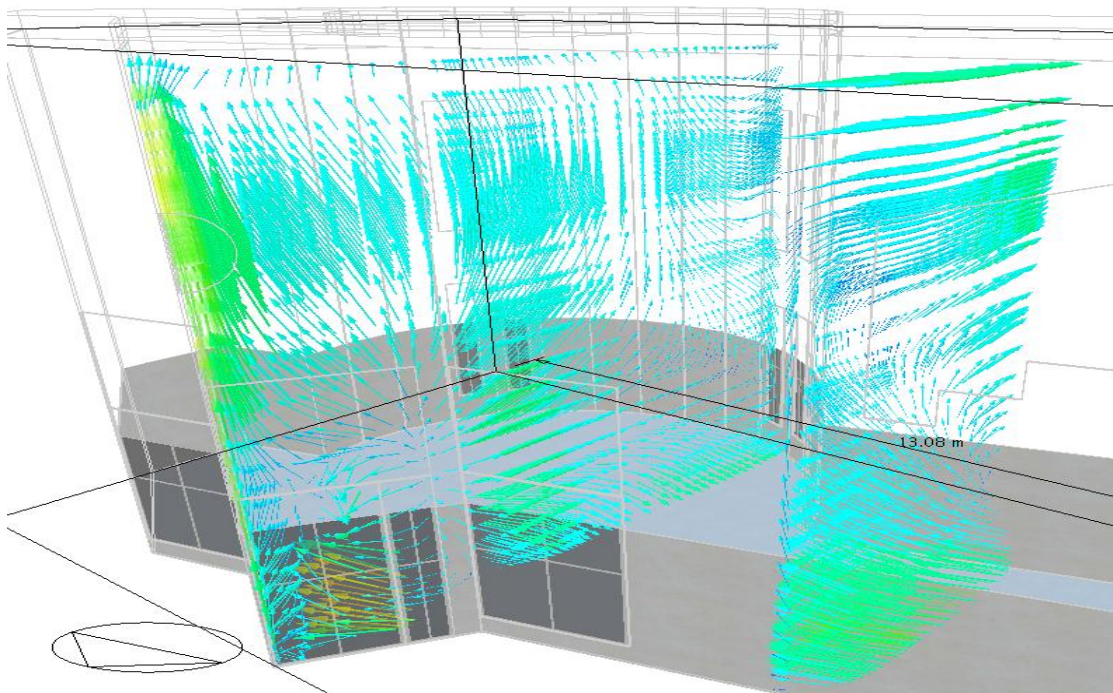


*Figure 3.35: Air circulation in the atrium area.*

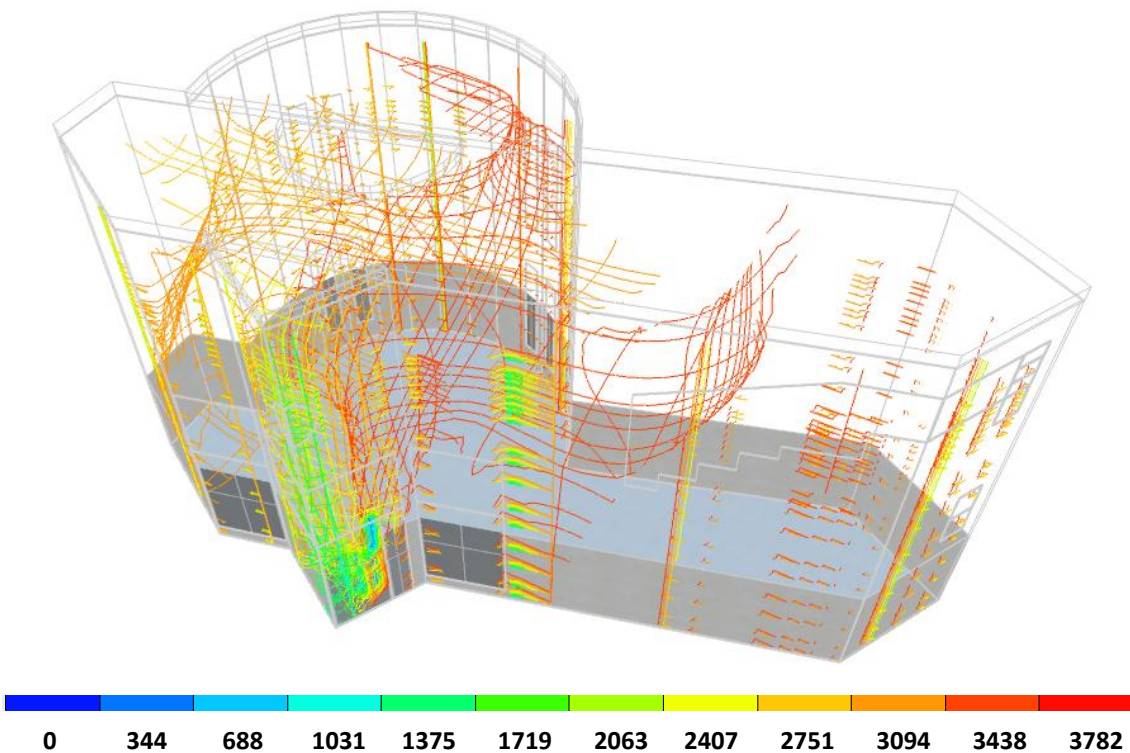


Figure 3.36: Age of air in the atrium area-3D contours (sec).

DesignBuilder can perform LMA calculations, measuring the time it takes for molecules of air to reach every edge in the calculation domain starting from an air supply node. In this case outside air is being supplied in the atrium area through the external door. According to *Figure 3.36* the age of air colored with red is more than an hour without renewal. Particularly in the upper area near the skylight and along the corridor on the right the warmer air, having lower density, is rising due to the stack effect and remains at the top for more than an hour.

Due to the fact that the skylight is not shaded causes a considerable temperature difference between the hot air trapped at the top of the building and the outside air introduced by the open external door. However taking advantage of the stack effect, natural ventilation can be achieved by creating vents at the top of the building enhancing the air flow.

Although thermal simulation and CFD analysis can quite accurately represent the under-examination building, its current state concerning the airtightness of the building is examined through thermal imaging inspection in order to examine the effects of climate conditions such as high temperature, humidity and wind speed on construction materials. In the next section the thermal imaging inspection of the building is discussed.

## 4. Energy auditing process-Further actions

### 4.1 Thermographic inspection

To corroborate and further amplify the simulation results, thermographic imaging, applied in the under examination building, was used. The aim of the energy audit using a thermal imaging camera was mainly to detect areas of energy waste, moisture and air infiltration throughout the building envelope in order to evaluate its airtightness. Moreover, thermal imaging was used to identify and affirm the construction materials bedding of the building envelope. Several modifications took place in the building during the years. These modifications were not imprinted in the drawings and thus the use of the thermal imaging camera assisted in the detection of the materials bedding.

The first thermographic inspection that took place was during summer and the second one during winter. The summer inspection took place on the 12<sup>th</sup> of June 2010 after the sunset. The mean outside air temperature during the day was 25.3°C while the maximum air temperature of the day was 30.4°C. The winter inspection took place on the 31<sup>st</sup> of January during the afternoon. The sky was cloudy; the mean outside air temperature during the day was 6.7°C while the minimum air temperature was 4.7°C.

*Figure 4.1* depicts the thermal image of the façade of the building. The development of the maximum temperature of 38.8°C is observed in part of the outside door of the building consisted only of concrete while the minimum temperature of 30.5°C is observed in the glazing surface. Intense rise of surface temperature is observed in building joints and around window frames. Humidity can be observed in blue color in the left side of the central door due to the presence of a small garden.

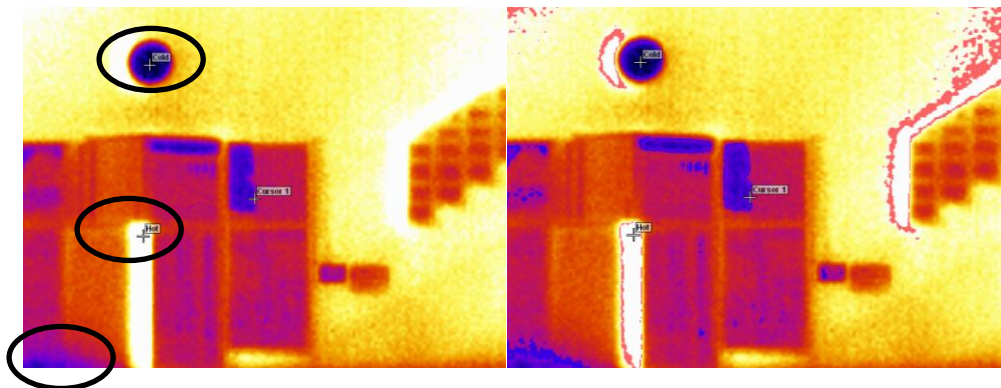


*Figure 4.1: Summer thermal image of the building façade.*

Air leakage through window frames can be observed in *Figure 4.2* and *Figure 4.3* (winter thermal images) due to high temperature difference between the inside and the outside environment of the building. During the time of the inspection the heating system of the building was on. The window lintels can be clearly noticed just above the window frames along the outside wall surface in a warmer color than the rest of the wall surface. The lintels are consisted of concrete having less thermal resistance.



*Figure 4.2: Winter thermal image of the façade of the building.*



*Figure 4.3: Winter thermal image of the façade of the building.*

Figure 4.4 and Figure 4.5 depict heat emission through the building joints acting as thermal bridges due to the temperature difference caused by the construction materials. Once again air leakage is detected in the perimeter area of the glazing. Even though the maximum air temperature of the day was 30.4°C, the highest temperature detected is 38.6°C in the roof.

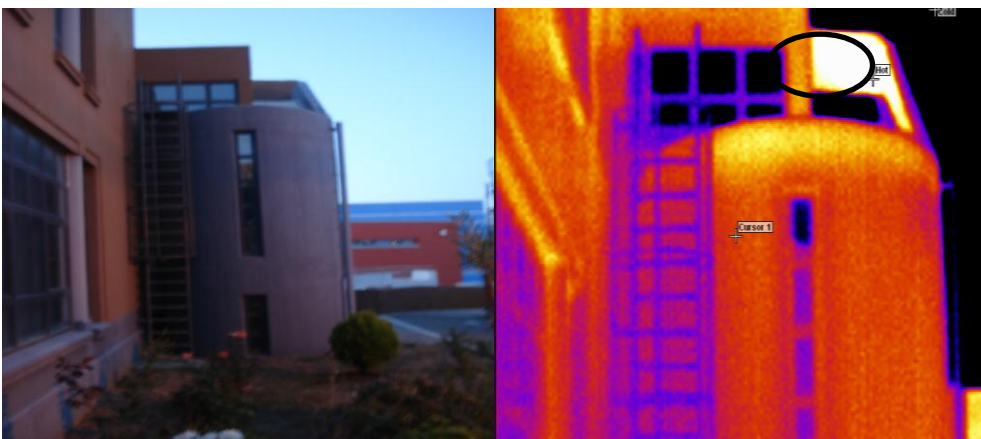


*Figure 4.4: Depiction of the south-west side of the building (Summer thermal image).*

In the south-west side of the building (Figure 4.5) the detected temperature from the thermal imaging camera revealed a temperature difference of 5.5°C between two surface parts of the same side of the building. A considerable temperature difference of 10°C between the wall

surface and the window frame joints is enforcing the heat transfer phenomenon from the outside environment to the inside and vice versa.

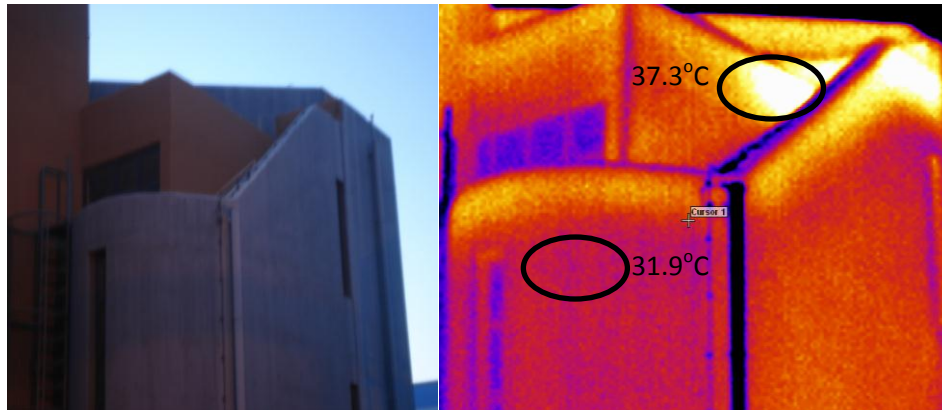


*Figure 4.5: Depiction of the south-west side of the building during summer.*

The same effects are noticed during winter period with a temperature fluctuation from 0°C in the surfaces junctions to 6.4°C around the window frames (Figure 4.6).

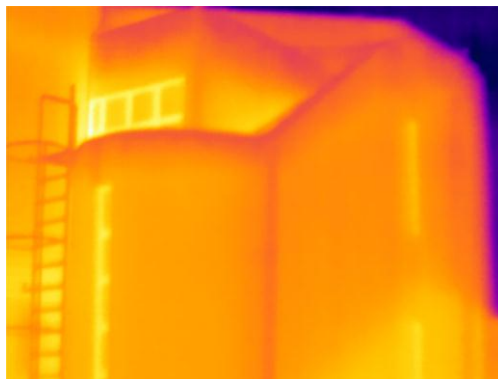


*Figure 4.6: Depiction of the south-west side of the building during winter.*

Intense temperature stratification is revealed in this specific part of the façade of the building (Figure 4.7) that could be caused not only by air leakage through the window frames but also from possible alteration in the thermal characteristics of the construction materials due to high humidity percentages in the area that outreached 85% during the day of the inspection.

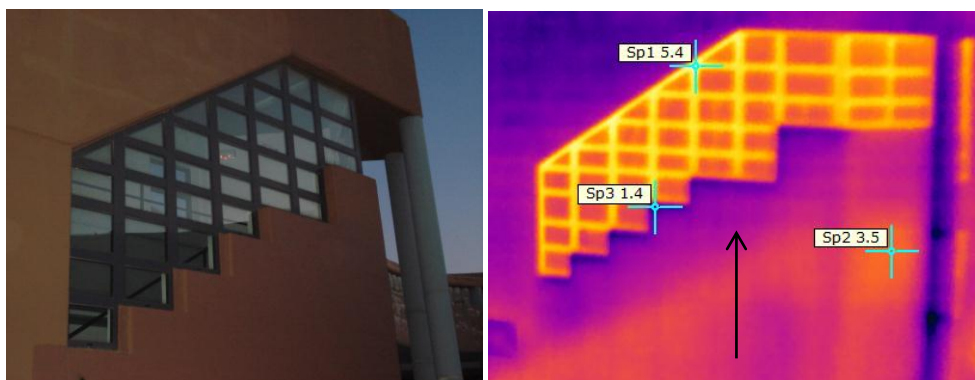


*Figure 4.7: Thermal imaging of the glazing part of the façade during winter.*

In the inside environment of the building, thermal bridging is enforced by discontinuity of construction materials due to the positioning of lintels in the brick wall and due to the building joints in the ceiling that cause a temperature difference of 4°C (*Figure 4.8*).

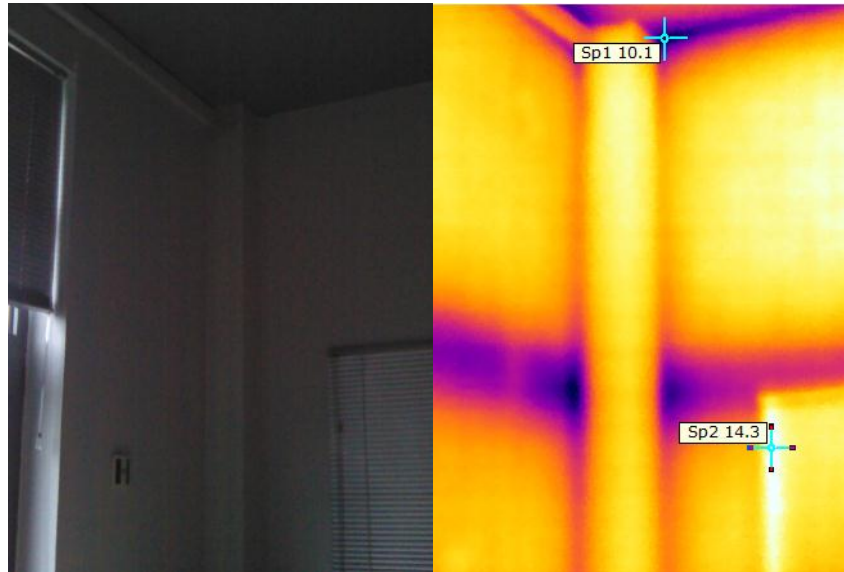


*Figure 4.8: Internal thermal imaging of the building.*

In *Figure 4.10* inappropriately installed and poorly insulated parts of the ceiling frame of the building are deteriorating the shielding of the building in terms of airtightness. The decreased surface temperatures of inside parts of the building can result quite often in condensation problems especially in the corners where it is mostly detected increasing at the same time heat losses.

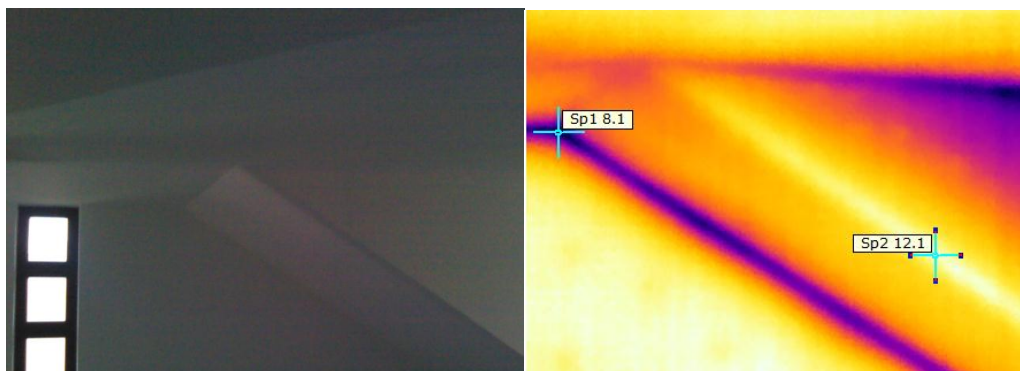


*Figure 4.9: Internal thermal imaging of the building.*

Bridging between the installed BATT insulation and the plasterboard semicircle internal partition of the building can be seen in *Figure 4.10*. The semicircle part of the building leads to the skylight. During summer large amounts of heat due to solar radiation are trapped inside the building and heat transferred to the offices is facilitated through thermal bridging in the plasterboard internal partitions causing a significant rise of the inside temperature and thus augmenting energy consumption for cooling the thermal zone in order to maintain comfort conditions.



*Figure 4.10: Internal thermal imaging of the building.*

Conducting the energy auditing process with a thermal imaging inspection assisted in the verification of the construction materials and the evaluation of the building's airtightness. Thermal losses through the inappropriately insulated envelope of the building is leading to the use of the supplementary heating system (split units) apart from the basic central one during winter. Even worse consequences are observed during summer when the surface temperature of the building façade tend to rise considerably.

The simulation-based energy auditing will be completed in the following section by introducing the buildings Energy Performance Certificate using the TEE-KENAK simulation software.

## 4.2 Building Energy Performance Rating

After the energy inspection which took place in the TUC building all the appropriate information gathered are introduced into the TEE-KENAK simulation software. The information gathered comprised dimensions of all the surfaces, information concerning the openable and non-openable surfaces and their characterization (wall, roof, window, door), the HVAC specification data, equipment, use of the building, number of users.

The data were introduced in the TEE-KENAK software and the shading coefficients were calculated for summer and winter period for each surface.

### 4.2.1 Calculation Parameters

The data used to calculate energy waste is the internal temperature of the building, the outside temperature the construction materials heat transfer coefficient, data for natural ventilation ( $\text{m}^3/\text{h}/\text{person}$ ) and data for infiltration. To take into account thermal gains, data related to solar gains and human activity contributing to thermal gains, should be provided such as solar radiation/building surface/orientation, window solar transmittance, surface shading percentage, number of people, activity type, equipment (number of devices, type).

The basic energy equations according to ISO 13790 (monthly timestep) for the heating and cooling energy demands are:

$$Q_{H,nd} = Q_{tr} + Q_{ve} - n_{gn} * (Q_{int} + Q_{sol})$$

$$Q_{c,nd} = Q_{int} + Q_{sol} - n_{gn} * (Q_{tr} + Q_{ve})$$

In order to calculate the primary energy consumption for heating and cooling, the HVAC system coefficients of performance should be acquainted and then conversion of the energy consumption to primary energy is taking place according to the appropriate factors.

To describe the buildings structure, the software requires information upon the surface and volume of heated and non-heated zones and sunspaces. In regard to the zoning of the building, (4) due to the fact that there is one type of HVAC system and the offices have the same use, the same working hours and the same comfort temperature values, the TUC building is examined as one thermal zone.

To describe the buildings envelope, information upon opaque external surfaces are introduced such as the type of the surface (wall, roof, door etc.). Moreover, information upon transparent surfaces should be given (openable, non-openable) and information concerning the internal partitions (opaque, transparent).

As far as the HVAC system is concerned, its specifications are entered, such as production, distribution, terminals, auxiliary systems. Lighting data are only introduced for dwellings that belong to the industrial sector.

Construction and glazing data are selected by the user and generated from the software's library data set for each introduced surface.

Library data set of climatic data comprises the latitude of the area, the heating period duration, the cooling period duration (4) and monthly values for mean external temperature (7) global horizontal radiation and global horizontal for gradient surfaces ( $\text{MJ}/\text{m}^2$ ).

#### 4.2.2 Results

Since the necessary data were introduced and all the appropriate calculations were conducted, the results of a simulation run can be seen in *Table 4.1*.

Category	Reference Building ( $\text{kWh}/\text{m}^2/\text{year}$ )	TUC Building ( $\text{kWh}/\text{m}^2/\text{year}$ )
Heating	10.4	16.9
Cooling	85.3	123.7
DHW	11.6	13.6
Lighting	71.5	66.7
Total	178.8	220.9
<b>Rating</b>	-	<b>Γ</b>

*Table 4.1: Simulation results through TEE-KENAK simulation software (23).*

Observing *Table 4.1*, the total building energy consumption requirement according to its necessities is  $220.9\text{kWh}/\text{m}^2/\text{year}$  while the reference buildings energy consumption is  $178.8\text{kWh}/\text{m}^2/\text{year}$ . The quotient of these results gives the rating of the building in  $\Gamma$  category. The acceptable rating concerning the energy efficiency is B category and therefore this rating is an indicator on the energy reduction changes that have to occur in order to re-evaluate the performance of the building.

#### 4.2.3 Modeling assumptions- Comparison with EnergyPlus

In order to evaluate the efficiency of TEE-KENAK simulation software, it should be mentioned that the two software, EnergyPlus and TEE-KENAK, differ in terms of the general aim of their use. Through EnergyPlus, an accurate representation of the buildings energy consumption and behavior can be achieved while TEE-KENAK is used in order to give an overall picture of the efficiency of the under inspection building under many assumptions and restrictions. The results of TEE-KENAK lack in accuracy comparing to EnergyPlus but the software offers less complexity in the modeling and significantly less time consuming simulations. The purposeful architecture of the software is aiming to its wide use by energy inspectors in order to facilitate them to apply energy reduction techniques by evaluating them in TEE-KENAK.

The first restriction of TEE-KENAK software is the library climatic data. According to KENAK Greece is separated into four climatic zones according to the climatic data which characterize each area (*Figure 4.11*). The TUC building which is located in Crete belongs to the forth climatic area. Thus there are no climatic data for Chania but for the whole grouping area. These data include temperature, humidity, solar radiation and wind speed in mean monthly values for the period 1993-2003.

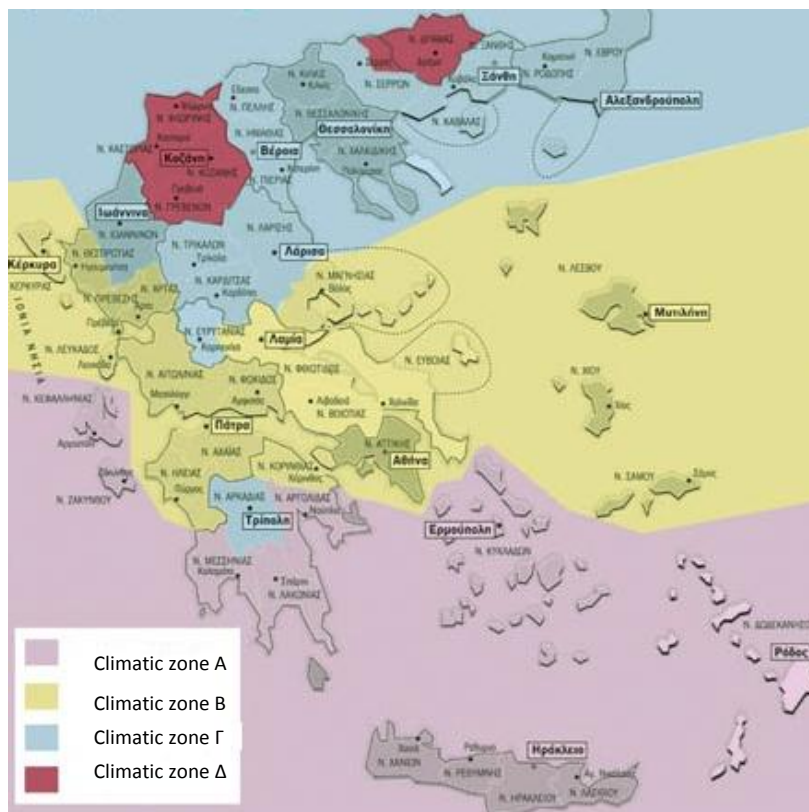


Figure 4.11: Greek climatic zones.

Thus, the simulation results are based on monthly mean values for temperature, humidity and radiation while EnergyPlus runs in sub-hourly timesteps providing results for every ten minutes. The time step data include dry bulb and dew point temperature, relative humidity, station pressure, solar radiation (global, extraterrestrial, horizontal infrared, direct, and diffuse), luminance, wind direction and speed, sky cover, and current weather. The results of TEE-KENAK are consumption results for heating, cooling, DHW (Domestic Hot Water) and lighting. Through EnergyPlus results, the behavior of the building, its spaces, its systems and its users can be examined. A variety of modeling options and results are offered to the user comprising building energy consumption and CO<sub>2</sub> emissions, internal temperatures and comfort indicators, integrated daylighting simulation in order to take advantage of natural light, modeling lighting control systems, airflow calculation and natural ventilation modeling, HVAC sizing and much more.

Referring to the geometry introduction and zoning, TEE-KENAK uses a description method for the construction materials and the volume and dimensions of the building and its surfaces and through the use of library data calculates its energy waste and demands. In EnergyPlus, building description can be achieved by several graphical user interfaces such as Google SketchUp, CYPE-Building Services, DesignBuilder, EFEN, EPlusInterface and more but it can be used as a stand-alone simulation software too. Through the graphical user interfaces, a detailed 3D geometry of the building is introduced to EnergyPlus simulation engine.

Moreover, in EnergyPlus a detailed zoning of the building can be achieved that will provide an in depth examination of the behavior of each zone and the interaction between them. The zoning can take place using partitions that already exist in the actual building or virtual ones.

Using a detailed zoning provides a more accurate determination of the load and energy distribution within the examined building.

In TEE-KENAK, buildings are categorized according to their use. One of these categories is the office-buildings category with the corresponding library data. According to the Technical Guideline TOTEE-20701-1 the examined building, which is an office-building, is operating ten hours per day, five days per week and twelve months per year. The actual operation of the building is around six hours per day and five days per week excluding Christmas, Easter, summer and local holidays when it remains closed. EnergyPlus allows the user to set a daily schedule and holidays schedule in order to take into account or not the operation of the HVAC system, lighting system, human activity and all the appropriate parameters that affect the energy consumption.

Another constrain in the modeling is the Domestic Hot Water (DHW) production. In the actual building such a system does not exist so it is not modeled in EnergyPlus. Even though there is a lack of a DHW production system, TEE-KENAK obligates the user to model such a system with the characteristics of the DHW production system of the reference building (4). To calculate the energy consumption to produce hot water, TEE-KENAK uses empirical values for each building category. For office-buildings the consumption of DHW is assumed to be 5 l/person/day, 0.5 l/m<sup>2</sup>/day and 0.13 m<sup>3</sup>/m<sup>2</sup>/year with a mean temperature value of 19.7°C for the water of climatic zone A. The differences between the consumption results (*Table 4.1*) of the reference building and the under-examination building occur due to the fact that the reference building uses mainly solar collectors for hot water production while the hypothetical introduced system is an electric system.

Concerning the lighting comfort levels, EnergyPlus uses a lighting control system to preserve the lighting comfort levels that the user indicates which mean that whenever the natural light does not reach the comfort level of 500 lux (office-buildings) artificial lighting is on. The consumption of artificial lighting is based upon the power of the lighting system. In TEE-KENAK, even though lighting power is introduced to the software by the user, this information is only applied in the heating and cooling load calculation and not in comfort conditions (4).

As far as the heating system of the actual building is concerned, heating is achieved, as mentioned before, by two systems, a central one using hot water radiators and an oil boiler and an auxiliary one that comprises heat pumps in each room used mainly for cooling the space but also in heating mode when the power of the central system cannot cover the heating needs of each zone according to the comfort conditions. EnergyPlus provides the user with the opportunity to model these two systems using priority vectors while through TEE-KENAK only one system can be modeled, the central one which is the main heating system.

Summarizing, one should take into consideration that the two simulation software tools were created for different uses. There may be significant differences in the accuracy of the results, according to the complexity of the modeling and calculations, but both have advantages and disadvantages. EnergyPlus is quite demanding software that needs a lot of effort to be able to handle it and use it correctly while TEE-KENAK is quite simple and is addressed to any engineer.

Finally the complexity of the modeling in EnergyPlus implies time-consuming simulations and advanced survey cost.

## Conclusions

In the current study a simulation-based energy auditing is presented. The energy auditing process comprised the creation of an integrated thermal model of the under-examination building with the EnergyPlus simulation engine and a CFD internal and external airflow analysis using DesignBuilder CFD software tool. In addition a thermal imaging inspection took place in order to the airtightness of the under-examination building. Finally the rating procedure according to the Energy Performance Certificate is applied and discussed.

The accurate representation of the under examination building through advanced simulation modeling can be used to account for further improvements on buildings energy performance in order to reduce energy requirements while maintaining comfort conditions. Thus the more integrated the simulation model is the more accurate the evaluation procedure of energy conservation measures will be facilitating assessors to undertake feasible and cost-effective measures.

The models produced from such a procedure are used not only towards the evaluation of the energy-performance of the building but they can also be used towards the evaluation of different control strategies applied on Building Energy Management Systems.

In the specific study, DesignBuilder CFD tool assisted in the evaluation of the heating and cooling system of the building so as to gain information and reach conclusions concerning the effectiveness of any HVAC system and to evaluate its position, its extract and intake nodes. The CFD calculations will be also used for determining the acceptable areas of the various sensor installations, such as temperature, presence and luminosity sensors, in all the offices of the TUC building. The conclusion reached was that the skylight space should additionally be ventilated through construction activities either by vents or by a mechanical method. Warmer air was moving upwards in the atrium area and heat was transferred through internal windows and partitions with low thermal resistance to the neighbor offices. Due to EnergyPlus constrains in modeling the Airflow Network, external CFD calculations can be used to more carefully ascertain the infiltration gains and particularize the pressure coefficients to the building. Currently  $C_p$  values are typical approximate values subjected to varying degrees of shelter and wind directions.

Finally thermal imaging inspection of the building revealed the poor airtightness of the building due to multiple thermal bridges in the envelope and air leakage through window frames reinforced by the buildings complex geometry.

## References

1. European Environmental Agency. [Online] [Cited: February 9, 2012.] <http://www.eea.europa.eu/>.
2. Directive 2010/31/EU of the EUROPEAN PARLIAMENT AND OF THE COUNCIL on the energy performance of buildings. *Official journal of the European Union*. May 2010.
3. Elena G. Dascalaki, Kalliopi G. Droutsas, Constantinos A. Balaras, Simon Kontoyiannidis. Building typologies as a tool for assessing the energy performance of residential buildings – A case study for the Hellenic building stock. *Energy and Buildings*. 2011, Vol. 43, pp. 3400-3409.
4. *Technical Guideline-TOTEE 20701-1*. 2010.
5. *Technical Guideline-TOTEE 20701-2*. 2010.
6. *Technical Guideline-TOTEE 20701-3*. 2010.
7. *Technical Guideline-TOTEE 20701-4*. 2010.
8. D. Kolokotsa, D.Rovas, E Kosmatopoulos, K. Kalaitzakis. A roadmap towards intelligent net zero-and positive-energy buildings. *Solar Energy*. 2011, Vol. 85, pp. 3067-3084.
9. Giannakis, G. "Development of model-based predictive control strategies to improve energy performance of existing office buildings." MSc thesis. Technical University of Crete, Chania : s.n., 2011.
10. Hellenic National Meteorological Service. [Online] [http://www.hnms.gr/hnms/english/climatology/climatology\\_region\\_diagrams\\_html?dr\\_city=C hania\\_Souda](http://www.hnms.gr/hnms/english/climatology/climatology_region_diagrams_html?dr_city=C hania_Souda).
11. EnergyPlus Documentation. [Online] [http://apps1.eere.energy.gov/buildings/energyplus/energyplus\\_documentation.cfm](http://apps1.eere.energy.gov/buildings/energyplus/energyplus_documentation.cfm).
12. DesignBuilder. *Technical Manual*.
13. America, Illuminating Engineering Society of North. *Lighting Handbook: Reference & Application*. New York : s.n., 1993. p. p. 335.
14. *ASHRAE Handbook of Fundamentals*. 2005.
15. Regulation of energy efficiency in buildings. [Online] April 2010. [http://portal.tee.gr/portal/page/portal/TEE\\_HOME/D6-5825%20KENAK-FEK%20407-B-2010.pdf](http://portal.tee.gr/portal/page/portal/TEE_HOME/D6-5825%20KENAK-FEK%20407-B-2010.pdf). 407.
16. Directive 2002/91/EC of the European Parliament and of the Council of 16 December 2002 on the energy performance of buildings.
17. Qiong Li, Hiroshi Yoshino, Akashi Mochida, Bo Lei, Qinglin Meng, Lihua Zhao, Yufat Lun. CFD study of the thermal environment in an air-conditioned train station building. *Building and Environment*. 2009, Vol. 44, pp. 1452–1465.
18. Nikola Tanasićca, Goran Jankesa, Håkon Skistadb. Cfd analysis and airflow measurements to approach large industrial halls energy efficiency: A case study of a cardboard mill hall. *Energy and Buildings*. 2011, Vol. 43, pp. 1200–1206.
19. Patankar, Suhas V. *Numerical Heat Transfer and Fluid Flow*.
20. J.H. Ferziger, M.Peric. *Computational Methods for Fluid Dynamics*. 3rd.
21. H.K.Malalasekera, W. Versteeg. *An Introduction to Comutational Fluid Dynamics*. 1995.

22. B. E. Launder, D. B. Spalding. *The numerical Computation of Turbulent Flows*. 1974, Vol. 3, pp. 269-289.
23. A. Vasilomichelaki, P. Exizidou, M. Tsirantonakis. *Building Energy Auditing through TEE-KENAK simulation software*. Environmental Engineering Department, Technical University of Crete. Chania : s.n., 2011. Term for the postgraduate course "Energy Management in the Built Environment".
24. [Online] <http://www.designbuilder.co.uk/>.
25. B. Blocken, T. Defraeye, D. Derome, J. Carmeliet. High-resolution CFD simulations for forced convective heat transfer coefficients at the facade of a low-rise building. *Building and Environment*. 2009, Vol. 44, pp. 2396–2412.
26. Omar S. Asfour, Mohamed B. Gadi. A comparison between CFD and Network models for predicting wind-driven ventilation in buildings. *Building and Environment*. 2007, Vol. 42, pp. 4079–4085.
27. Center for Renewable Energy Sources. [Online] [Cited: January 23, 2012.] [www.cres.gr](http://www.cres.gr).
28. P. Exizidou, G. Giannakis, D. Rovas. *Deliverable Report "Integrated Thermal Simulation Montels", PEBBLE*. 2010.

## Appendix: Building's envelope information and comfort results

### Window-Wall Ratio

	Total	North (315 to 45 deg)	East (45 to 135 deg)	South (135 to 225 deg)	West (225 to 315 deg)
Gross Wall Area [m2]	675.67	209.3	172.02	169.03	125.33
Window Opening Area [m2]	85.48	34.62	15.56	23.33	11.97
Window-Wall Ratio [%]	12.65	16.54	9.04	13.8	9.55

### Skylight-Roof Ratio

	Total
Gross Roof Area [m2]	196.38
Skylight Area [m2]	18.32
Skylight-Roof Ratio [%]	9.33

### Performance

	Area [m2]	Conditioned (Y/N)	Volume [m3]
UNDERGROUND FLOOR:ZONE2	62.39	No	155.99
UNDERGROUND FLOOR:ZONE6	10.02	No	25.05
GROUND%FLOOR:CORRIDORSTAIRS	26.28	No	88.05
GROUND%FLOOR:OFFICE1	18.76	Yes	62.85
GROUND%FLOOR:OFFICE2	10.51	Yes	35.2
GROUND%FLOOR:CENTRALCORRIDOR1	22.86	No	76.58
GROUND%FLOOR:OFFICE3	13.53	Yes	45.49
GROUND%FLOOR:CENTRALCORRIDOR2	26.29	Yes	88.06
GROUND%FLOOR:WC	5.08	Yes	17.02
GROUND%FLOOR:OFFICE56	17.81	Yes	59.66
GROUND%FLOOR:ATRIUMCORRIDOR	16.43	No	55.03
GROUND%FLOOR:OFFICE4	23.26	Yes	77.93
GROUND%FLOOR:STORAGEAREAELEVATOR	6.56	No	21.97
GROUND%FLOOR:HALLELEVATOR	4	No	13.4
GROUND%FLOOR:HALOFFICES	3.13	No	10.49
FIRSTFLOOR4STAIRS:STAIRS	2.75	No	3.96
FIRSTFLOOR2:OFFICE8	15.07	Yes	73.45
FIRSTFLOOR2:OFFICE9	15.19	Yes	74.43
FIRSTFLOOR2:OFFICE10	13.71	Yes	66.57
FIRSTFLOOR2:HALOFFICES2	1.37	No	6.48
FIRSTFLOOR2:HALOFFICES1	1.9	No	9.32

Simulation-based energy auditing

FIRSTFLOOR3CORRIDOR:CORRIDOR2	25.29	Yes	102.21
FIRSTFLOOR3CORRIDOR:CORRIDOR1	3.68	No	86.9
FIRSTFLOOR1:OFFICE11	28.14	Yes	151.48
FIRSTFLOOR1:STORAGEAREAELEVATOR	6.37	No	34.39
FIRSTFLOOR1:HALLELEVATOR	4.45	No	24.11
FIRSTFLOOR1:EQUIPMENTROOM	7.86	No	42.34
FIRSTFLOOR1:HOLE	0.19	No	81.53
FIRSTFLOOR1:OFFICE13	10.39	Yes	55.94
FIRSTFLOOR3STAIRS:STAIRS	23.15	Yes	93.04
FRSTFLRENTRNCTRNGL:HOLE	0.01	No	0.77
Total	426.44		1739.69
Conditioned Total	246.18		1003.34
Unconditioned Total	180.26		736.36

Time Not Comfortable Based on Simple ASHRAE 55-2004

	Winter Clothes [hr]	Summer Clothes [hr]	Summer or Winter Clothes [hr]
GROUND%FLOOR:OFFICE1	1154.5	1573.67	817.67
GROUND%FLOOR:OFFICE2	1188.17	1560.67	838.33
GROUND%FLOOR:OFFICE3	1282.5	1547.33	922.83
GROUND%FLOOR:OFFICE56	1093.33	1414.83	623.67
GROUND%FLOOR:OFFICE4	1282.33	1540.5	945
FIRSTFLOOR2:OFFICE8	1341	1645.17	1074.17
FIRSTFLOOR2:OFFICE9	1260.5	1590.5	939.33
FIRSTFLOOR2:OFFICE10	1508.33	1629.5	1224
FIRSTFLOOR1:OFFICE11	1233.17	1714.17	1035.83
FIRSTFLOOR1:OFFICE13	1308.17	1668.17	1087.5
Facility	1749.83	1889.83	1573.83

Time Setpoint Not Met

	During Heating [hr]	During Cooling [hr]	During Occupied Heating [hr]	During Occupied Cooling [hr]
GROUND%FLOOR:OFFICE1	7	10.67	7	10.67
GROUND%FLOOR:OFFICE2	8.33	7.67	8.33	7.67
GROUND%FLOOR:OFFICE3	4	7.83	4	7.83
GROUND%FLOOR:OFFICE56	1.5	0.5	1.5	0.5
GROUND%FLOOR:OFFICE4	4.33	12.17	4.33	12.17
FIRSTFLOOR2:OFFICE8	12.17	12	12.17	12
FIRSTFLOOR2:OFFICE9	8.83	9.5	8.83	9.5
FIRSTFLOOR2:OFFICE10	10	10.17	10	10.17
FIRSTFLOOR1:OFFICE11	11.67	24.17	11.67	24.17
FIRSTFLOOR1:OFFICE13	1.33	9.83	1.33	9.83

---

Simulation-based energy auditing

---

GROUND%FLOOR:WC	819.83	403	0	0
Facility	819.83	405.5	13	24.17

---